IEA INTERNATIONAL ENERGY AGENCY

Demonstration test results for grid interconnected photovoltaic power systems

Task V
Report IEA-PVPS T5-02:1999
March 1999

PVPS

PHOTOVOLTAIC POWER SYSTEMS PROGRAMME

IEA PVPS
International Energy Agency
Implementing Agreement on Photovoltaic Power Systems

TASK V
Grid Interconnection of Building Integrated
and Other Dispersed Photovoltaic Power Systems

Report IEA PVPS T5-02: 1999

DEMONSTRATION TEST RESULTS FOR GRID INTERCONNECTED PHOTOVOLTAIC POWER SYSTEMS

March 1999

Prepared by:
Akio KITAMURA
The Kansai Electric Power Co., Technical Research Center
11-20, Nakoji 3-chome, Amagasaki, Hyogo, Japan
e-mail: K516204@KEPCO.CO.JP

To obtain additional copies of this report or information on other
IEA-PVPS publications, contact the IEA website: http://www.iea.org

CONTENTS

Foreword

The International Energy Agency (IEA), founded in November 1974, is an autonomous body within the framework of the Organisation for Economic Co-operation and Development (OECD) which carries out a comprehensive programme of energy co-operation among its 23 member countries. The European Commission also participates in the work of the Agency.

The IEA Photovoltaic Power Systems Programme (PVPS) is one of the collaborative R&D agreements established within the IEA, and since 1993 its participants have conducted various joint projects on the photovoltaic conversion of solar energy into electricity.
The twenty-two members are: Australia, Austria, Canada, Denmark, European Commission, Finland, France, Germany, Israel, Italy, Japan, Korea, Mexico, Netherlands, Norway, Portugal, Spain, Sweden, Switzerland, Turkey, United Kingdom and United States.

This report has been prepared under the supervision of PVPS Task V by
Akio KITAMURA
The Kansai Electric Power Co., Technical Research Center
11-20, Nakoji 3-chome, Amagasaki, Hyogo 661, Japan
Telephone +81 6 6484 9786, Fax +81 6 6494 9827
in co-operation with experts of the following countries:
Australia, Austria, Denmark, Germany, Italy, Japan, Netherlands, Portugal, Switzerland, United Kingdom and United States and approved by the Executive Committee of the PVPS programme.

The report expresses as accurately as possible the international consensus of opinion on the subjects addressed.

ABSTRACT AND KEYWORD

This report describes the data obtained from experimental tests for PV system grid interconnection using the test facility at Rokko Island Test Centre in Japan. These tests were intended to show the actual phenomena of grid interconnection of PV systems. This report was written as a reference for people with a technical background, such as electricity company personnel, manufactures and researchers.

Keywords: Photovoltaic power generation, Grid interconnection, Utility distribution system, PV inverters, Harmonics, Islanding, Short circuit fault in distribution system, DC injection, PV output variation, PV array temperature

Executive Summary

Background and objectives

Grid interconnection of photovoltaic (PV) power generation system has the advantage of more effective utilisation of generated power. However, the technical requirements from both the utility power system grid side and the PV system side need to be satisfied to ensure the safety of the PV installer and the reliability of the utility grid. Clarifying the technical requirements for grid interconnection and solving the problems are therefore very important issues for widespread application of PV systems.

The International Energy Agency (IEA), Implementing Agreement on Photovoltaic Power Systems (PVPS) Task V : *Grid Interconnection of Building Integrated and Other Dispersed Photovoltaic Power Systems*, has conducted research into the grid interconnection issues through a process of international collaboration. The main objective of Task V was to develop and verify technical requirements which may serve as technical guidelines for grid interconnection of building integrated and other dispersed PV systems. In order to achieve the objectives of Task V, three sub-tasks were established, as follows:

- Sub-task 10 : Review of existing PV grid interconnection guidelines, grid structure and previously installed PV experiences

- Sub-task 20 : Theoretical studies on various aspects for grid interconnection and configuration of PV systems

- Sub-task 30 : Experimental tests using the Rokko Island and/or other test facilities

In sub-task 30, actual experimental tests for PV system grid interconnection were conducted using the test facility at Rokko Island Test Centre in Japan. These tests were intended to show the actual phenomena of grid interconnection with reference to the subtask 20 work. Although some of the tests were not directly related to subtask 20, much data for future reference purposes was obtained. Subjects of tests conducted in Rokko Island are listed below.

- Harmonics generated by PV systems
- Islanding
- Short circuit fault contribution in the LV distribution system
- DC injection
- Output power variation of many PV systems
- Temperature measurement of PV array

This report describes the data obtained from these tests. This report was written as a reference for people with a technical background, such as electricity company personnel, manufactures and researchers. Although the inverters used for some of the tests are no longer commercially available, the information is still considered valuable for the targeted readers.

Findings

Summaries of the experimental results are described below for each tested subject.

1. Measurement of Harmonics Distortion Caused by PV Systems

Problems and Objectives

Grid interconnected photovoltaic power generation systems generates harmonics because it has AC/DC converters and isolation transformers. These harmonics may affect the quality of electricity and cause damage to equipment.

As the number of units of grid interconnected photovoltaic power generation systems increase, the total harmonic content in the system may increase when each harmonic from each photovoltaic power generation system superimposes one another or may decrease when each harmonic cancels one another. It is important to examine what is the general tendency of total harmonic when a lot of photovoltaic power generation systems are interconnected to one distribution line. Relation between the number of interconnected PV units and total harmonic current was measured.

Findings and conclusions

It was found that the third and the fifth harmonic current increased with the increase in the number of connected units of inverters. However, the higher harmonics did not always increase or sometimes decreased with the number of units, especially when the photovoltaic power generation inverters manufactured by the different manufacturer (having different control scheme) are interconnected to the same distribution line.

From these results, it can be concluded that third and fifth harmonic current from inverters have almost the same phase displacement and the total harmonic current could be superimposed, while higher harmonics from inverters have different phase displacement even if the same control scheme is employed and total harmonic current could be cancelled. The phenomenon that the third harmonic and the fifth harmonic increase with the number of connected units is considered to be caused by exciting current of the isolation transformers.

2. Measurement of Islanding Characteristics

Problems and Objectives

Islanding may cause problems such as human safety and equipment maintenance if it continues for a long time. It is therefore important to clarify the conditions under which continued islanding occurs, and verify the necessity of measures for preventing islanding and effectiveness of these countermeasures, especially when a large number of PV systems are interconnected to one distribution line.

Findings and conclusions

When many PV systems whose inverters have only ordinary protective relays such as over/under voltage relays and over/under frequency relays, islanding can be continued for a long time if total output power from PV systems is higher than total load in distribution system. This result shows that some measures for detecting islanding conditions are required. Various kind of islanding detection or prevention function, including passive and active schemes, have been proposed.

Islanding phenomenon does not continue for a long period of time if multiple photovoltaic power generation systems having islanding detection functions for their inverters were interconnected to power distribution line. Especially when inverters manufactured by different manufacturers were interconnected together, that means different schemes of islanding detection were exist, islanding is hardly occur. It was confirmed that mainly the passive scheme detected islanding phenomenon, while the contribution of active scheme islanding detection was not clarified. It was also found that islanding detection time increases when a load which can sustain a distribution line voltage such as induction motor load.

3. Characteristics under Distribution Line Short Circuit

Problems and Objectives

Photovoltaic power generation systems may supply fault current under the short circuit fault condition in distribution system. Fault current from PV systems could affect the fault detection in distribution system and causing delay of protection. Therefore, it is necessary to verify the effect of the short circuit current from PV systems on system fault detection.

Fault current from PV system was measured under the short circuit condition at the low voltage side of distribution transformer. Measurements were conducted for various output power of PV system.

Findings and conclusions

Some inverters do not supply fault current at all (only maintaining the current before short circuit fault) and stop the operation in a short period of time (within 1 or 2 cycles) by the under voltage relay. Even for inverters supplying fault current, magnitude of fault current is only twice of current before fault and lasts only 1 or 2 cycles. This result shows that output current control of inverter works well.

It was concluded that PV systems do not affect the protection for short circuit fault in distribution system.

4. Characteristics under AC/DC Mixing Fault

Problems and Objectives

If PV system has no isolation transformer, DC current component may injected to AC circuit of the power distribution system (DC injection), resulting magnetic saturation of utility transformer. This magnetic saturation causes distortion of exciting current and a large amount of harmonics in distribution system. The effect of DC injection could be examined by more severe situation, AC/DC mixing fault condition, in which DC circuit of PV array is directly connected to the AC system. In this AC/DC mixing fault condition, effect of AC current breaks into DC circuit of photovoltaic array can be also examined.

Propagation range of harmonics generated at the AC-DC mixing fault in the power system, the effect on other transformers connected to the same high voltage distribution line and the effect on other inverters for photovoltaic power generation connected to the same low voltage distribution line are examined.

Findings and conclusions

Exciting current of utility transformer starts to increase immediately after AC/DC mixing fault and becomes stabilised (saturated) in several to ten-odd seconds. At this time, magnetic saturation occurs and harmonic current of even orders are generated on the high voltage side of the utility transformer. Distortion of current waveform was also seen in other utility transformers connected to the same high voltage side of distribution line and the isolation transformers of other photovoltaic power generation systems connected to the same low voltage distribution line.

However, even though the AC/DC mixing fault continues for several minutes, no overheating, vibration or sound were observed for the utility transformers. Also, no effect was observed for the operation of photovoltaic power generation systems connected to the low voltage side of utility transformers located in the vicinity of the utility transformer generating mixing fault. For conclusion, effect of DC current injected to the AC system is negligible.

5. Output Fluctuation of PV systems

Problems and Objectives

The output of photovoltaic power generation fluctuates with solar irradiance. Solar irradiance varies in second order owing to the movement of cloud except for a very fine day and a totally cloudy day. The fluctuation in output of the photovoltaic power generation causes the fluctuation in power flow, or fluctuation in voltage in the connected distribution line. If many PV systems are interconnected to a limited area, output fluctuation of PV system occur simultaneously then voltage fluctuation in the distribution line becomes larger than the fluctuation induced from load. Moreover, considering that the voltage fluctuation take places in second order, it may causes flicker in distribution system. That kind of fluctuation may become a technological issue for future introduction of photovoltaic power generation.

Power fluctuation from large number of PV systems interconnected to one distribution line within limited area was measured and relation between power fluctuation for individual system and whole system was obtained.

Findings and conclusions

In the case that many PV systems are connected, even if the output fluctuation of each PV system is large, both the magnitude and speed of fluctuation decrease to level off as the whole system. Accordingly, distribution voltage fluctuation due to output fluctuation also decreases.

It is difficult to measure the speed and magnitude of output fluctuation of the multiple interconnected photovoltaic power generation systems in actual installation. It was found that measured value brought by a pyranometer of slow response rate is similar to the actual values of the speed and magnitude of output fluctuation of multiple interconnected photovoltaic power generation systems. Therefore, measurement of the speed and magnitude of output fluctuation can be conducted with a pyranometer of slow response rate.

6. Measurement of PV Array Temperature

Problems and Objectives

The surface temperature of array is an important factor in evaluating characteristics of photovoltaic power generation systems. However, it is not clearly determined whether the temperature is for output period or for no output period. Therefore, the difference in the surface temperature of array "for the case that inverter is connected to photovoltaic array and output at full capacity" and "for the case that output terminal of array is opened, i.e., no output" was measured.

Findings and conclusions

The surface temperature of array of photovoltaic power generating systems is lower when the array have output power than when the array does not have output. This was confirmed by the measurement with three units of photovoltaic power generating arrays. Although the temperature difference was as low as 5℃ at the most in this measurement, the difference is considered to be bigger under actual conditions.

It should be studied in the future that which is appropriate to measure the surface temperature of array with output or array without output and what is the appropriate interval in evaluating the conversion efficiency of photovoltaic power generating systems.

Conclusions

In subtask 30, experimental studies using the test facilities at the Rokko Test Centre for Advanced Energy Systems were conducted. Experiments were conducted for various aspects such as harmonics, islanding, distribution line short circuit, AC-DC mixing fault, PV system output variation, and PV array temperature evaluation. These experiments were conducted to provide reference data for grid interconnection of PV systems. Subjects like harmonics, islanding, AC-DC mixing fault and PV system output variation are closely related to the activities of subtask 20, while some of the subjects such as distribution line short circuit and PV array temperature measurement were not directly related to subtask 20 activities.

Test results showed that grid interconnection of multiple photovoltaic power generation systems has little effect on distribution line short circuit, AC-DC mixing fault, and output variation, but does affect harmonics and islanding. Further consideration of these effects, especially the islanding conditions, is required.

1. Introduction

Task V is a working group of the International Energy Agency (IEA), Implementing Agreement on Photovoltaic Power Systems (PVPS). The title of the working group is "Grid Interconnection of Building Integrated and Other Dispersed Photovoltaic Power Systems."

The main objective of Task V is to develop and verify technical requirements that may serve as pre-normative technical guidelines for the network interconnection of building-integrated and other dispersed photovoltaic (PV) systems. These technical guidelines are intended to ensure the safe, reliable and low-cost interconnection of PV systems to the electric power network. Task V considers PV systems connected to the low-voltage network with a typical peak power rating of 1 to 50 kilowatts.

Task V has three subtasks:

10 Review of PV guidelines, grid structures and PV experiences
20 Theoretical studies on utility aspects of PV systems
30 Experimental tests using Rokko Island and/or other test facilities

Subtask 10 defines the status quo of grid connected PV systems. A survey on current guidelines produced information on the interconnection of PV systems with the utility network. A second survey showed the different network structures of the participating countries. Subtask 10 identified existing and possible problems in the near future regarding the network connection of PV systems.

The scope of work of subtask 20 was to analyse these problems and to draft possible recommendations for improvement. Some problems, however, appeared to be too complex and additional experimental work was required. These experiments are co-ordinated in subtask 30.

In subtask 30, experimental studies using the Rokko Island test facility were conducted. Experiments were conducted for many aspects such as harmonics, islanding, PV system output variation, dc-ac mixing and others. These experiments were conducted as a reference for grid interconnection of PV systems and some of the subjects were not directly related to the activities of subtask 20.

This report describes the experimental results of subtask 30, and is written by subtask 30 leader.

2. Outline of Rokko Test Centre for Advanced Energy Systems

The Rokko Test Centre for Advanced Energy Systems was built at Rokko Island in Kobe, Japan to verify technical problems arising from grid interconnection of various new energy generation systems through field tests. The new energy generation systems to be tested are photovoltaic power generators, wind power generators and fuel cell generators, and these power generators are interconnected to simulated utility distribution lines. Among these systems, in the field tests for IEA task V, simulated distribution lines and photovoltaic power generation systems were used. A total of 200 photovoltaic power generators with a total capacity of 500 kW were installed in order to conduct various tests regarding grid interconnection.

The Rokko Test Centre for Advanced Energy Systems has two simulated high voltage overhead distribution lines (line 1 with a transformer capacity of 500 kVA and line 2 with a transformer capacity of 2000 kVA) and each line has ten blocks equivalent to a total of 10 km, one block being equivalent to 1 km of line length. Two pole transformers with a capacitance of 20 kVA or 30 kVA are mounted every one block of the simulated distribution lines. The simulated distribution lines are Japanese standard overhead distribution lines, where the high voltage distribution line is the 6.6 kV three-phase, three-wire system (neutral point ungrounded) and the low voltage distribution line is the single-phase, three-wire system (100, 200 V). All the photovoltaic power generation systems are interconnected to the low voltage distribution lines.

In line 1, five photovoltaic power generation systems with a capacity of 2 kW each are mounted on each pole transformer, hence a total of 100 units with 200 kW are connected. In line 1, to simulate the utility distribution system configuration in Europe, the high voltage distribution line can be changed to the neutral line grounding system and the impedance of the cable system can be simulated (although the line voltage is kept to 6.6 kV and the power supply frequency is 60 Hz).

In line 2, five photovoltaic power generation systems consisting of two units having a capacity of 2 kW, another two units having a capacity of 3 kW and one unit having a capacity of 5 kW are mounted on each pole transformer, hence a total of 100 units with 300 kW are connected. With regard to loads, simulated loads (constant impedance load and motor load) and actual loads are mounted for each of the high voltage and low voltage distribution lines. For grid interconnection inverters for photovoltaic power generation, line 1 has 50 voltage controlled type units and 50 current controlled type units, while all the units in line 2 are current controlled type.

Fig.2-1 shows the electrical configuration of the simulated distribution lines of Rokko Test Centre for Advanced Energy Systems. Fig.2-2 shows installation layout of the photovoltaic power generation systems in Rokko Test Centre for Advanced Energy Systems. Table 2-1 shows the specifications for the high voltage transformers, the simulated distribution lines, the pole transformers, the photovoltaic power generation systems and the simulated loads.

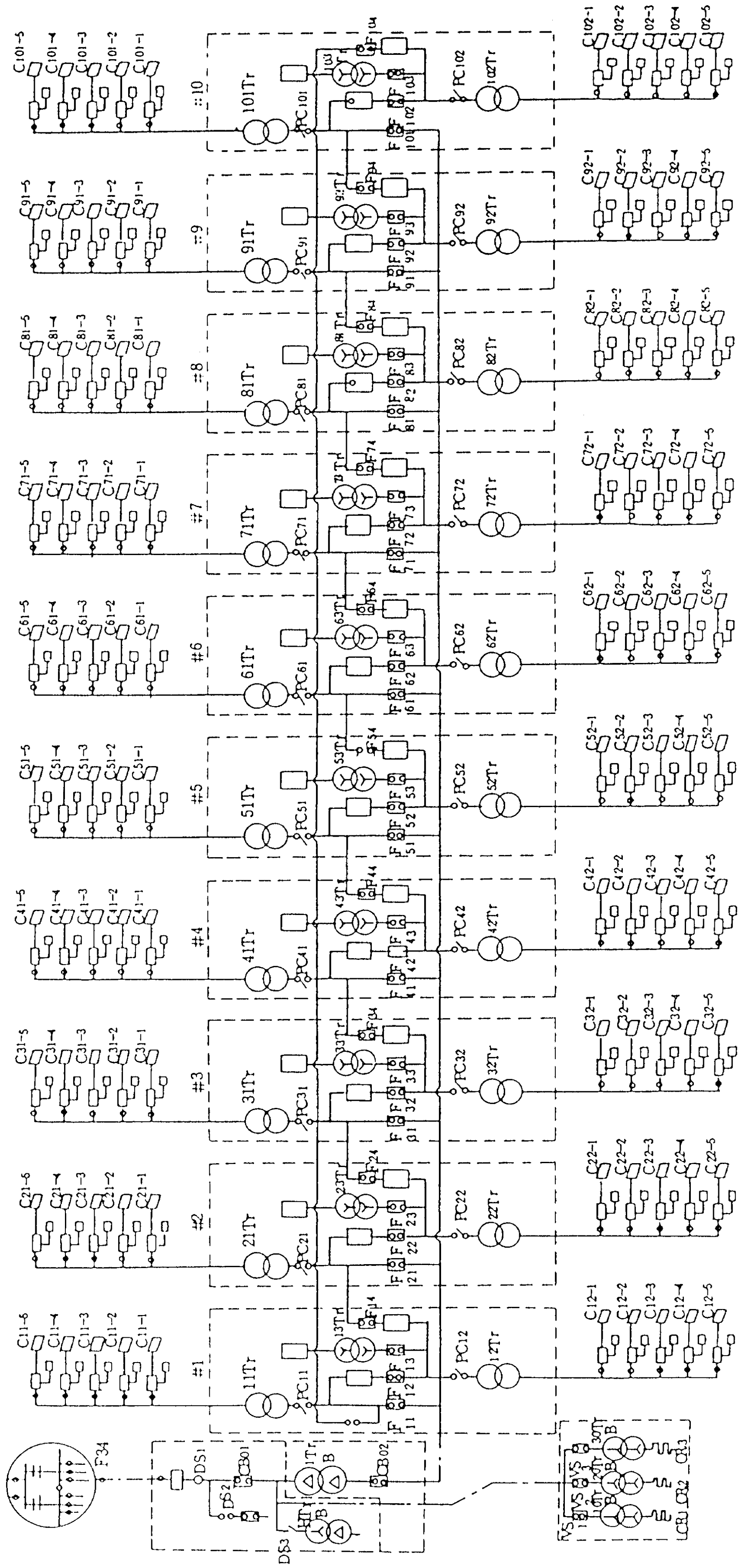

Fig. 2-1 The Electrical Configuration of The Simulated Distribution Lines of Rokko Test Centre for Advanced Energy Systems
(a) Line 1

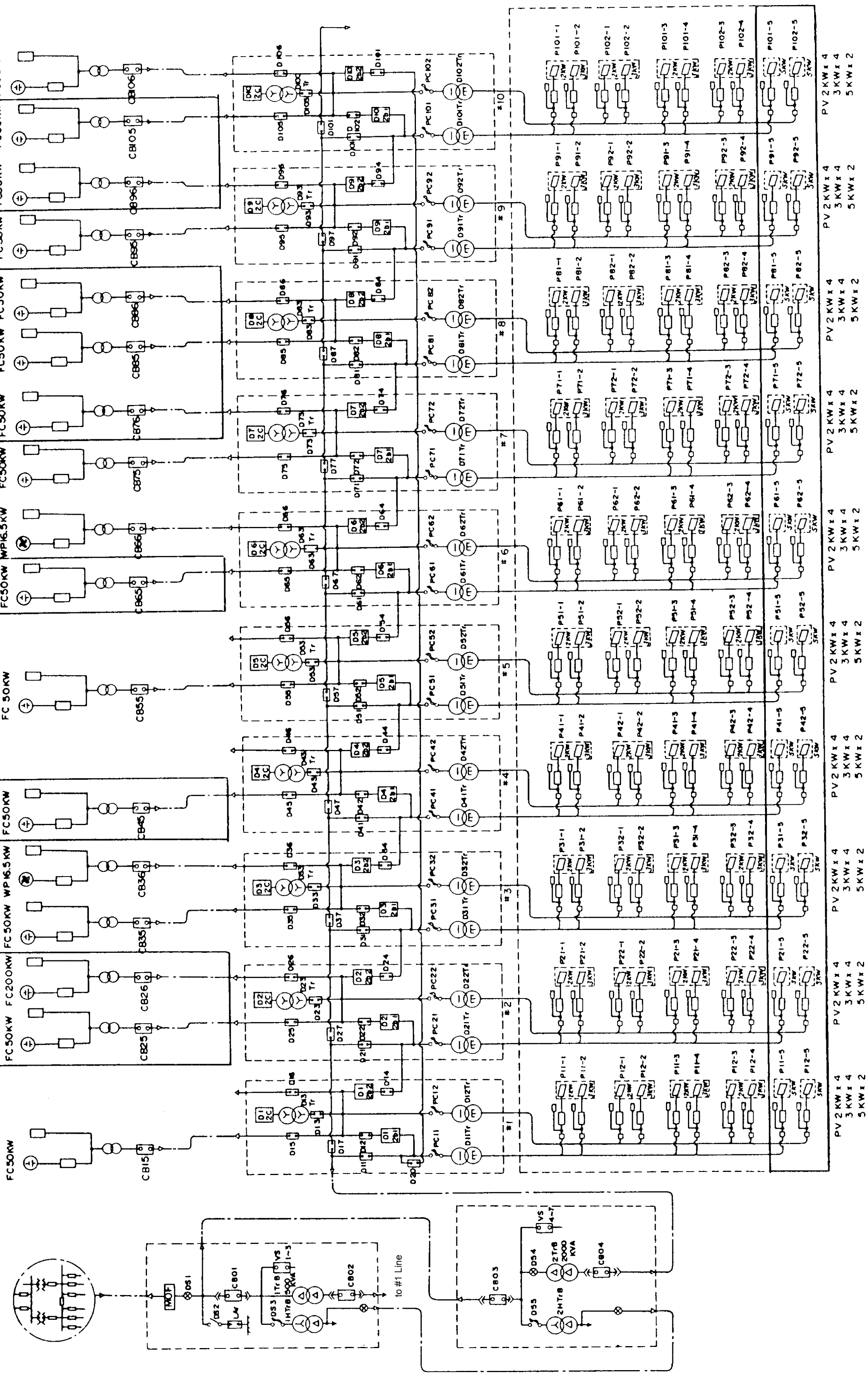

Fig. 2-1(b) Line 2

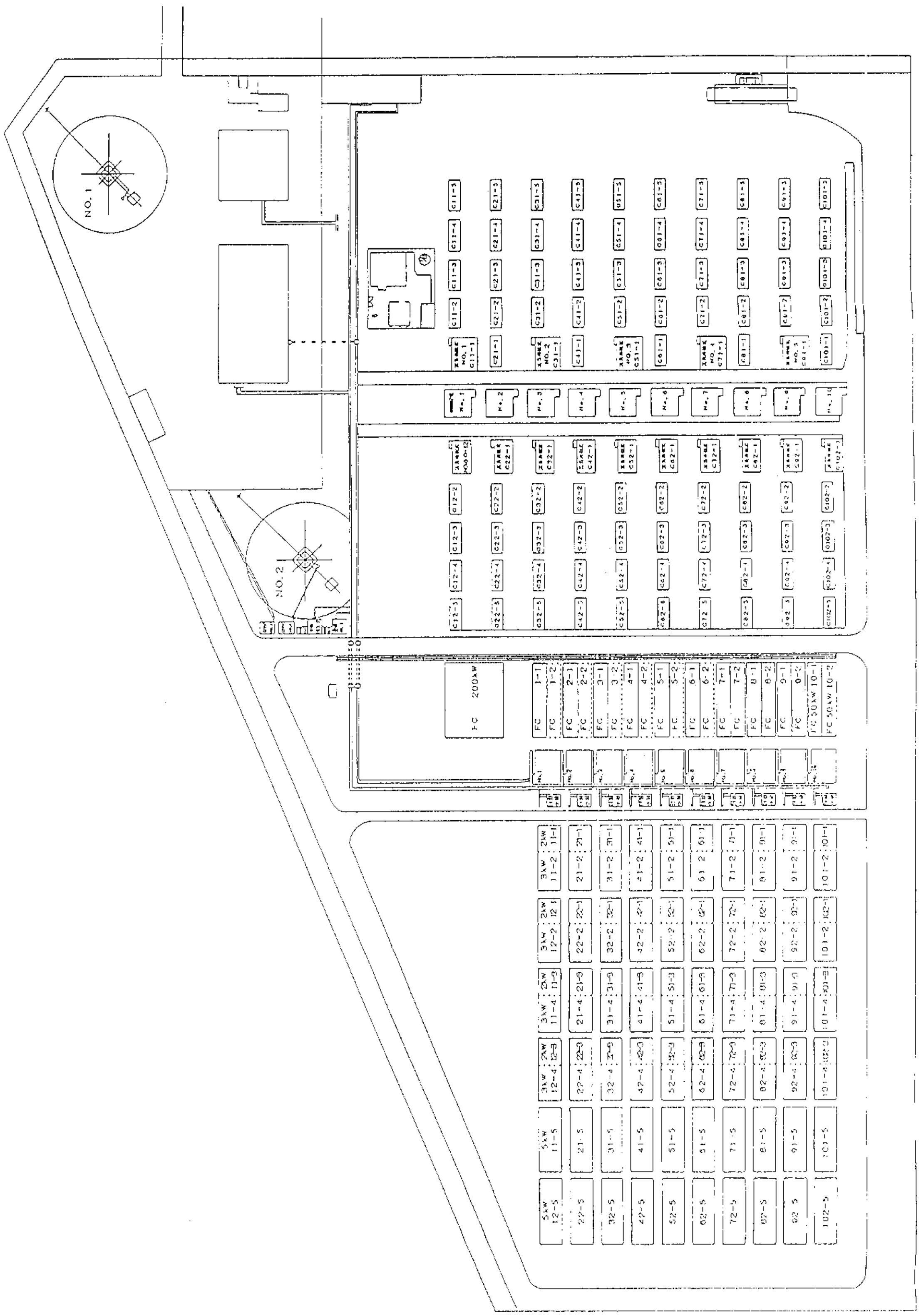

Fig. 2-2 Installation Layout of Photovoltaic Power Generation Systems in Rokko Test Centre for Advanced Energy Systems

Table 2-1 Specifications of Rokko Test Centre for Advanced Energy System

	#1 Simulated Distribution Line	#2 Simulated Distribution Line
Power Receiving Facility	Receiving Voltage: 6.6 kV (3 phase, 60 Hz) Capacity: 500kVA Short Circuit Capacity: 12.5kA Protection Relay: 67G, 51, 27, 59, 95, 85R	Receiving Voltage: 6.6 kV (3 phase, 60 Hz) Capacity: 2000kVA Short Circuit Capacity: 12.5kA Protection Relay: 67G, 51, 27, 59, 95, 85R
Simulated 6.6kV Distribution Line	Number of Blocks: 10 (1km/block) Inductance: 0.1-0.5 mH × 20 Capacitance: 0.3 μF × 4 (for simulating cable)	Number of Blocks: 10 (1km/block) Inductance: 0.1-0.3-0.5 mH × 20 Capacitance: 0.3 μF × 4 (for simulating cable)
Simulated 6.6 kV Load	Capacity: 20kVA (3 phase, 60 Hz) Power Factor: 0.85-1.0 Number of Loads: 10	R-L Capacity: 46kVA (3 phase, 60 Hz) Capacitor: 20 kVA Power Factor: 0.85-1.0 Number of Loads: 10 each for R-L and Capacitor
Low Voltage Distribution Line	Pole Transformer Capacity: 30 kVA (single phase, 3 wire, 210/105 V) × 20 Number of Feeders per Transformer: 5	Pole Transformer Capacity: 20 kVA (single phase, 3 wire, 210/105 V) × 20 Number of Feeders per Transformer: 5
Low Voltage Load	Capacity: 2 kVA (max.) × 100 (Real Load 15, Simulated Load 85)	Capacity: 2 kVA (max.) × 40, 3 kVA (max.) × 40 5 kVA (max.) × 20 (All simulated Load)
PV Array	Output Capacity: 2 kWp × 100	Output Capacity: 2 kWp × 40, 3 kWp × 40 5 kWp × 20
Inverter for PV System	Capacity: 2 kVA × 100 Type: Self-commutated, Voltage Source, Voltage Controlled and Current Controlled PWM Operation Window: AC 101± 10V, 60Hz ± 1.5% Protection Relay: 51, 51G, 27, 59, 95	Capacity: 2 kVA × 40, 3 kVA × 40 (AC 100V, 1 ph) 5 kVA × 20 (AC 200V 1ph) Type: Self-commutated, Voltage Source, Current Controlled PWM Operation Window: AC 101± 10V (AC 202± 20V) 60Hz ± 1.5% Protection Relay: 51, 51G, 27, 59, 95

3. Measurement of Harmonics Distortion Caused by PV Systems

3.1 Background

Grid interconnected photovoltaic power generation systems generate harmonics because they have AC/DC converters and isolation transformers. As the number of grid interconnected photovoltaic power generation systems increase, the total harmonic content of the system may increase when each harmonic from each photovoltaic power generation system superimposes on one another or may decrease when harmonics cancel out one another. It is important to examine the general tendency of the total harmonics when many photovoltaic power generation systems are interconnected.

This section describes the results of measurements for the changes in harmonics when the connected number of photovoltaic power generation systems is increased.

3.2 Experimental Procedure

The relationship between the number of installed photovoltaic power generation systems and harmonic content in the system was investigated by measuring the current harmonic distortion ratio before and after a sequential disconnection of each photovoltaic power generation system. The field tests compared a case where the photovoltaic power generation systems installed are manufactured by the same manufacturer, meaning these systems have the same types of inverter and control, and a case where the systems are manufactured by different manufacturers, meaning these systems have different types of inverter and control.

Four or five 2 kW PV systems were connected to the same phase of the secondary side (single-phase, three wires) of the 30 kVA pole transformer. The test was carried out under a no-load condition to remove the effect of harmonic current from loads. Fig.3-1 shows the measurement test circuit.

The photovoltaic power generation systems were successively (at 1-second intervals) disconnected from the operating state, while the harmonic distortion at each location was measured continuously using a memory recorder. The locations of measurement were the following.

a. Power source side of each inverter. (current)
b. Secondary side of pole transformer. (current)

The current harmonics for individual target inverters were measured in advance.

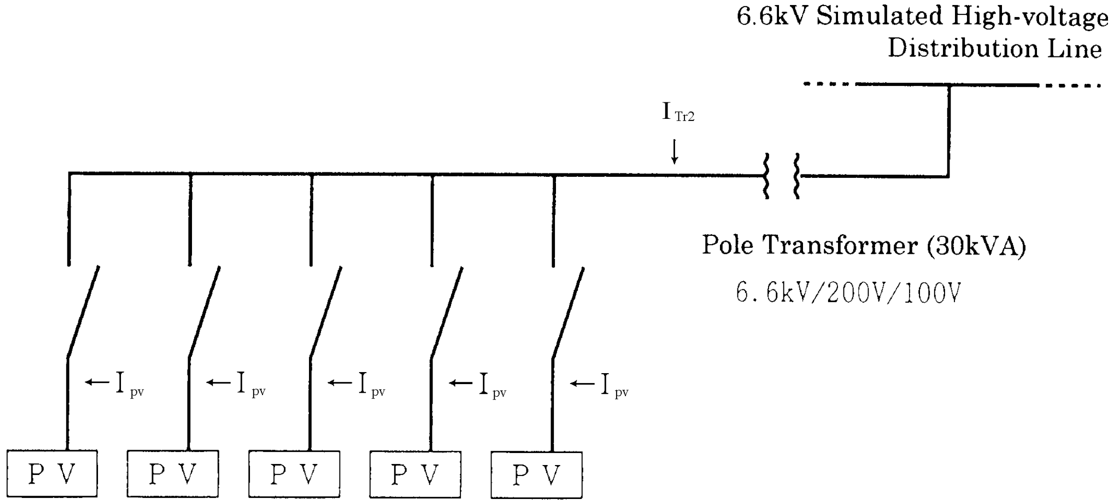

Fig. 3-1 Harmonic distortion test circuit

3.3 Experimental Results

3.3.1 The case of five units manufactured by the same manufacturer

The current harmonic contents for each of five individual inverters manufactured by the same manufacturer were measured first. The results are given in Fig.3-2 through 3-6. The applied inverters are self-commutated voltage controlled, sine wave PWM type, having switching frequency of 20 kHz. They have a harmonic filter of reverse L shape, fo = 1.3 kHz. These figures suggest that the third harmonic and fifth harmonic are predominant, giving 200 to 300 mA.

The state viewed from the ratio (%) to the fundamental current is shown in Figs. 3-7 through 3-11. The third and the fifth harmonics are around 4% ratio. The current harmonic from individual inverters appeared very small except for inverter 81-2.

Table 3-1 and Fig. 3-12 show the changes in harmonics in the case when the above-described same manufacturer’s five inverters were connected to the grid at first, and then the connected number of inverters was successively reduced. The table and figure show that the third harmonic and the fifth harmonic increased with the increase in connected number of inverters. The abrupt increase in harmonics when four units were connected was caused by the generation of large harmonics from the fourth inverter (81-2) as described above. On the other hand, for the seventh and higher harmonics, very little change in total harmonics was observed even when the number of connected inverters was changed.

3.3.2 The case of four units manufactured by different manufacturers

Similar measurements were made for a total of four inverters (two of the voltage controlled type and two of the current controlled type) each made by different manufacturers. Figures 3-13 through 3-16 show the measured data of harmonic current, and Figs. 3-17 through 3-20 show the ratio (%) to the fundamental current for each inverter. These figures indicate that harmonic current less than the fifth is dominant for these inverters, similar to the inverters described in

Section 3.3.1. The current controlled type inverter (51-2 and 51-5), especially inverter 51-2, produces less harmonic current than the voltage controlled type inverter (51-3 and 51-4), while harmonic current from current controlled type inverter 51-5 varies with time.

Table 3-2 and Fig. 3-21 show the changes in harmonic current in the case when the above-described different manufacturers' inverters were connected together to the system and then the connected number of inverters was successively reduced. The first inverter and the fourth inverter among the connected inverters in Fig. 3-21 are current controlled type inverters, and the second and third inverters are voltage controlled type inverters. As seen in Fig. 3-21, the third and fifth harmonics increase as the connected number of units is increased, though the rate of increase differs depending on the individual characteristics of the inverters, similar to the case of Fig. 3-12. Because the voltage controlled type inverters and the current controlled type inverters generate different amount and phase of each order of harmonic current, the rate of increase is not necessarily proportional to the increase in the number of connected units.

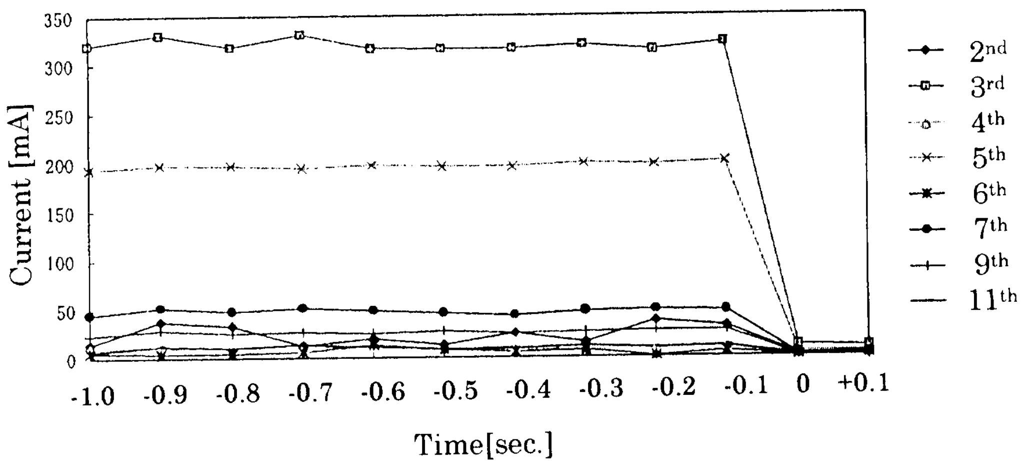

Fig. 3-2 Current harmonics (INV. 81-1: Secondary side of transformer)

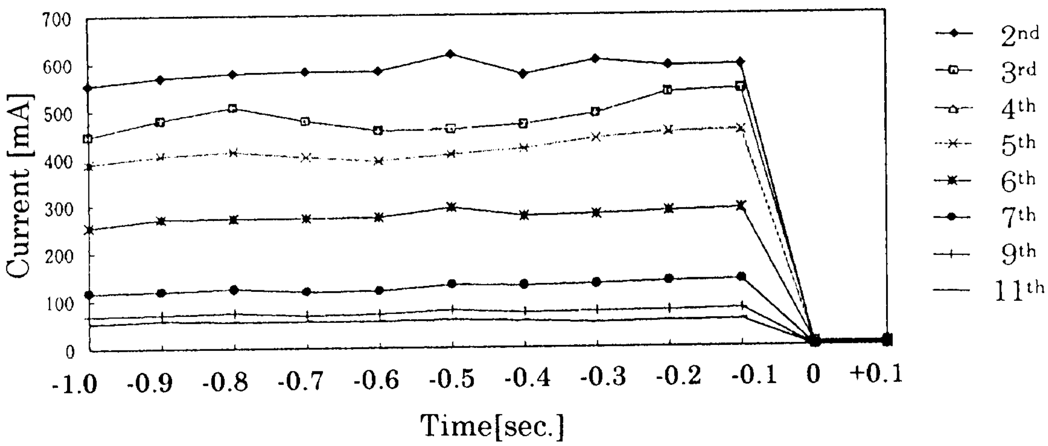

Fig. 3-3 Current harmonics (INV. 81-2: Secondary side of transformer)

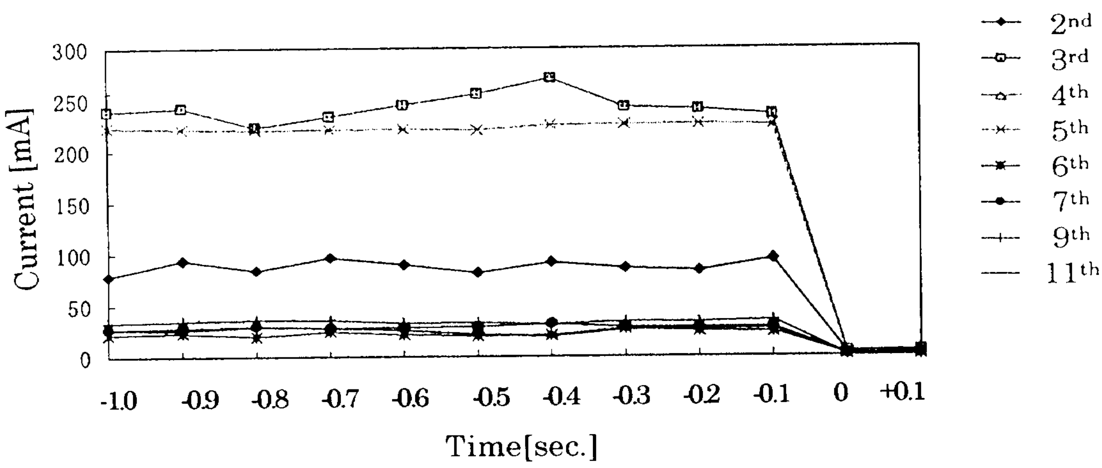

Fig. 3-4 Current harmonics (INV. 81-3: Secondary side of transformer)

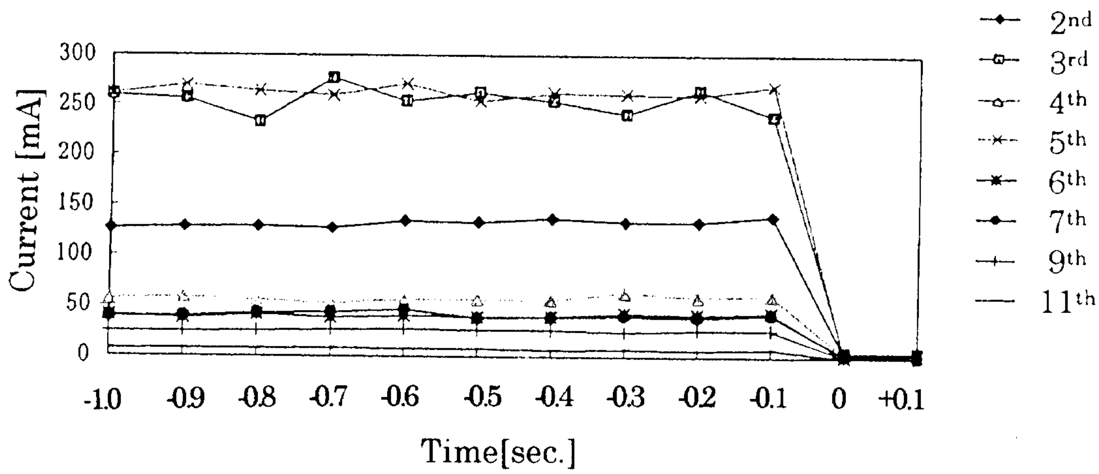

Fig. 3-5 Current harmonics (INV. 81-4: Secondary side of transformer)

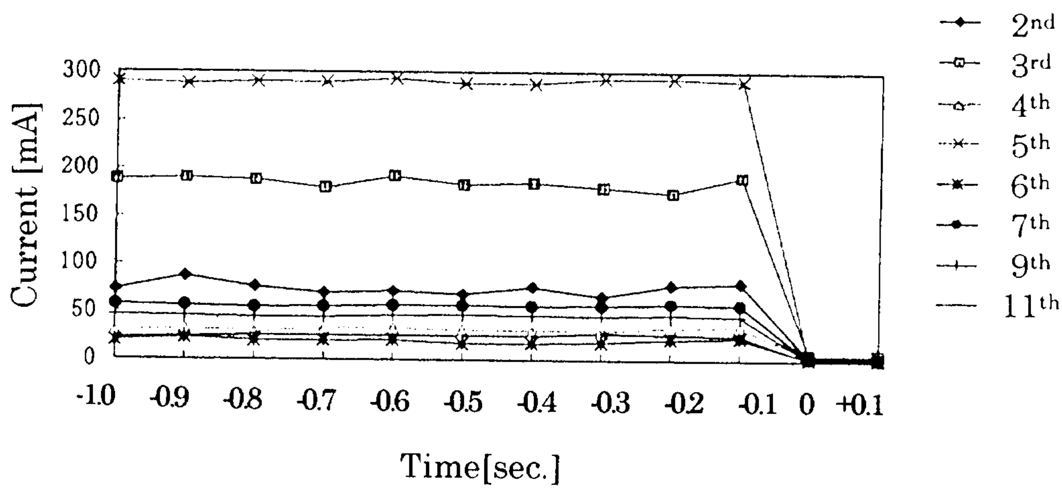

Fig. 3-6 Current harmonics (INV. 81-5: Secondary side of transformer)

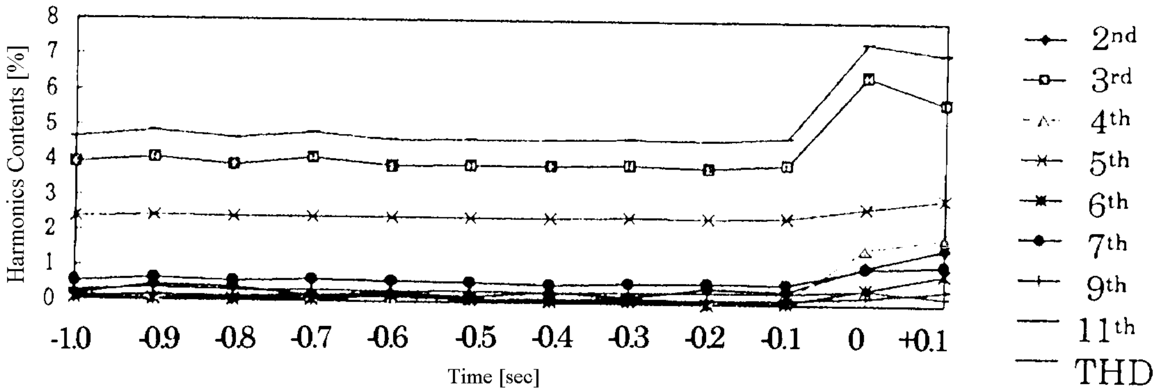

Fig. 3-7 Current harmonic content ratio (INV. 81-1: Secondary side of transformer)

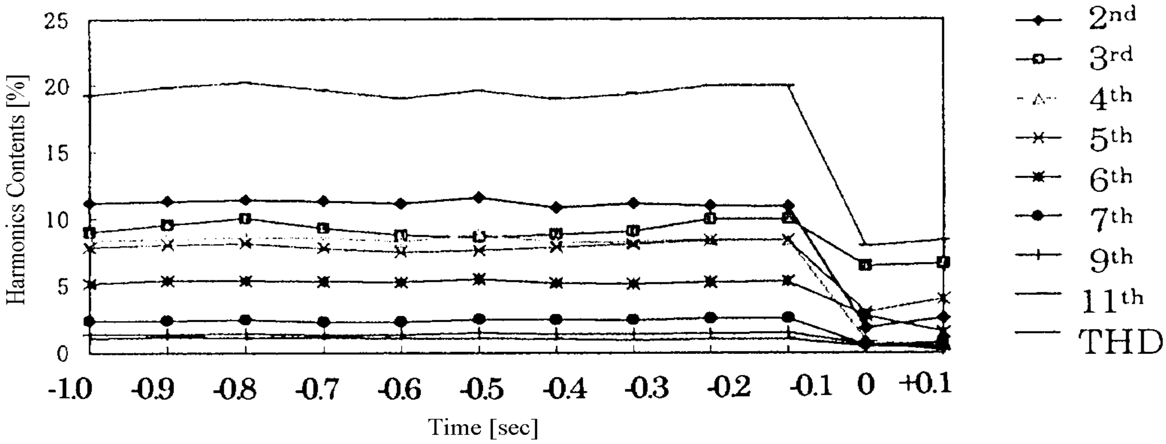

Fig. 3-8 Current harmonic content ratio (INV. 81-2: Secondary side of transformer)

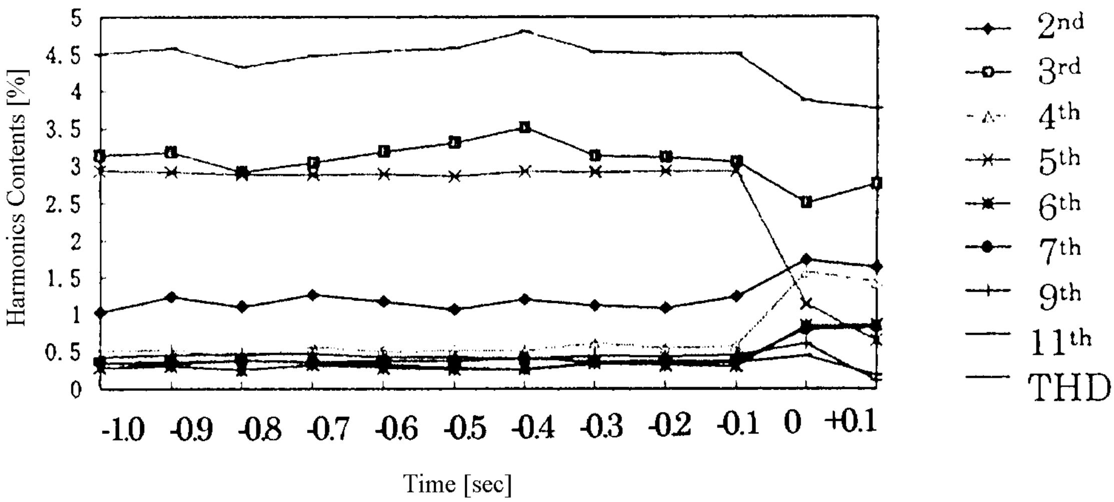

Fig. 3-9 Current harmonic content ratio (INV. 81-3: Secondary side of transformer)

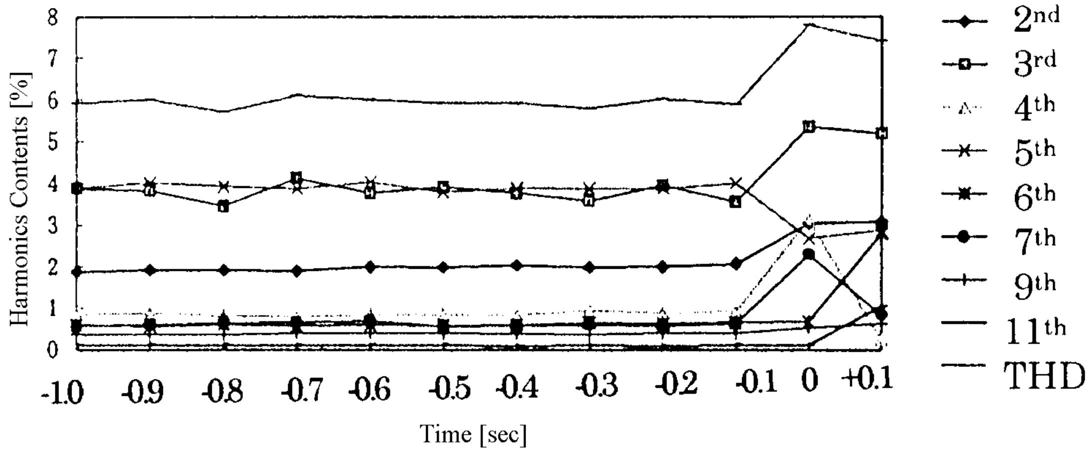

Fig. 3-10 Current harmonic content ratio (INV. 81-4: Secondary side of transformer)

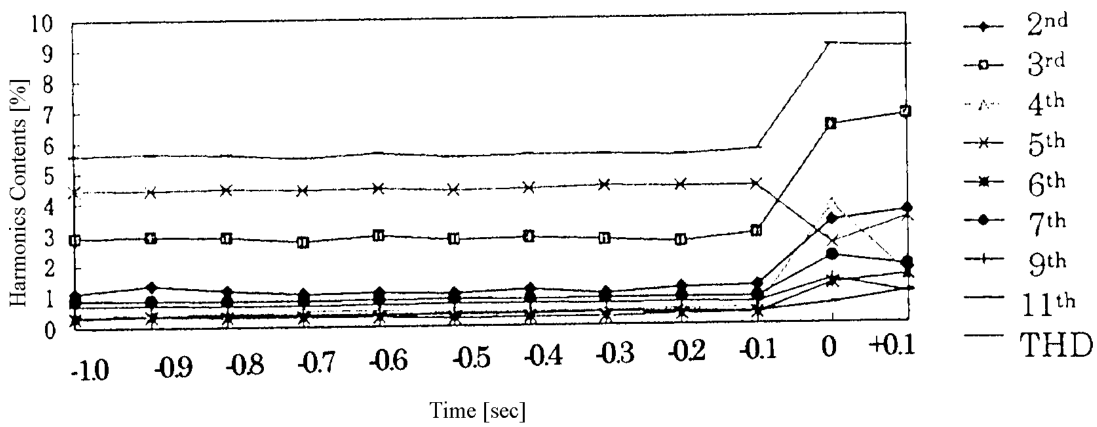

Fig. 3-11 Current harmonic content ratio (INV. 81-5: Secondary side of transformer)

Table 3-1 Change in current harmonics

	No unit connected	1 unit connected	2 units connected	3 units connected	4 units connected	5 units connected
2nd	7.563	125.65	137.84	144.51	546.75	507.78
3rd	8.478	260.95	694.52	892.84	1458.3	1737.9
4th	3.392	75.794	96.632	34.091	420.73	448.04
5th	3.007	302.14	581.51	740.18	1263.8	1392.1
6th	1.9	55.046	63.344	24.56	253.31	258.35
7th	3.594	67.913	143.7	147.22	321.64	355.47
9th	1.731	40.29	84.44	93.066	173	197.09
11th	0.49	13.394	25.146	7.647	57.58	74.21
- Number of connected inverters made by the same manufacturer is changed - On the secondary side of the pole transformer [mA]						

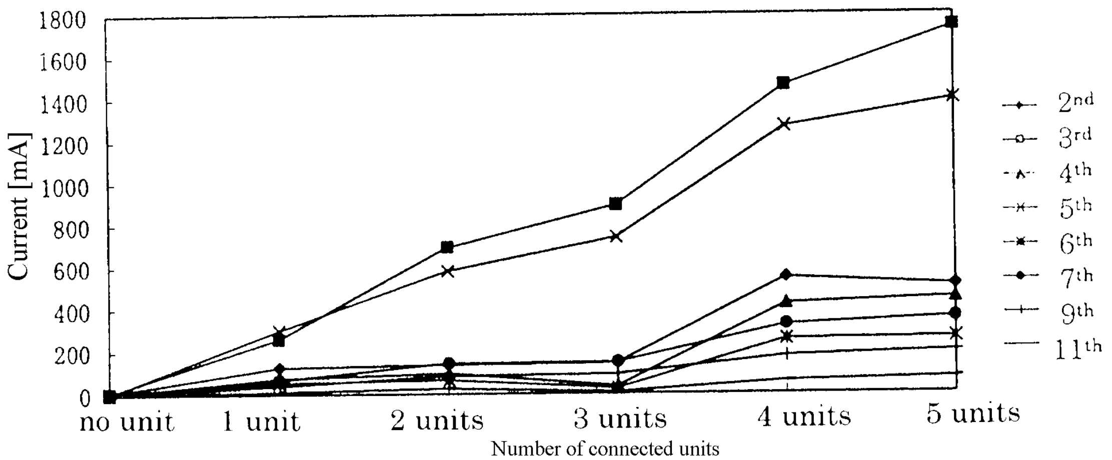

Fig. 3-12 Current harmonics for each number of connected inverter units

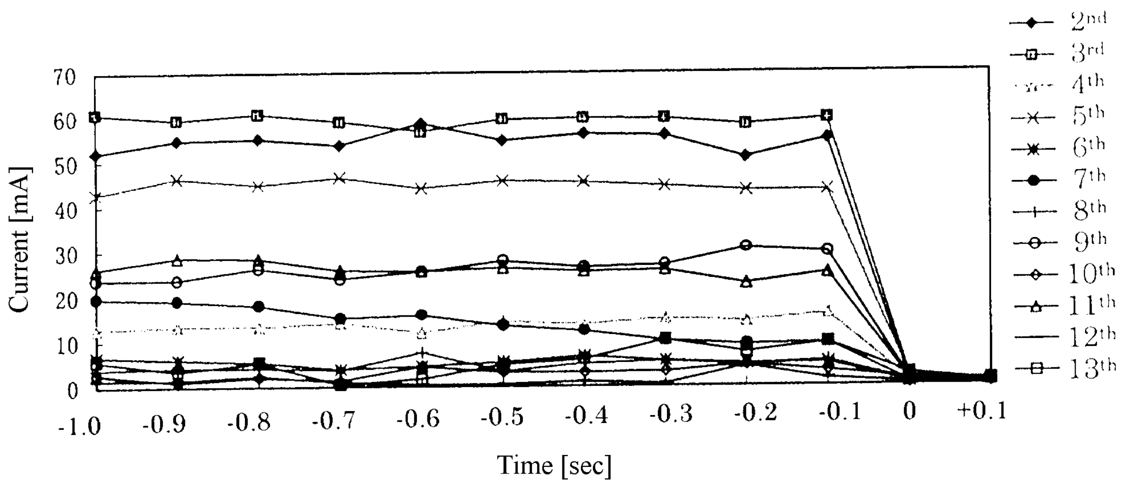

Fig. 3-13 Current harmonics (INV. 51-2: Secondary side of transformer)

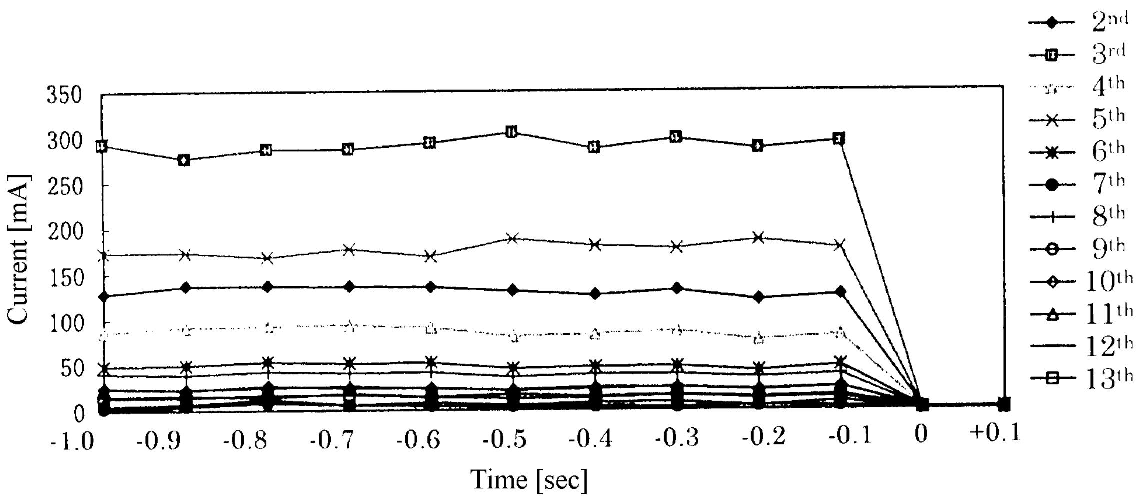

Fig. 3-14 Current harmonics (INV. 51-3: Secondary side of transformer)

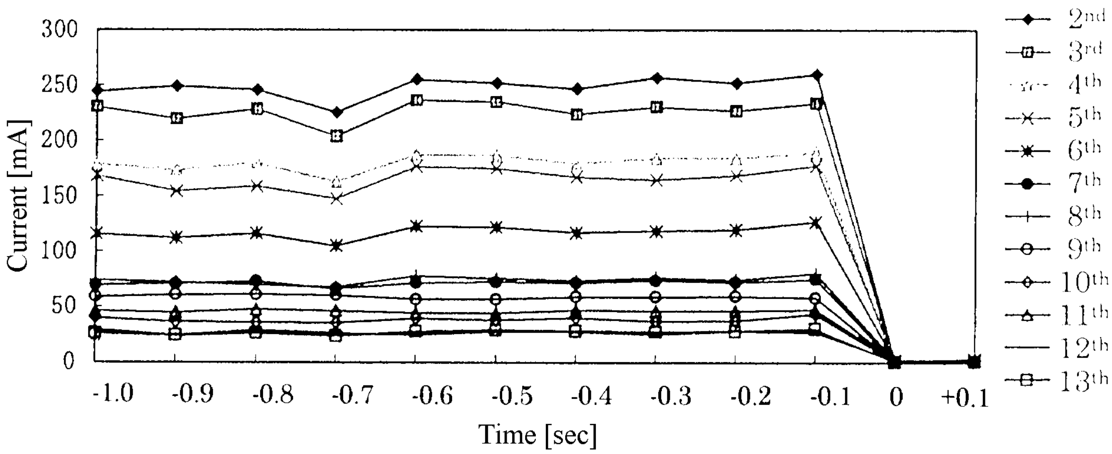

Fig. 3-15 Current harmonics (INV. 51-4: Secondary side of transformer)

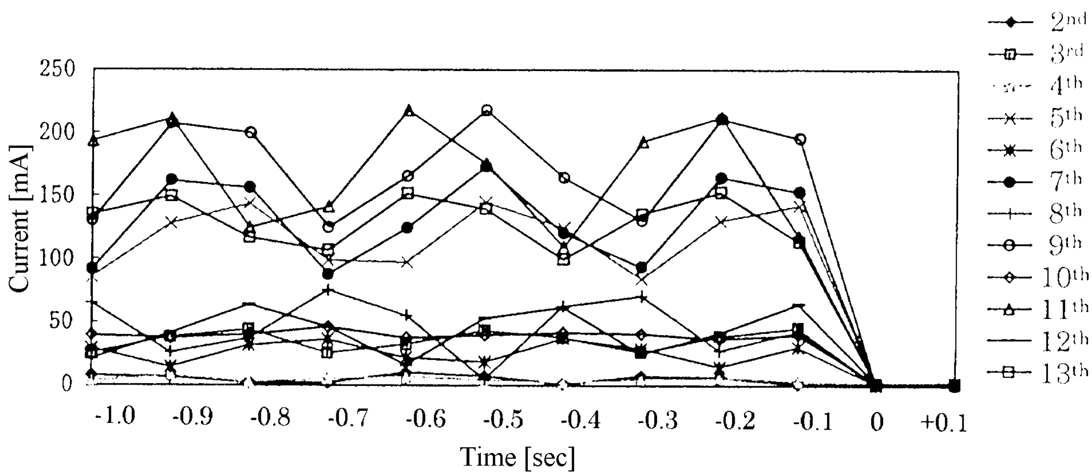

Fig. 3-16 Current harmonics (INV. 51-5: Secondary side of transformer)

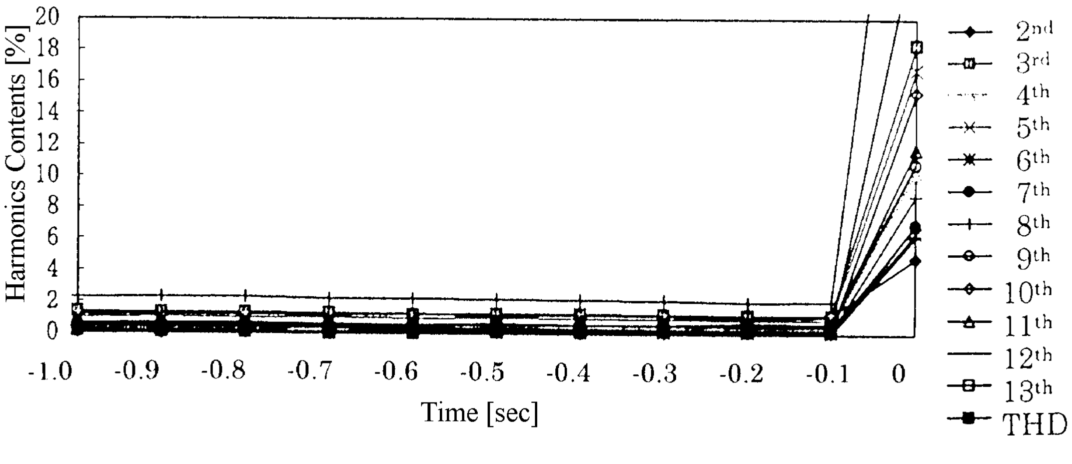

Fig. 3-17 Current harmonic content ratio (INV. 51-2: Secondary side of transformer)

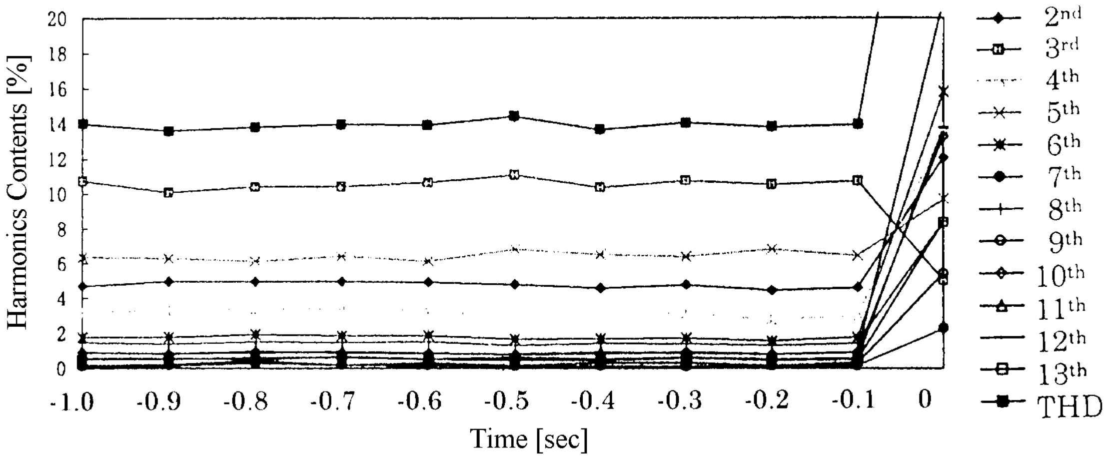

Fig. 3-18 Current harmonic content ratio (INV. 51-3: Secondary side of transformer)

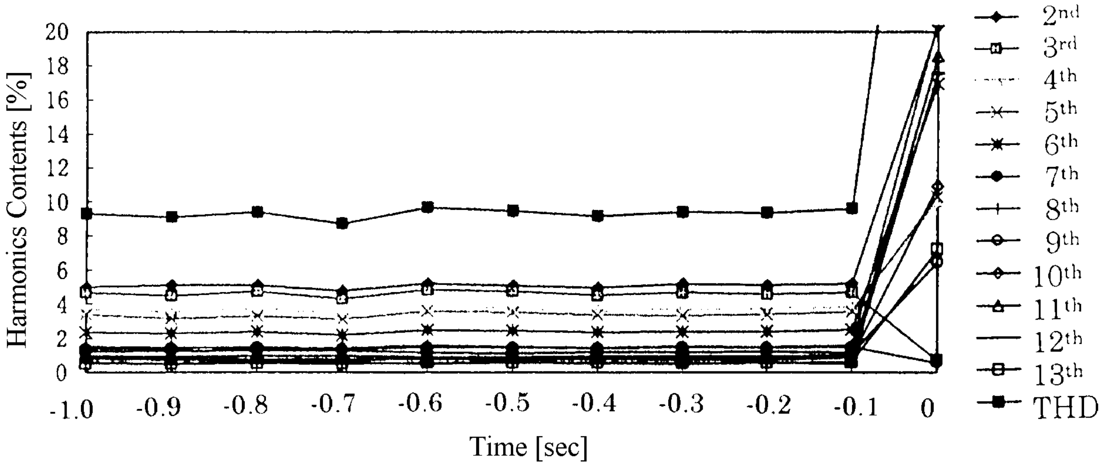

Fig. 3-19 Current harmonic content ratio (INV. 51-4: Secondary side of transformer)

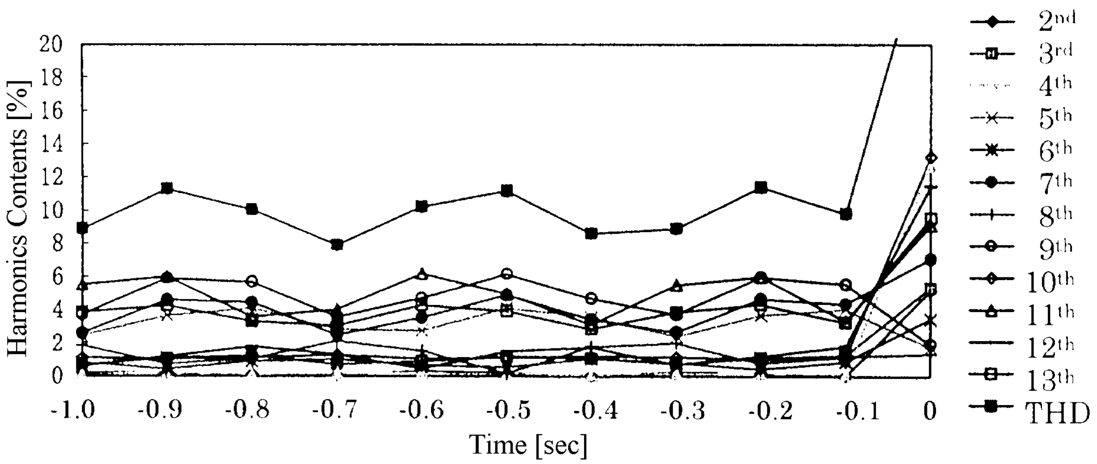

Fig. 3-20 Current harmonic content ratio (INV. 51-5: Secondary side of transformer)

Table 3-2 Change in current harmonics

	No unit connected	1 unit connected	2 units connected	3 units connected	4 units connected
2nd	1.888	4.228	153.3	204	216.5
3rd	1.908	46.16	84.39	531.9	569
4th	1.573	11.15	93.61	165.5	195.3
5th	2.318	192.6	449.4	763	811.6
6th	1.593	55.12	27.96	103.2	114.8
7th	0.2087	227.5	225.7	197.3	285.3
8th	1.991	29.8	19.23	67.24	56.9
9th	1.027	325	258.6	257	156.7
10th	1.07	36.78	27.18	37.35	42.57
11th	0.8194	187.5	243	237	162.3
12th	0.6763	31.49	8.078	47.84	48.9
13th	1.485	82.92	13.69	48.46	96.45
- Number of connected inverters made by the different manufacturer is changed - On the secondary side of the pole transformer [mA]					

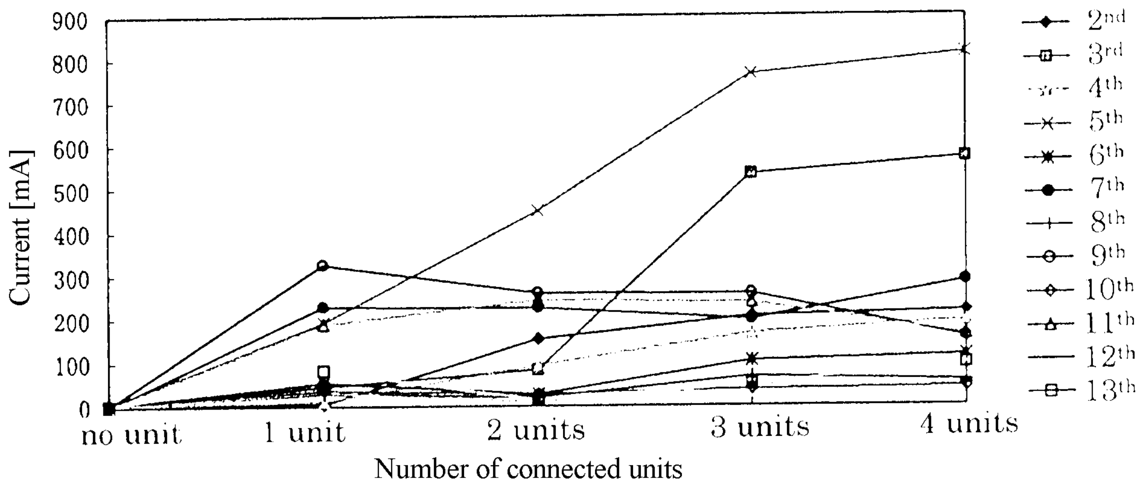

Fig. 3-21 Current harmonics for each number of connected inverter units

3.4 Conclusions

In the case of photovoltaic power generation inverters manufactured by the same manufacturer (i.e. having the same control scheme) being interconnected to the same distribution line, it was found that the third harmonic current and the fifth harmonic current increased almost in proportion to the increase in the number of connected inverter units, although the higher harmonics did not always increase.

Even in the case of photovoltaic power generation inverters manufactured by different manufacturers (i.e. having different control schemes) being interconnected to the same distribution line, it was found that the third harmonic current and the fifth harmonic current increased with the number of connected inverter units and the total harmonic current is almost the sum of each individual harmonic current. However, higher harmonics do not always increase and, in some cases, may decrease (i.e. some cancellation of harmonic current takes place).

From these results, it can be concluded that third and fifth harmonic currents from inverters have almost the same phase displacement and the total harmonic current could be superimposed, while higher harmonics from inverters have different phase displacement even if the same control scheme is employed and total harmonic current could be cancelled. The phenomenon that the third harmonic and the fifth harmonic increase with the number of connected units is considered to be caused by the excitation current of the isolation transformers.

Unfortunately, we have no experimental result for harmonic measurement from transformerless inverters as they were not available at the time of measurements. We hope that measurement for harmonics from transformerless inverters could be conducted in the future.

4. Measurement of Islanding Characteristics

4.1 Background and Objective

Islanding means the phenomenon whereby the power distribution line is opened for some reason and the power supply from the utility company is cut off, but the generators interconnected to the distribution line continue to operate so supply power to the loads connected to the distribution line. If islanding continues, problems such as human safety and equipment maintenance arise. It is therefore important to clarify the conditions under which continued islanding occurs, and verify the necessity of preventing islanding and the effectiveness of the countermeasures.

In this section, the conditions for occurrence of islanding are studied for a power system having a large number of photovoltaic generators interconnected to distribution lines where only conventional voltage/frequency relays are provided. The effectiveness of the islanding prevention countermeasures is verified and reported.

4.2 Islanding Condition

The inverters of photovoltaic power generation systems are operated in synchronism with the power system voltage at interconnection points. Under this condition, islanding occurs even when the voltage on the power system side is lost, because the voltage at the interconnection point is maintained as the inverters attempt to continue operation in synchronism with their own voltage output. However, the system voltage and frequency are decreased if the total load on the power system is larger than the output power of the photovoltaic generators, and they are increased if the total load is smaller than generator outputs. Therefore, if relays that detect voltage/frequency anomalies are installed, continuation of islanding can be almost avoided. However, if the total load is almost equal to the photovoltaic power generation output, the deviation of voltage and frequency is small, being within the detecting sensitivity of relays, and islanding may continue. Here, if the number of photovoltaic power generators is small, the probability of the load being equal to generator output is very small, and hence the probability of continuous islanding is also small.

On the other hand, if many photovoltaic power generation systems are connected to the distribution line, the line load may be almost equal to the total output. The occurrence of islanding has been tested under this condition. The test was conducted on distribution line 1 at Rokko Test Centre for Advanced Energy Systems, to which 100 photovoltaic power generation systems (with total output of 200 kWp) were connected. The ratio of distribution line load to total output of photovoltaic power generation was changed, and the duration of islanding was measured. The islanding was created by opening the sending end circuit breaker of high voltage distribution line 1. There were constant impedance loads (resistance loads) having power factor of 1 and one 3-phase induction motor load, 25 kW with power factor of 0.998 by using power factor correcting capacitor. Fifty of the inverters are voltage controlled type, and the other 50 inverters are current controlled type. Inverters are protected by overvoltage relays (+10%), undervoltage relays (-10%), over frequency relays (+1 to 2%) and under frequency relays (-1 to 2%).

The test results are shown in Fig.4-1. This result indicates that the duration of islanding is short when the distribution line load is larger than total photovoltaic generator output, but duration is increased as the load decreases and approaches the generator output, reaching several tens of seconds or more. This test also verified that islanding also continues when the load is smaller than photovoltaic generation output. This phenomenon occurs, when there are many generators, as voltage and frequency deviations occur, some photovoltaic generators having more sensitive relays drop off, thereby leaving the output power of the remaining photovoltaic generators almost equal to the load. Then the voltage/frequency deviation of the surviving system becomes small and islanding continues. This tendency is enhanced when induction motor load is present.

The test results indicated that the probability of occurrence of islanding is higher when a large number of photovoltaic power generation systems are interconnected. For this reason, some device for detecting islanding is required, in addition to conventional voltage/frequency protection, in order to prevent islanding.

Various islanding detection schemes have been proposed, which are classified into passive schemes and active schemes. In a passive scheme, a higher sensitivity detection is realised by monitoring not only the absolute values of voltage and frequency, but also their rates of change and phase deviation. In the active scheme, disturbance is intentionally introduced via an inverter control function or outside attachment to forcibly deviate voltage and/or frequency to provide detection even if load is at near equilibrium with generator output. A passive system has the advantage of giving no extra disturbance to the power system and enabling short detection time, but an insensitive zone remains in principle. On the other hand, the active system has the disadvantage of providing an extra disturbance to the power system although there is no insensitive zone in this system. Therefore, the combination of a passive scheme and active scheme, which is deemed to be effective when a single photovoltaic power generation system supplies the power to the load, is now being considered.

On the other hand, when many photovoltaic power generation systems are connected to the same distribution line, more than one protection system could interfere with one another even if they are composed of the same scheme. In the following section, the test results on the duration of islanding of a large number of photovoltaic systems, each provided with islanding detection device, are discussed.

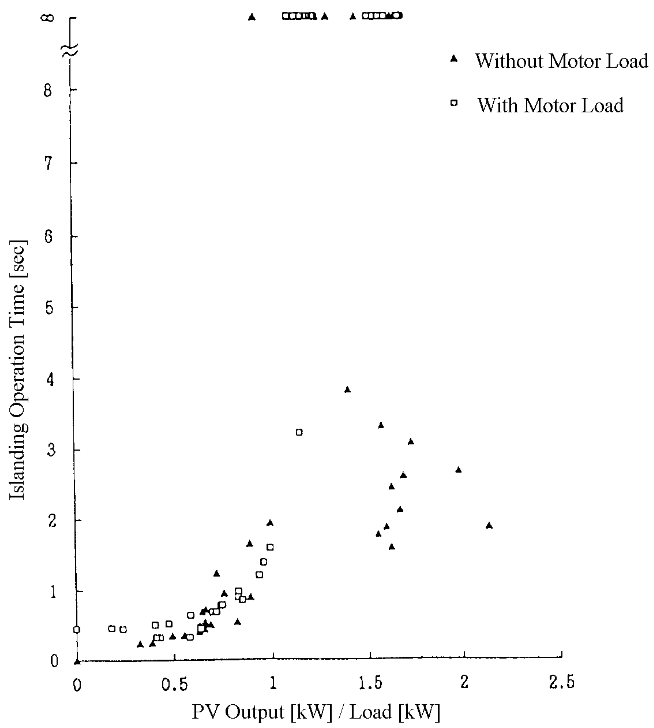

Fig.4-1 Islanding Test Result

4.3 Effect of Islanding Detection

As a method of preventing islanding of photovoltaic power generation systems, inverters manufactured recently in Japan are equipped with both active and passive schemes of islanding detection functions. However, in the case when many inverters are interconnected to one grid, the function of the active scheme may be lowered due to mutual interference. On the other hand, there is an insensitive zone in the passive scheme and there is a possibility that islanding cannot be detected.

To examine the mutual effect between islanding detection functions, in Section 4.3.1, islanding characteristics within high voltage lines were measured for the case that many photovoltaic power generation systems manufactured by different manufacturers having different active and passive scheme islanding detection functions were interconnected to different low voltage distribution lines. In Section 4.3.2, the characteristics of islanding within low voltage distribution lines were measured for the case that some photovoltaic power generation inverters manufactured by one manufacturer and having the same active and passive scheme islanding detection functions were interconnected to one low voltage distribution line.

4.3.1 Islanding within High Voltage Distribution Line

4.3.1.1 Experimental Procedure

With five kinds of commercially available inverters for photovoltaic power generation, having an islanding detection function and each manufactured by different manufacturers, (four kinds supplied from Japanese manufacturers, one kind supplied from a foreign manufacturer), islanding tests were conducted. The main specifications of the inverters are given in Table 4.1.

Table 4-1 Specifications of inverters tested

Manufacturer	A (Japan) (7 units)	B (Japan) (5 units)	C (Japan) (7 units)	D (USA) (6 units)	E (Japan) (9 units)
DC voltage range[V]	160 - 230	160 - 350	0 - 350	180 - 300	120 - 350
Nominal DC voltage[V]	200	200	200	210	200
Nominal AC voltage[V]	200	202	202	120(200)	202
Nominal AC output[kW]	5.0	3.5	4.0	4.0	3.5
DC/AC conversion efficiency [%]	90	93	92	94.5	92
PWM switching frequency [kHz]	15.6	17.0	18.0	12.0	20.0
Passive islanding detection	Frequency fluctuation rate, voltage waveform abnormality	Phase jump	Frequency fluctuation rate	Unknown	Phase jump
Active islanding detection	Reactive power modulation	Frequency shifting	Reactive power modulation	Frequency shifting	Reactive power modulation

34 units of five types of photovoltaic power generation system were connected to a 6.6 kV high voltage distribution line via 100/200 V low voltage distribution lines. Loads with reactance component and resistance component were connected as adjustable loads to the distribution line on both the low voltage and high voltage sides. In addition, a capacitor for improving the power-factor was connected to the high voltage distribution line. Moreover, a rotary machine (induction motor) load was connected as a load having dynamic properties.

The field test circuits are shown in Fig. 4-2. The field tests were conducted for the case that the rotary machine load was not connected to the power system and for the case that the rotary machine load was connected to the power system. Loads of reactance component, resistance component and capacitance component and rotary machine load were adjusted to cancel the active power component and reactive power component of the total output of the photovoltaic power generation system group, respectively. Islanding was realised by opening the delivery circuit breaker of the substation (CB04).

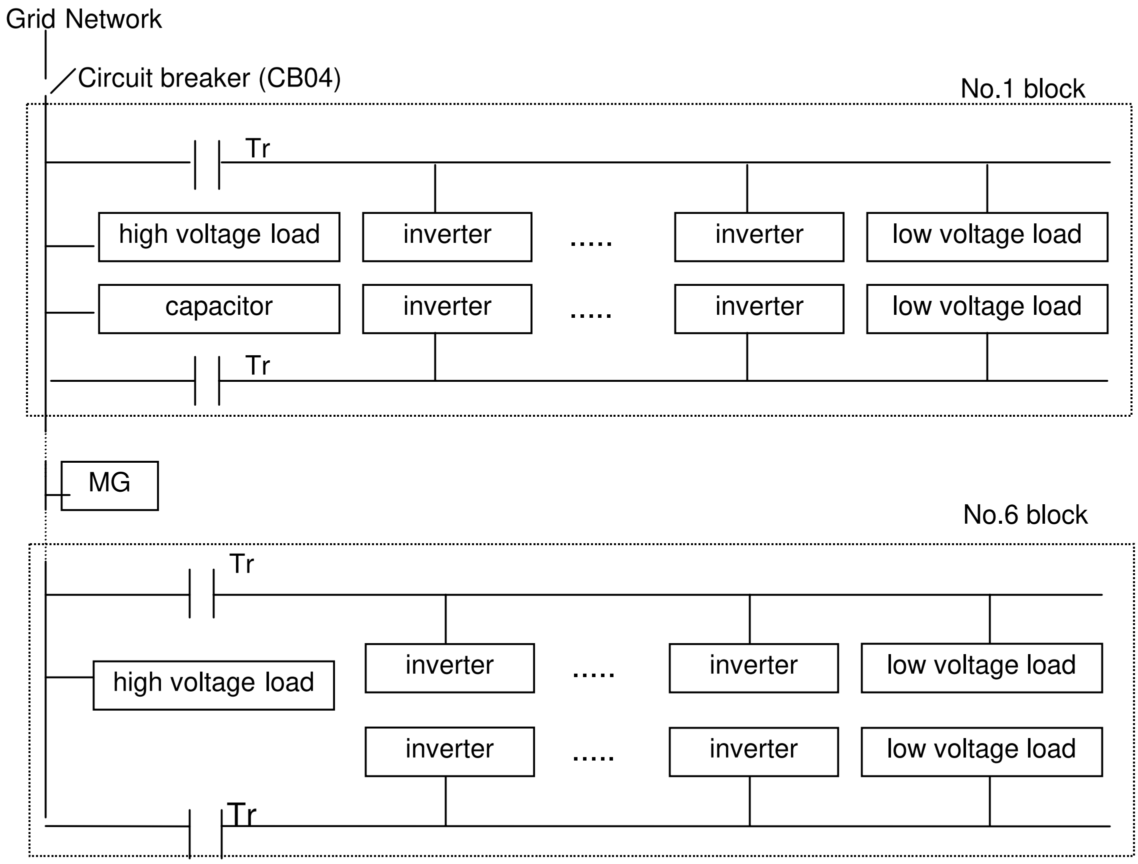

Fig. 4-2 Islanding test circuit

4.3.1.2 Experimental Results

It was confirmed that the islanding phenomenon hardly occurs in multiple photovoltaic power generation systems having active scheme and passive scheme islanding detection functions. The islanding state was detected mainly by the passive scheme, but it could not be confirmed how much the active scheme contributes to the detection of islanding.

1) Islanding test without induction motor load
The test results are shown in Fig. 4-3. It was confirmed that islanding hardly occurs if many photovoltaic power generation systems having various kinds of active and passive scheme islanding detection functions were interconnected to the grid. In this test, the longest duration of islanding was 1.6 seconds. The power flowing at the line breaking point immediately before interruption was an active power of -1 kW and a reactive power of -1 kVar, which was near the

point of balanced power flows, where the positive sign of active power and reactive power indicates power receiving and inductive respectively.

2) Islanding test without induction motor load
The test results are shown in Fig. 4-4. Since the induction motor load helps sustain the voltage after the power line breaker (CB04) is opened, the duration of islanding tends to be longer for all the inverters connected to the line. As a result, we experienced several islanding operations continuing more than one second in the nearly power balanced condition. The longest duration of islanding was 8.15 seconds at an active power flow of 0 kW and a reactive power flow of 4 kVar. The conditions for load were that all the simulated distribution lines were charged, induction motor load was set to 0 kW (no load operation) and the low voltage load was set to 20 kW, and that four high voltage capacitors were connected to the system. Except for one inverter (made by company A) that stopped, all remaining 33 units continued their islanding operation. Finally, the operation was successively stopped in sequential order of units of company A, C, and E, and the units of companies B and D were operated until the final stage. Fig.4-5 and 4-6 show examples of waveforms during the longest continuous islanding before and after the breaker was opened, and before and after the inverters were stopped, respectively. Immediately after the breaker (CB04) was opened, the voltage waveform was sustained with a slight reduction of magnitude, and there was no change in inverter current. Fig.4-6 suggests that the stopping time differs with each inverter. The tests showed that when induction motor load is present, islanding is relatively easily sustained at near the point of balanced power flows, and that islanding can be sustained even if islanding detection schemes are employed.

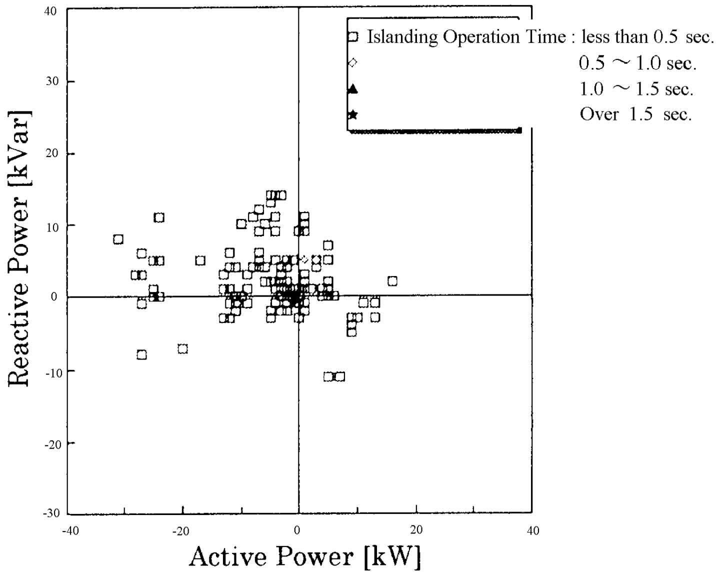

Fig. 4-3 Test result of islanding (without induction motor load)

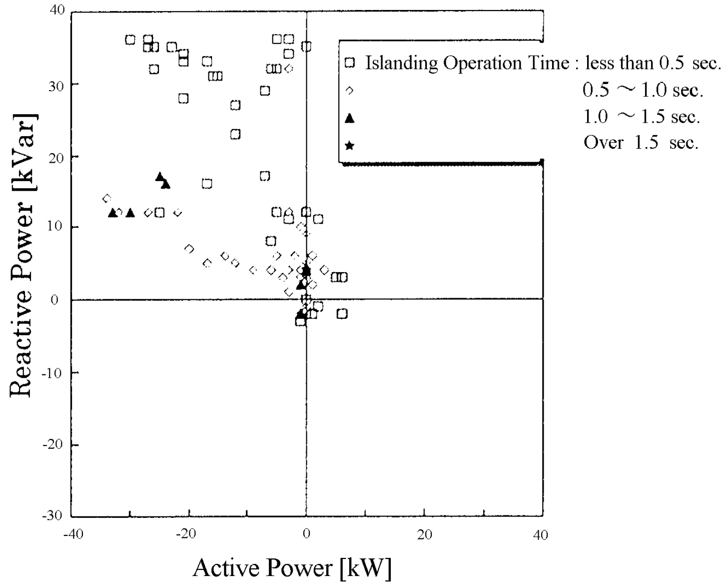

Fig. 4-4 Test result of islanding (with induction motor load)

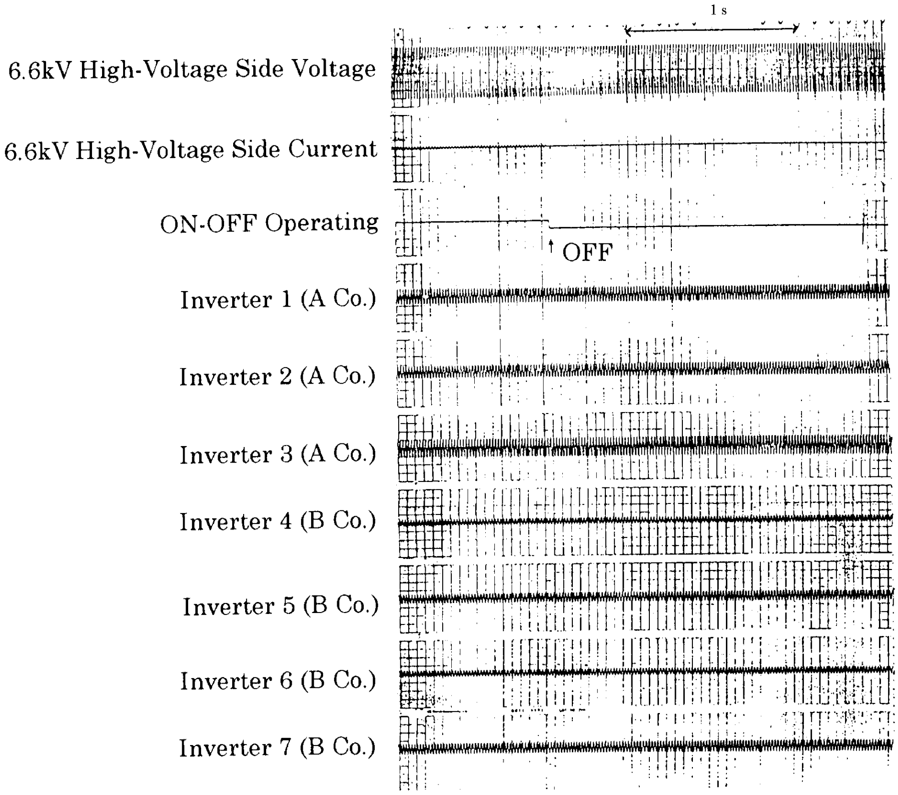

Fig. 4-5 Examples of waveform of islanding test
(before and after the opening of breaker: with induction motor load, 8.15 sec duration)

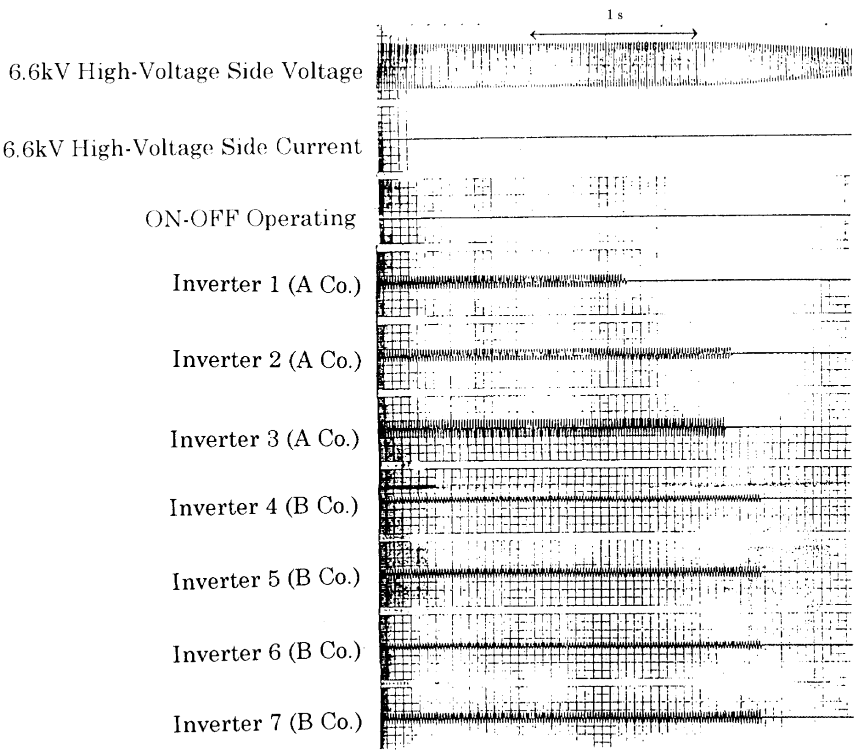

Fig. 4-6 Examples of waveform of islanding test
(before and after the stopping of inverters: with induction motor load, 8.15 sec duration)

4.3.2 Islanding within Low Voltage Distribution Line

4.3.2.1 Experimental Procedure

Islanding duration for multiple photovoltaic generation systems interconnected to one low voltage distribution line was measured. The islanding condition was established by opening the circuit breaker installed on the high voltage side of the pole transformer. Figure 4-7 shows the islanding test circuit. Simulated load, single-phase induction motor, reactor, and capacitor are connected to the low voltage power distribution line. The active and reactive power flowing through the pole transformer can be controlled by adjusting these loads.

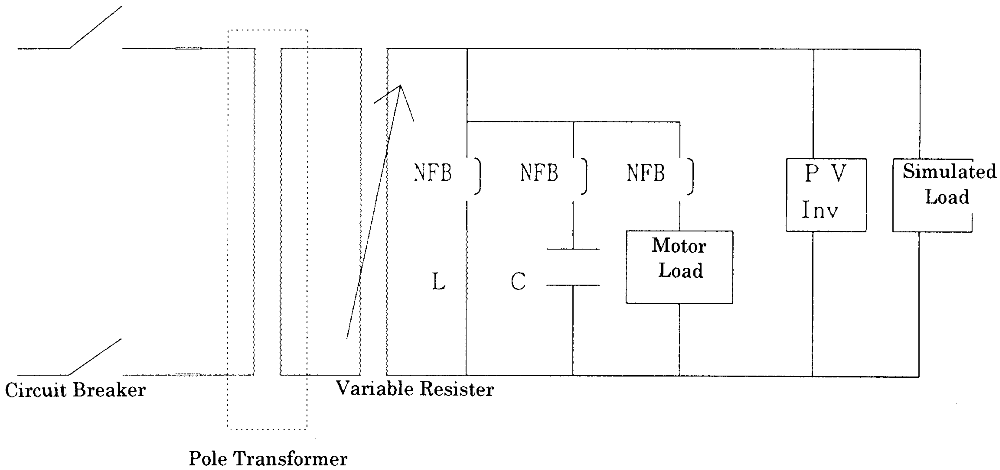

L: 1 - 12 kVA (variable in 1 kVA increments)
C: 0.75 - 9 kVA (variable in 0.75 kVA increments)
Motor load: 1 kW single-phase induction motor (with fly wheel)
PV Inv (rated): 12 - 20 kW (depending on distribution line)
Simulated load (maximum): 10 - 15 kW (depending on distribution line)

Fig. 4-7 Islanding test circuit

Islanding duration was obtained by measuring the voltage waveform and current waveform of the distribution line and output of the inverters. Active and reactive power flows on the low voltage side of the pole transformer were changed as the parameters for test conditions. Experimental tests were conducted mainly for the conditions that both active and reactive power flows are nearly zero.

To examine the effect of interaction for islanding detection schemes between interconnected inverters, tests were conducted for the case that only inverters made by the same manufacturer and having the same scheme of islanding detection were connected to the grid. Also, the tests were conducted for the case that five inverters made by five different manufacturers were connected to the grid. The test cases are listed below.

1) Only inverters made by the same manufacturer are connected to the grid
   a. Inverter made by company A: 3 units connected
   b. Inverter made by company B: 4 units connected
   c. Inverter made by company C: 3 units connected
   d. Inverter made by company D: 3 units connected
   e. Inverter made by company E: 4 units connected

2) Five inverters, each made by a different manufacturer, are connected to the grid
The specifications for the inverters are the same as shown in Table 4.1.

4.3.2.2 Experimental Results

It was found that the passive scheme islanding detection function worked very well, while the effects of the active scheme could not be identified. Moreover, a reduction in the ability to detect islanding for the active scheme was observed in some cases due to interaction between multiple inverters.

1) Only inverters made by the same manufacturer are connected to the grid

a. Inverter made by company A: 3 units connected
As seen in Fig.4-8, even when the output from PV systems and power consumption by loads were nearly balanced for both active and reactive power, the inverters stopped operation within 1 second. Islanding was effectively detected mainly by the passive scheme detection.

b. Inverter made by company B: 4 units connected
In Fig.4-9, the inverters stopped within 0.2 second by the passive scheme islanding detection, even when the output from PV systems and power consumption by loads were almost balanced for both active and reactive power.

c. Inverter made by company C: 3 units connected
In Fig. 4-10, the inverters stopped within 0.7 second at the longest by the passive scheme islanding detection independent of the balance condition of active and reactive powers.
As for these inverters in Fig.4-8 through 4-10, islanding was detected effectively at a relatively early stage.

d. Inverter made by company D: 3 units connected
In Fig.4-11, islanding took a relatively long time to detect in a region where the output power from inverters was slightly less than the loads. These inverters only utilise active scheme islanding detection. Maximum islanding duration was observed in the case of power flow of 0.2 kW, -0.3 kVar (capacitive) and continued for 3.7 seconds.

e. Inverter made by company E: 4 units connected
Fig.4-12 shows a region where islanding detection was disabled and islanding continued. This phenomenon occurred when the reactive power flow was around -0.1 kVar and the inverter active power output was somewhat larger than the load. The longest islanding duration was 4 minutes and 28 seconds under the conditions of -0.4 kW and -0.1 kVar of active and reactive power flows, respectively. Sensitivity of the islanding detection function was set to normal as suggested by the manufacturer of the inverter. Islanding ended only when power balance was lost by sudden shading of the sun. A stable climate might further prolong the islanding time.
Even when the sensitivity of the passive method of islanding detection was maximised and induction motor load which helps sustain the grid voltage after opening of the breaker is eliminated, islanding continued for 56 seconds under the conditions of -0.3 kW and -0.1 kVar of active and reactive power flows, respectively. This result suggests that active islanding detection for inverters cancelled each other out under specific conditions.

These results show that, if inverters having only the same detection scheme against islanding are interconnected in one distribution line, islanding detection may be disabled even for the nearly-balanced state of active power and reactive power under certain circumstances, even when the number of connected units is relatively small.

2) Five inverters, each made by a different manufacturer, are connected to the grid
Fig.4-13 shows the test results. As shown, the islanding state was detected and inverters stopped operation within 0.9 second at the longest, regardless of the balance of active power and reactive power. Accordingly, the test with five inverters, each made by a different manufacturer, detected the islanding relatively quickly.

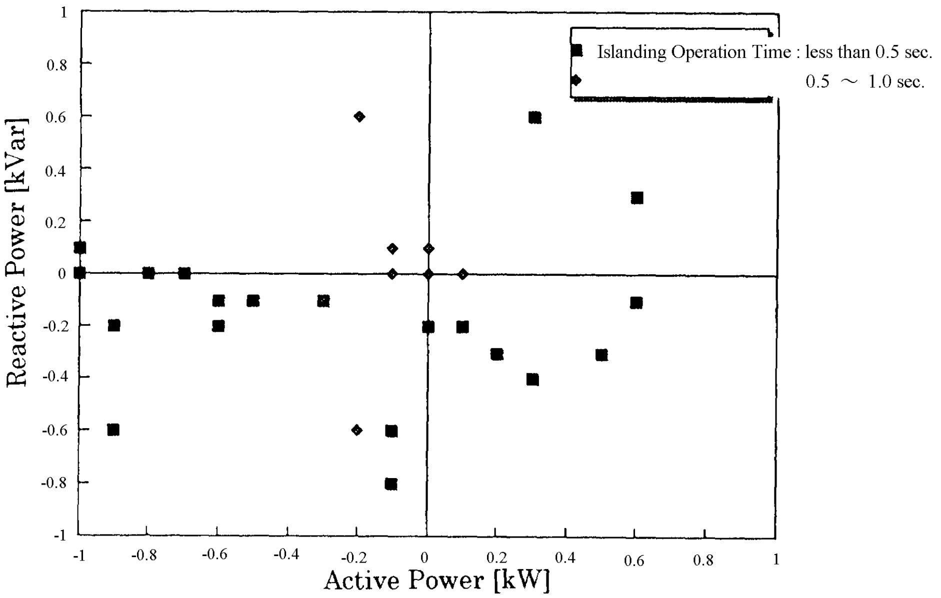

Fig. 4-8 Test result of islanding (with inverters made by company A)

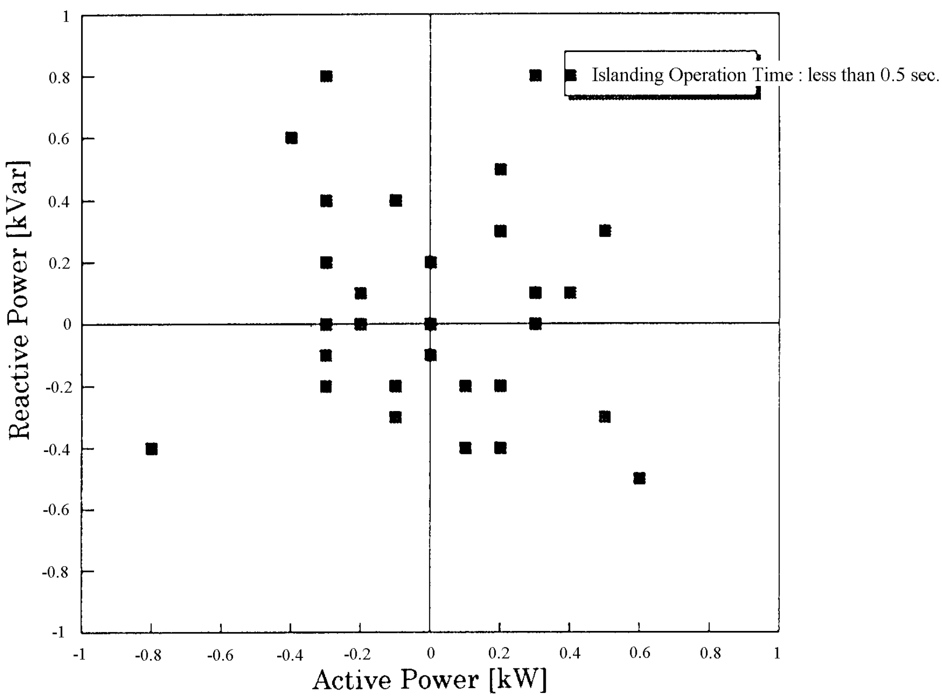

Fig. 4-9 Test result of islanding (with inverters made by company B)

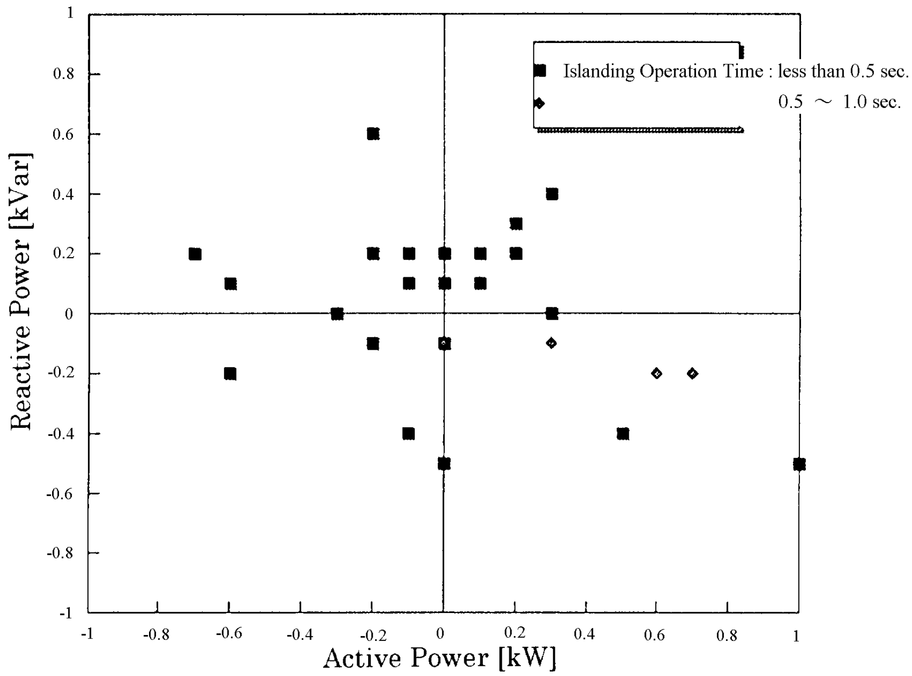

Fig. 4-10 Test result of islanding (with inverters made by company C)

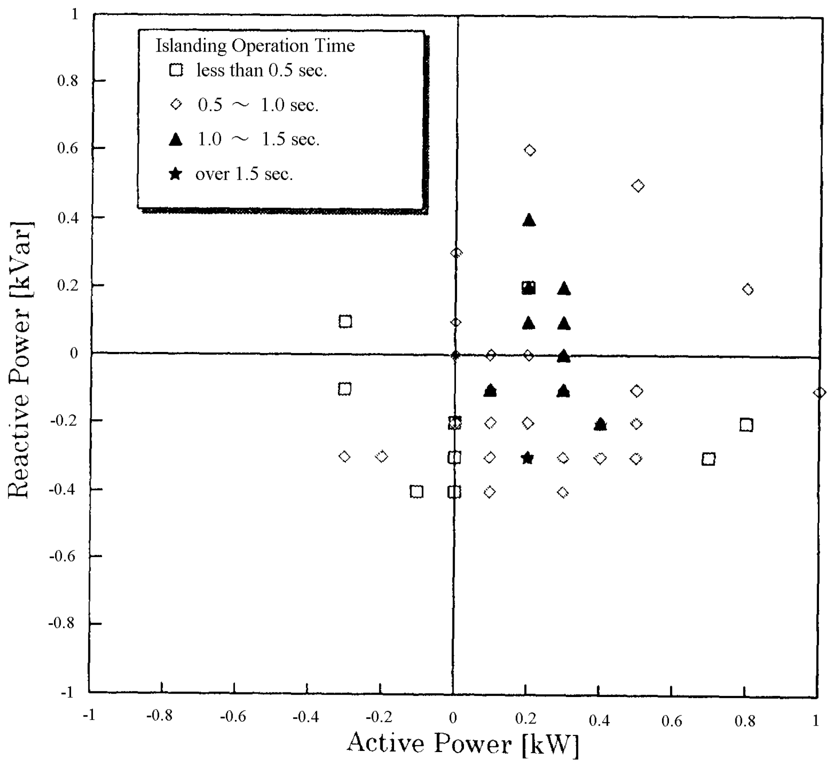

Fig. 4-11 Test result of islanding (with inverters made by company D)

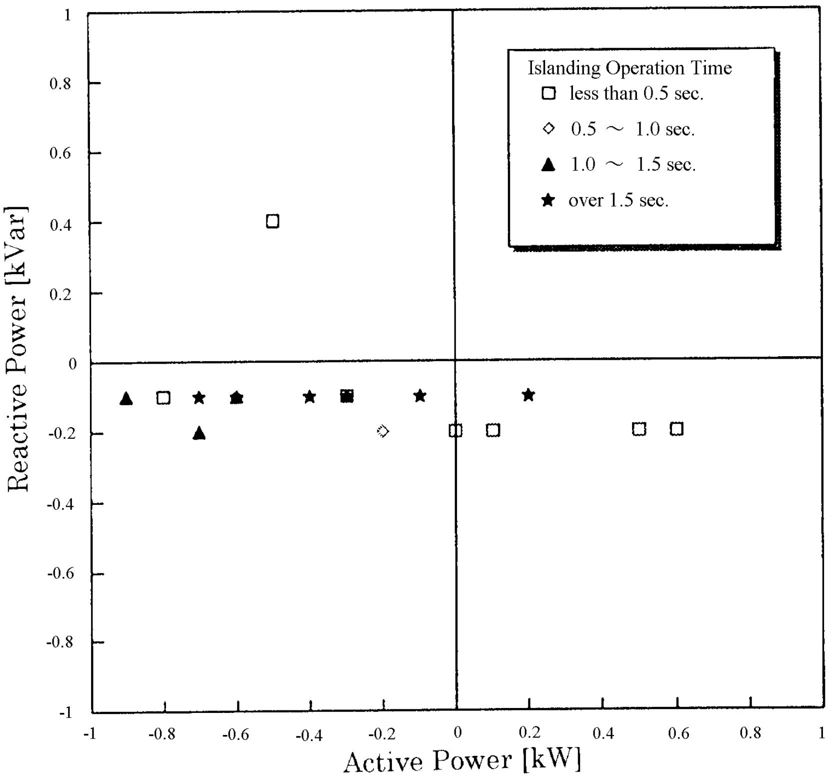

Fig. 4-12 Test result of islanding (with inverters made by company E)

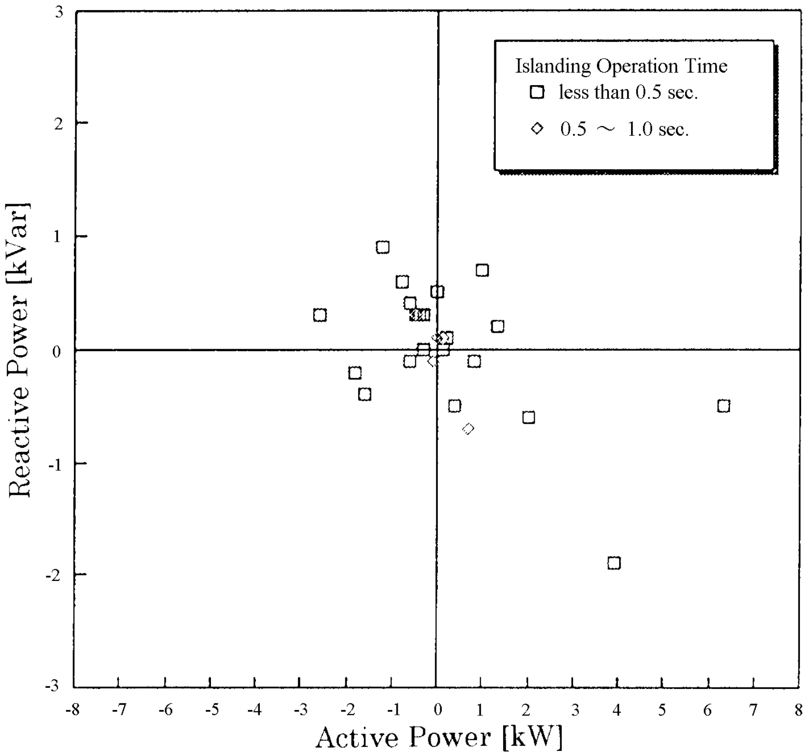

Fig. 4-13 Test result of islanding
(with inverters made by five different manufacturers interconnected)

4.4 Conclusions

The “Islanding” phenomena did not persist for a long period of time if multiple photovoltaic power generation systems having inverters with islanding detection functions are interconnected to the power distribution line. For the case when inverters manufactured by different manufacturers are interconnected (these inverters incorporating different islanding detection schemes) islanding rarely occurs. Even when an inverter having a known insensitive zone in islanding detection is used, other inverters complement the insensitive zone of that inverter and islanding can be prevented extremely effectively. It was confirmed that mainly the passive scheme detected islanding, whilst the contribution of the active islanding detection scheme was not clarified. It was also found that islanding detection time increases when a load that can sustain a distribution line voltage such as an induction motor load is connected.

On the other hand, when multiple photovoltaic power generation systems having inverters of exactly the same type of active islanding detection are interconnected they may interfere with one another and sometimes the detection function does not work effectively. This tendency appears even if islanding detection is confirmed to work effectively when only one inverter is interconnected to the grid.

It should be noted that these results covers only for the specific conditions of grid condition and inverters specifications. In fact, many types of islanding detection schemes, which were not available at the time of test have been proposed. Further examination for different types of grid configurations and inverter combinations will be required.

5. Characteristics under Distribution Line Short Circuit

5.1 Background

It is generally considered that photovoltaic power generators interconnected to the power distribution system do not supply short circuit fault current to the system in case of a short circuit fault on the system side. This is because the short circuit current of a solar call array is 10 to 20% more than the rated maximum output current at most and current controlled type inverters mainly used for photovoltaic generation have a function to limit the output current in case of a disturbance on the distribution system side. However, this operation may work over a relatively long term and some photovoltaic power generation inverters supply a rather large short circuit current in a short period of time (several cycles). If the current control does not work rapidly, current through semiconductor devices in photovoltaic power generation inverters should be limited to protect themselves by interrupting the fault current before it increases. Therefore, it was necessary to verify the effect of the short circuit current in a short period of time on system fault detection.

In this field test, the photovoltaic power generation system is connected to a low voltage distribution line, and measurements of the short circuit current supplied from the photovoltaic power generation system in case of a short circuit fault in the distribution line is described.

5.2 Experimental Procedure

Assuming that the photovoltaic power generation system is connected to a low voltage distribution line, the behaviour of inverters of the photovoltaic power generation system in case of a short circuit fault on the secondary side (200 V side) of the pole transformer is confirmed.

Four kinds of commercially available inverters for photovoltaic power generation (three from Japanese manufacturers and one from a foreign manufacturer), each made by a different manufacturer, were employed for the short circuit test. Table 5-1 shows the major specifications of these inverters. When the photovoltaic power generation system was connected to a low voltage distribution line for each kind of inverter, and when the secondary side of the pole transformer was short circuited, the short circuit current supplied from the inverter and the time between the occurrence of short circuit to stopping of operation were measured. The parameter adopted was the inverter output. Figure 5-1 shows the short circuit test circuit. The short circuit was made by closing the switch directly connected to the short circuit impedance.

Short circuit impedance was determined to cause enough over current to activate over current protection for inverter if the current control of inverter does not work sufficiently.

Table 5-1 Specifications of inverters

Manufacturer	B (Japan)	C (Japan)	D (USA)	E (Japan)
DC voltage range[V]	160 - 350	0 - 350	180 - 300	120 - 350
Nominal DC voltage[V]	200	200	210	200
Nominal AC voltage[V]	202	202	120(200)	202
Nominal AC output[kW]	3.5	4.0	4.0	3.5
AC overvoltage protection[V]	230	230	250	230
AC undervoltage protection[V]	160	160	160	160
AC overcurrent protection[A]	37.1	30	33.4	26.3

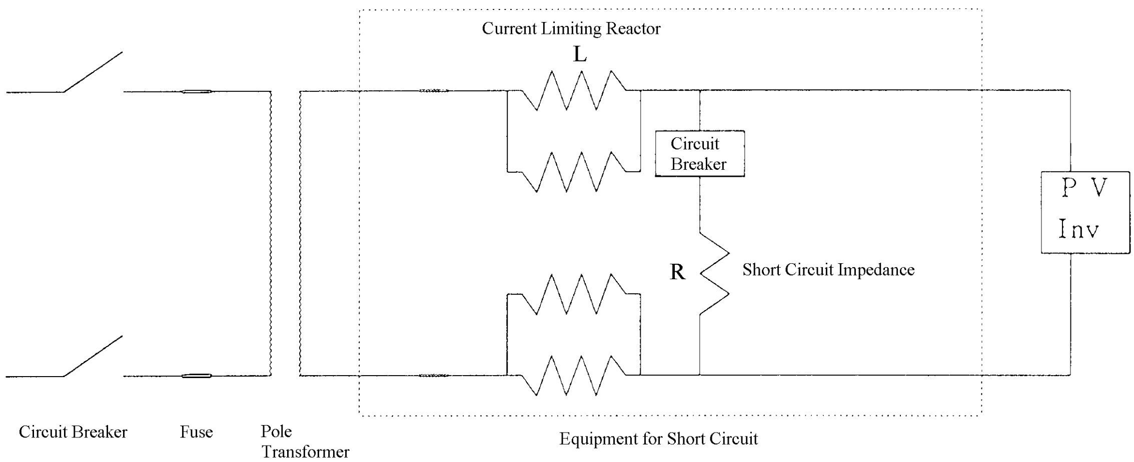

Current-limiting reactor L: 51.35 mH × 4 parallel
Short circuit impedance: 0.5 - 1.9 Ω
PV Inv (rated value): 3.5 kW - 4 kW

Fig. 5-1 Short circuit test circuit

A single inverter was connected to the grid, and the short circuit was made while the inverter was operating. The test was performed for each manufacturer's inverter. In addition, two inverters made by company E were connected to the grid and tested. The tested cases are listed below.

1) Connection of single unit of inverter for photovoltaic power generation
   a. One inverter made by company B is connected.
   b. One inverter made by company C is connected.
   c. One inverter made by company D is connected.
   d. One inverter made by company E is connected.
2) Connection of two inverters for photovoltaic power generation
   a. Two inverters made by company E are connected.

5.3 Experimental Results

In most of the photovoltaic power generation systems, no change in output current was observed before and after the short circuit fault and operation stopped quickly by under voltage protection. It was found that some photovoltaic power generation system inverters supplied about twice the current of that before the short circuit fault for a short period of 1 to 2 cycles.

1) Only one inverter for photovoltaic power generation is connected to the grid
Figures 5-2 through 5-5 show the test results, and Figs. 5-6 through 5-9 show the waveform examples.

a. Test result when one inverter made by company B is connected
As seen in Fig. 5-2, the maximum peak short circuit current does not change compared with the output current before the short circuit, nor change with inverter output. The short circuit resistance at that moment was 1.9 Ω. The inverter waveform in Fig. 5-6 shows that the inverter stopped operation within 1 or 2 cycles after the short circuit. Protection was provided by the undervoltage relay of the inverter.

b. Test result when one inverter made by company C is connected
In Fig. 5-3, with 1.9 Ω short circuit resistance, the maximum peak output current after the short circuit increased by up to 1.7 times and on average 1.3 times compared to the values before the short circuit. Figure 5-7 indicates that the inverter stopped operation within 1 to 2 cycles. The undervoltage relay functioned to stop the inverter.

c. Test result when one inverter made by company D is connected
In Fig. 5-4, the maximum peak output current changed very little after the short circuit. The short circuit resistance was 1.9 Ω. No change in maximum current after the short circuit was observed, regardless of the difference in inverter output. Figure 5-8 shows that the operation stopped within 1 to 2 cycles after the short circuit fault as seen from the output waveform of the inverter. The undervoltage relay functioned to stop the inverter.

d. Test result when one inverter made by company E is connected
In Fig. 5-5, the maximum peak short circuit current was increased to twice the average operating current before the short circuit. Three cases were tested: 0.6, 1.0, and 1.9 Ω short circuit resistance, but no difference was observed in the maximum peak current. Moreover, the trend of twice the maximum value did not change even when the output power at the short circuit varied. As seen in Fig. 5-9, the output waveform of inverters shows that the operation stopped within 1 to 2 cycles after the short circuit fault. The undervoltage relay functioned to stop the inverter.

These test results show that inverters for photovoltaic power generation supply a fault current of only about twice that before the short circuit at most when a short circuit fault occurs in the utility distribution system, and that the time to remove the fault is about 1 to 2 cycles.

2) Two photovoltaic power generation inverters are connected to the grid
(Two inverters made by company E are connected)

Figure 5-10 shows the test results and Fig. 5-11 shows the waveform examples. These figures show that, when two inverters are connected and when the distribution line is short circuited, each inverter generates a peak current that is on average twice that before the short circuit, and the undervoltage relay functions within 1 or 2 cycles to stop the inverter. Therefore, the results for two inverters are similar to those when only one inverter is connected.

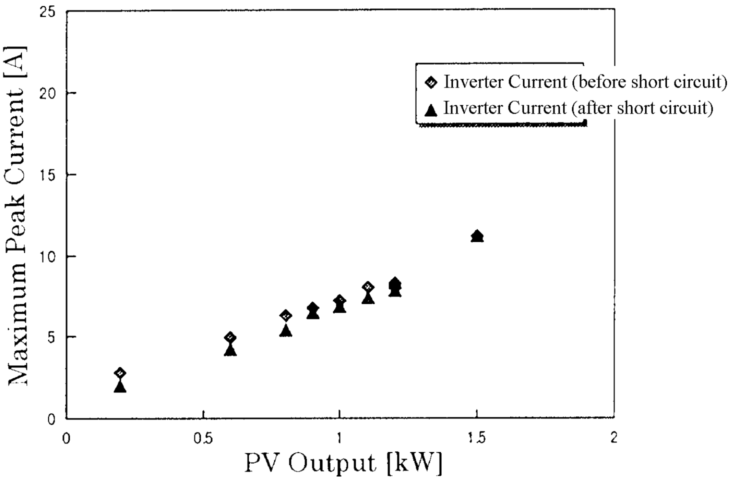

Fig. 5-2 Result of short circuit test (inverter made by company B)

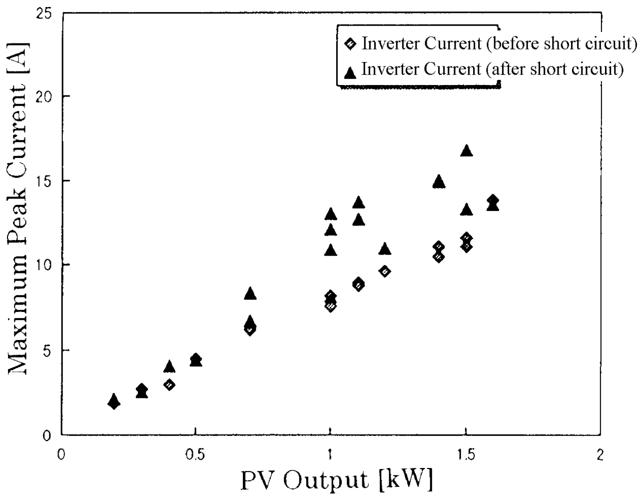

Fig. 5-3 Result of short circuit test (inverter made by company C)

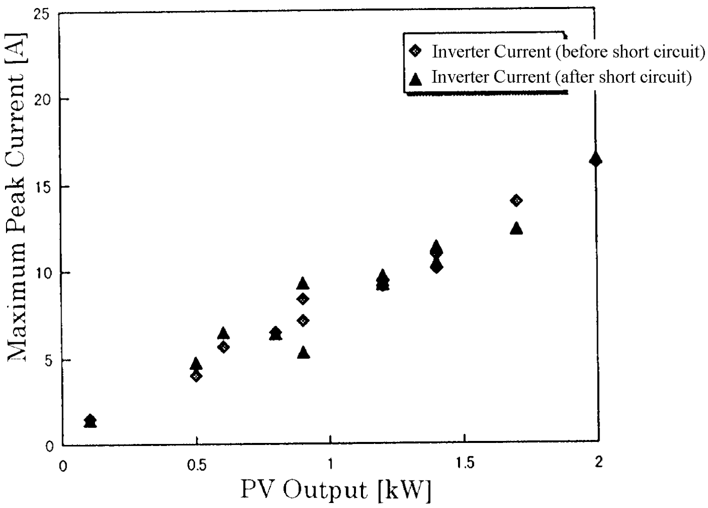

Fig. 5-4 Result of short circuit test (inverter made by company D)

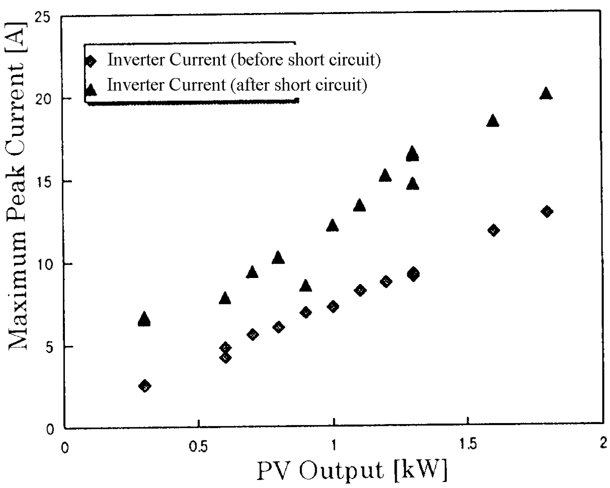

Fig. 5-5 Result of short circuit test (inverter made by company E)

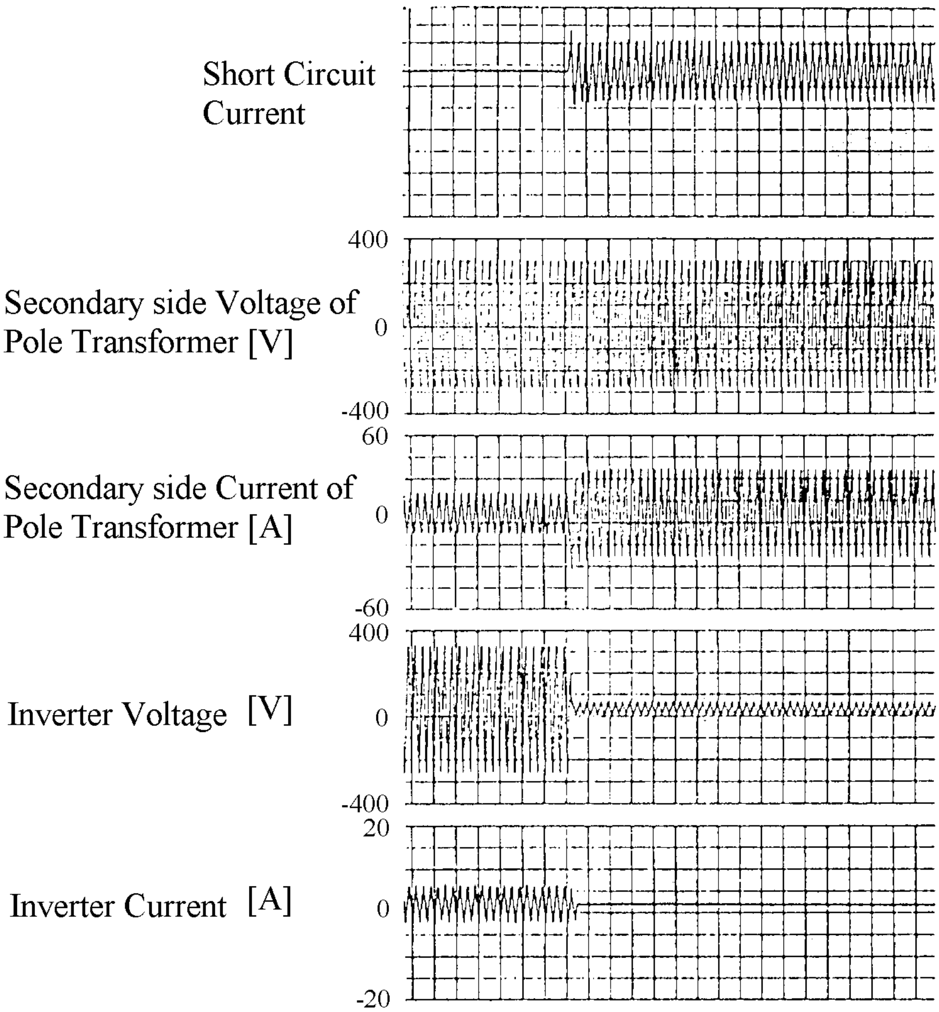

Fig. 5-6 Examples of waveform of short circuit test (inverter made by company B)

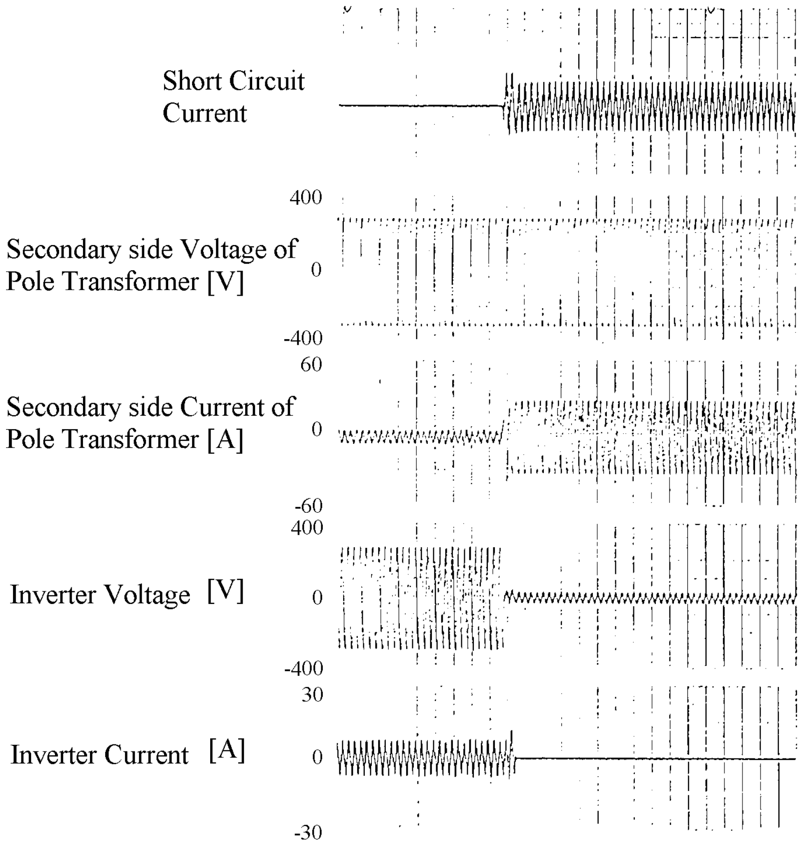

Fig. 5-7 Examples of waveform of short circuit test (inverter made by company C)

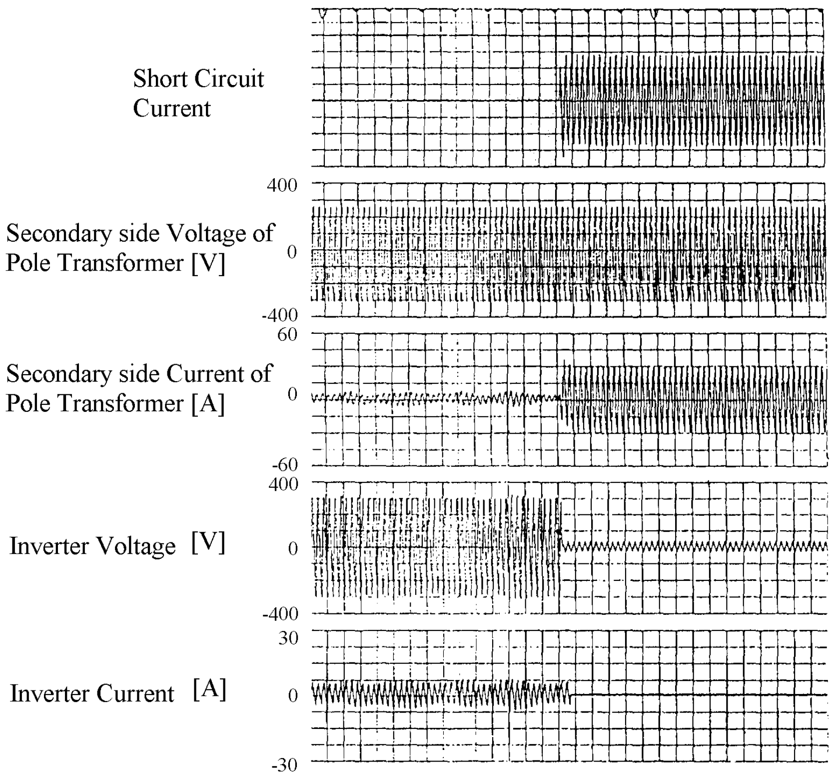

Fig. 5-8 Examples of waveform of short circuit test (inverter made by company D)

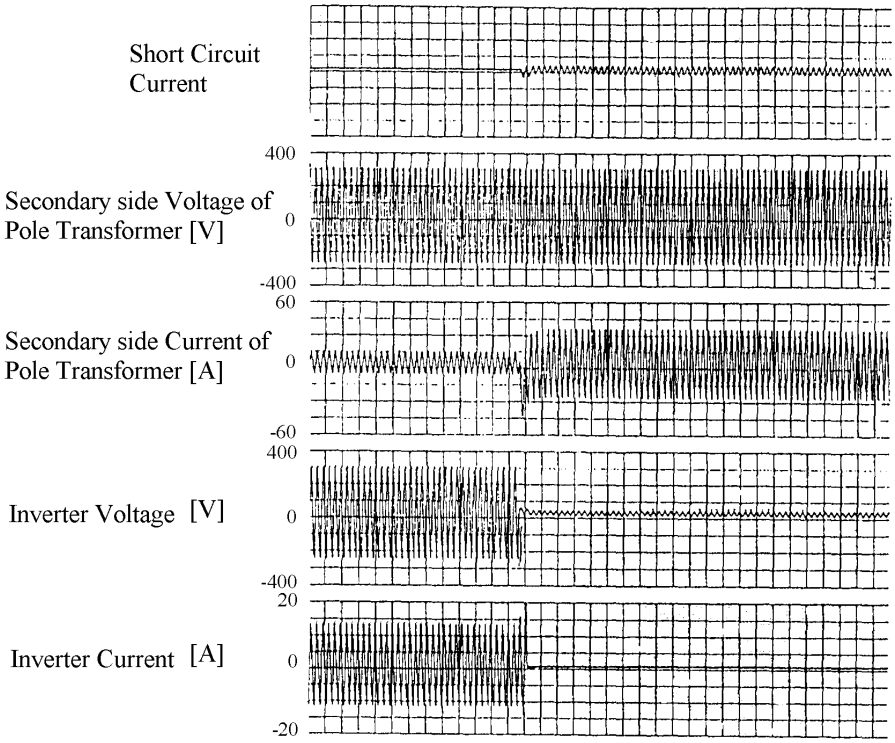

Fig. 5-9 Examples of waveform of short circuit test (inverter made by company E)

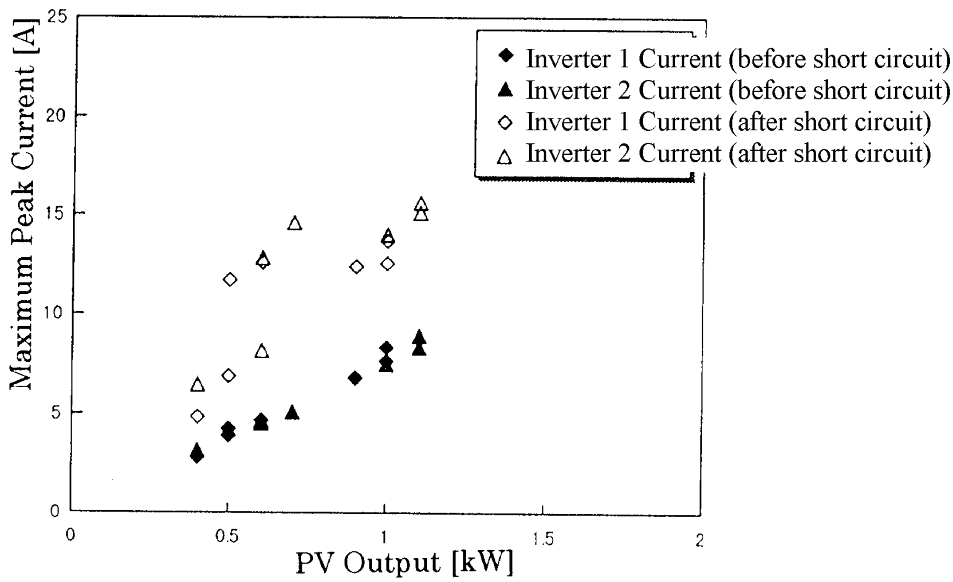

Fig. 5-10 Result of short circuit test (two inverters made by company E)

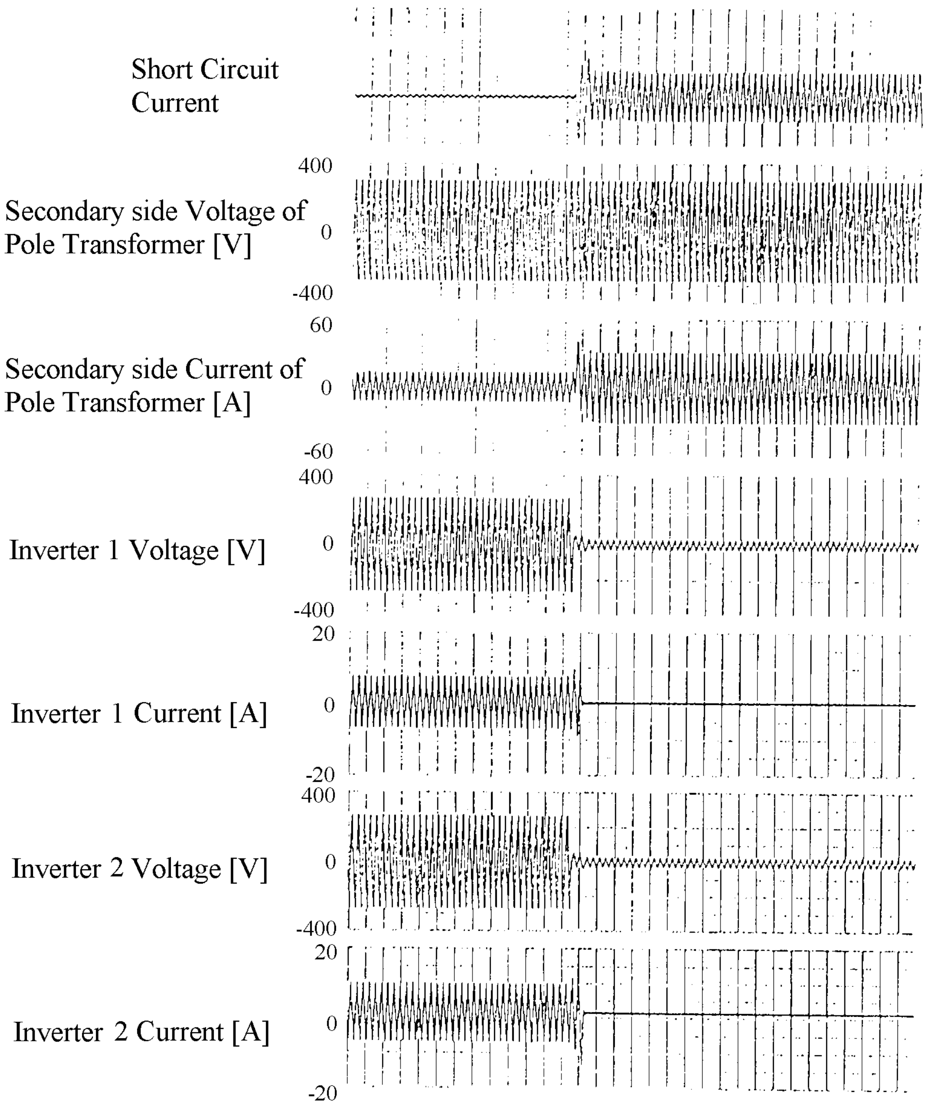

Fig. 5-11 Examples of waveform of short circuit test (two inverters made by company E)

5.4 Conclusions

Some inverters do not supply a short circuit current at all (the current is maintained at the level before the short circuit) and stop operation quickly (within 1 or 2 cycles). On the other hand, some inverters supply a short circuit current that is about twice that before the short circuit for a short period of time (for 1 to 2 cycles) before stopping operation. Furthermore, the short circuit current supplied from each photovoltaic power generation inverter does not change even when several units are connected.

Therefore, it was concluded that for the case of short circuit faults in a line to which photovoltaic power generation systems are connected, the short circuit current is within about twice that before the short circuit, well below the inverter over current protection level, and continues only for several cycles before under voltage protection takes place. As long as current controlled inverter is applied, short circuit current from PV inverter is negligible.

6. Characteristics under AC-DC Mixing Fault

6.1 Background

The phenomenon in which the AC circuit of the power distribution system directly contacts the DC circuit of the PV array of a photovoltaic power generation system is called an AC-DC mixing fault. AC-DC mixing faults occur in the following cases: if the DC current component flows out in an AC system if many inverters without isolation transformers are connected to the power system; and if the DC current component in the AC system increases due to a fault of multiple interconnected inverters without isolation transformers.

The DC current in case of an AC-DC mixing fault saturates the magnetic circuit of the pole transformers on the power system side, resulting in a large distortion of exciting current and large harmonics. Also, the AC current enters the DC circuit of the photovoltaic array and may blow DC circuit parts.

This field test investigated the propagation range of harmonics generated in case of an AC-DC mixing fault in the power system, the effect on other transformers connected to the same high voltage distribution line, and the effect on other inverters for photovoltaic power generation connected to the same low voltage distribution line.

6.2 Effect on inverters for photovoltaic power generation at AC-DC mixing fault

6.2.1 Experimental Procedure

It is difficult to generate the actual mixing fault condition caused by the DC current component from multiple interconnected transformerless inverters or a fault in a transformerless inverter. Therefore, the field test was conducted by connecting the output terminal of the photovoltaic array to the AC circuit directly. With the circuit illustrated in Fig. 6-1, we measured the pole transformer primary voltage and current, the transformer secondary voltage and current, the by-pass diode output voltage and output current under connection to the photovoltaic array. For the case in which the by-pass diode is not connected, the output current for a single string was measured.

The pole transformer primary voltage and current were measured before and after the occurrence of the AC-DC mixing fault, and the increase/decrease of harmonics before and after the AC-DC mixing fault were compared.

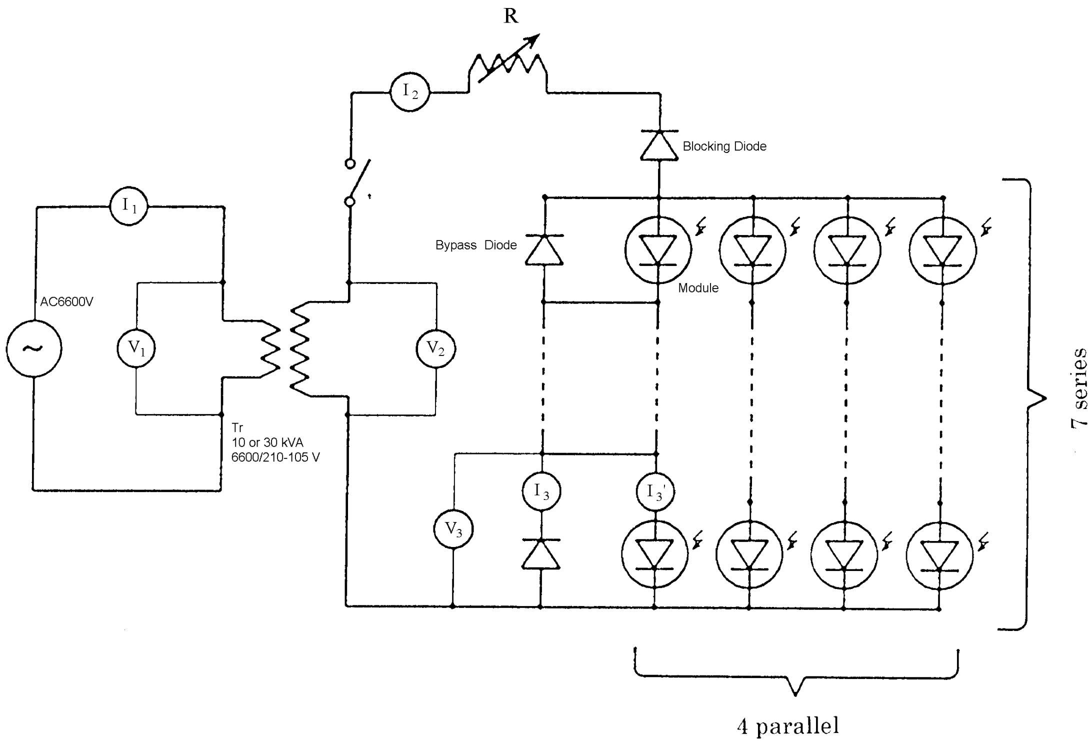

Fig. 6-1 AC-DC mixing fault test circuit

6.2.2 Experimental Results

The internal resistance of the photovoltaic module was measured first with no solar irradiation. The internal resistance was 10 kΩ in the 0 V forward direction and 50-100 kΩ in the backward direction as measured when a voltage of 500 V was applied to the output terminal of the PV module. Under this condition, even if an AC-DC mixing fault occurs, the current flowing in both direction for PV module is extremely small as to be insignificant. Therefore, if an AC-DC mixing fault occurs in case of connection to the by-pass diode and in the state that the PV cell array does not have output, the current flowing on the low voltage side of the pole transformer was subjected to half wave rectification, resulting in rapid burnout of the by-pass diode

When an AC-DC mixing fault occurs in the state that solar irradiation exists, the exciting current magnetically deflected by DC current starts to flow on the high voltage side of the pole transformers regardless of the connection of the by-pass diode, and it increases (Fig. 6-2 and 6-3). The increase in exciting current becomes saturated in several seconds or tens of seconds. A characteristic of the exciting current magnetically deflected by DC current is that harmonics of even orders occur, and both exciting current and harmonics of even orders rapidly increase. Even when DC current equivalent to 10% of the rated current is induced in the winding in the pole transformer with a capacitance of several tens of kW or over, no problem such as overheating was observed in the transformer.

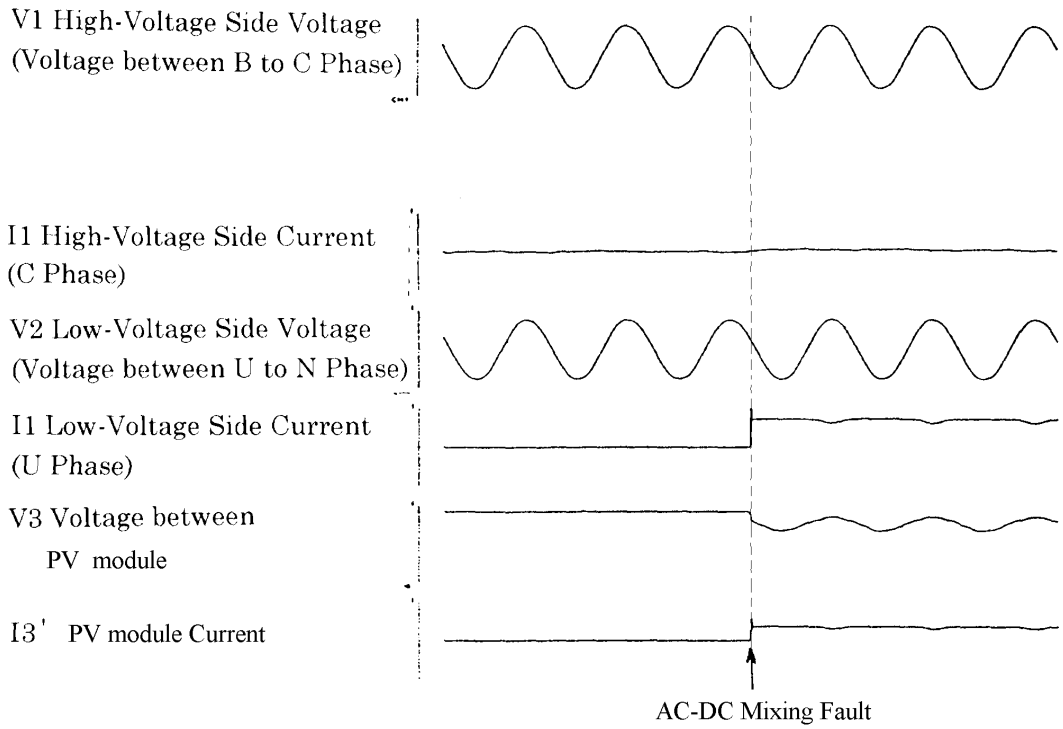

Fig. 6-2 Test result of AC-DC mixing fault
Conditions: transformer 10 kVA, limiting resistance 16 Ω,
four PV cells connected in parallel, without blocking and by-pass diode

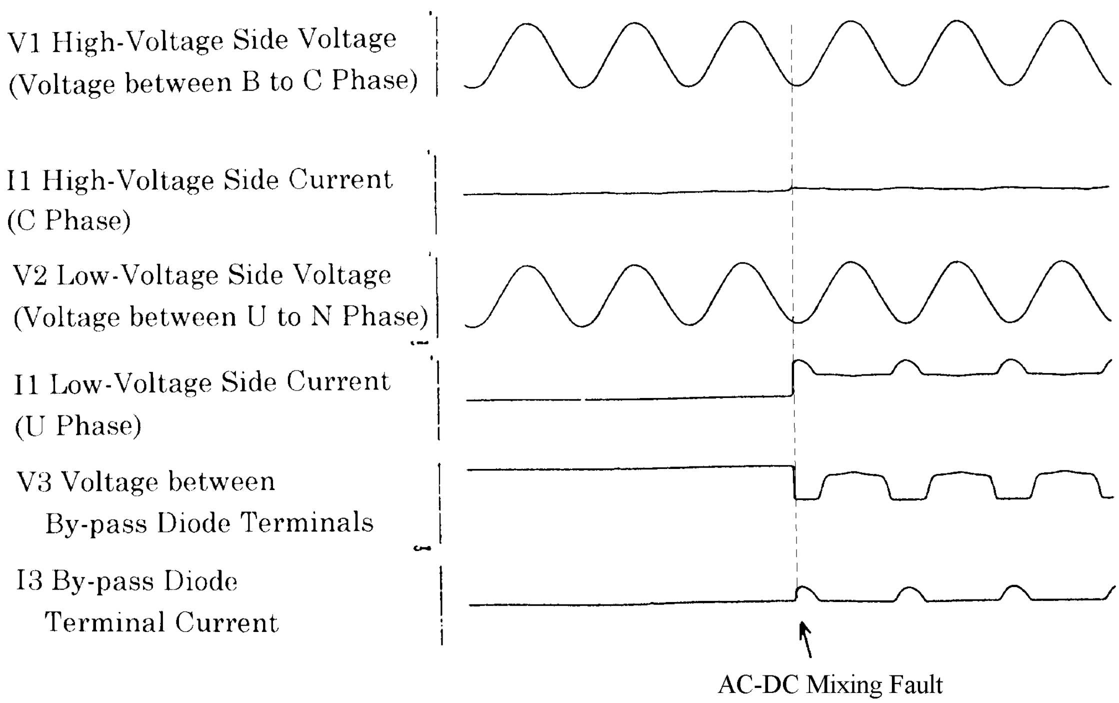

Fig. 6-3 Test result of AC-DC mixing fault
Conditions: transformer 10 kVA, limiting resistance 16 Ω,
four PV cells connected in parallel, with blocking diode and by-pass diode

When the exciting current harmonics were compared before and after the AC-DC mixing fault, the exciting current waveform on the primary side of the transformer induced distortion; in particular, the figures of even degrees increased to the level of odd degrees. The test results are shown in Figs. 6-4 and 6-5. For the AC voltage on the secondary side of the transformer, the wave height reduced by 1 to 3 V when the current limiting resistance was reduced.

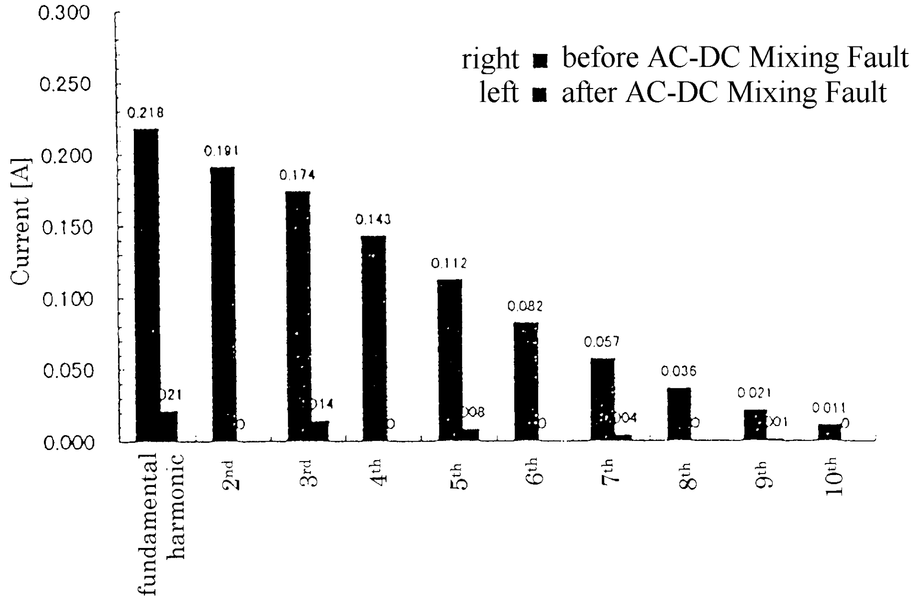

Fig. 6-4 Measurement of harmonics
Conditions: transformer 10 kVA, limiting resistance 16 Ω, four PV cells connected in parallel, without blocking or by-pass diode, irradiance 0.71 kW/m^2

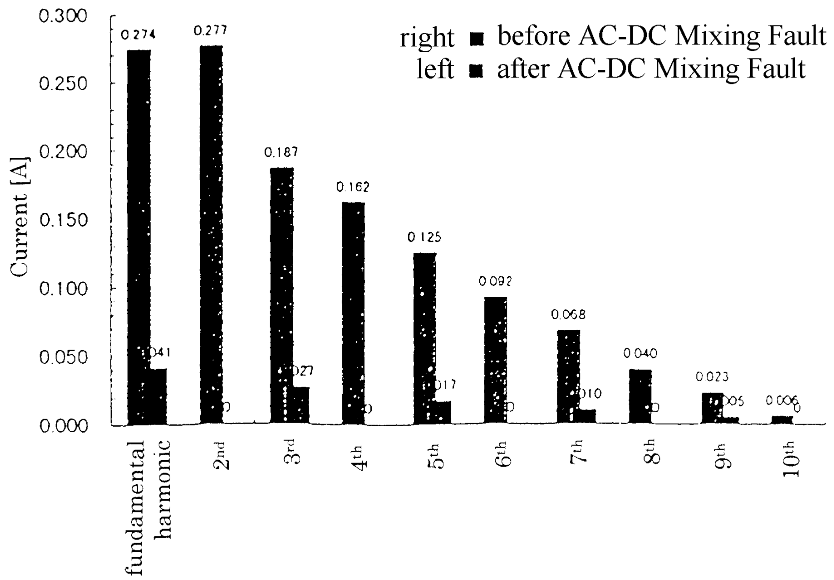

Fig. 6-5 Measurement of harmonics
Conditions: transformer 30 kVA, limiting resistance 5 Ω, four PV cells connected in parallel, applying blocking diode and by-pass diode, irradiance 0.71 kW/m^2

6.3 Effect on the power system and other inverters

6.3.1 Experimental Procedure

The extent of propagation of the effect of harmonics of even orders generated at an AC-DC mixing fault in the AC system was measured. At the same time, field tests confirmed whether or not there was any effect in the behaviour of inverters of photovoltaic power generation systems connected to the same distribution line and whether or not there was any change in characteristics such as reliance in the inverter itself. The test circuit is shown in Fig. 6-6. Using this test circuit the output current (measurement point: 42 PCT) for other inverters, and the current (measurement points: 0 CT, 4 PCT, 5 PCT) on the high voltage distribution line were measured.

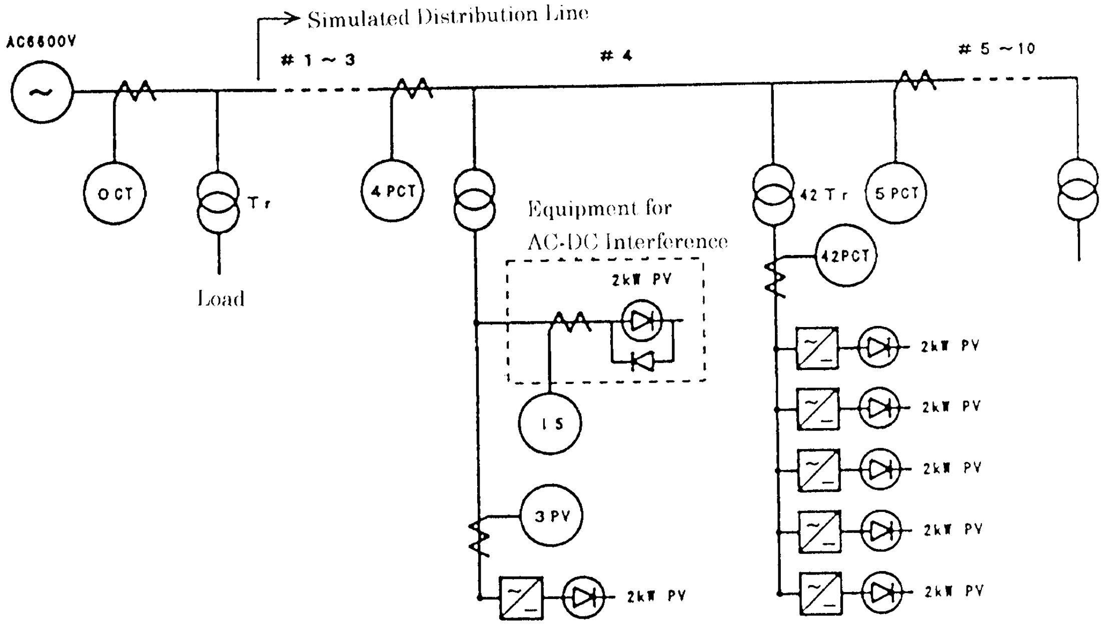

Circuit conditions: Capacity of transformer: 30 kVA
Limiting resistance: 16 Ω
Number of PV arrays connected in parallel: 4
Blocking diode: present
By-pass diode: present

Fig. 6-6 Test circuit

6.3.2 Experimental Results

It was confirmed that harmonics of even orders generated on the AC side by the AC-DC mixing fault propagate over a wide range. Distortion of the waveform for the output current of other photovoltaic power generation systems interconnected to the same low voltage line generating AC-DC mixing faults was also seen. It is considered that the DC current of the PV array generating mixing fault generates DC magnetic deflection phenomenon in the insulating transformers of other inverters to which it is interconnected. However, this did not cause other photovoltaic power generation systems to stop operating or detect a fault.

Distortion of current waveform by the AC-DC mixing fault was seen in other pole transformers of the same high voltage distribution line. This trend was observed in pole transformers located on the power supply side from the pole transformer generating AC-DC fault contact. No such trend was seen in the pole transformer located on the load side from the pole transformer generating the AC-DC mixing fault. This trend shows that harmonic current of even orders generated by an AC-DC mixing fault is supplied from the substation, i.e., from the power supply side.

Although the AC-DC mixing fault was continued for about 5 minutes to observe the status of the pole transformer, no problems such as overheating, vibration, unusual sound or odour were observed except the increase in harmonics (Figs. 6-7 and 6-8).

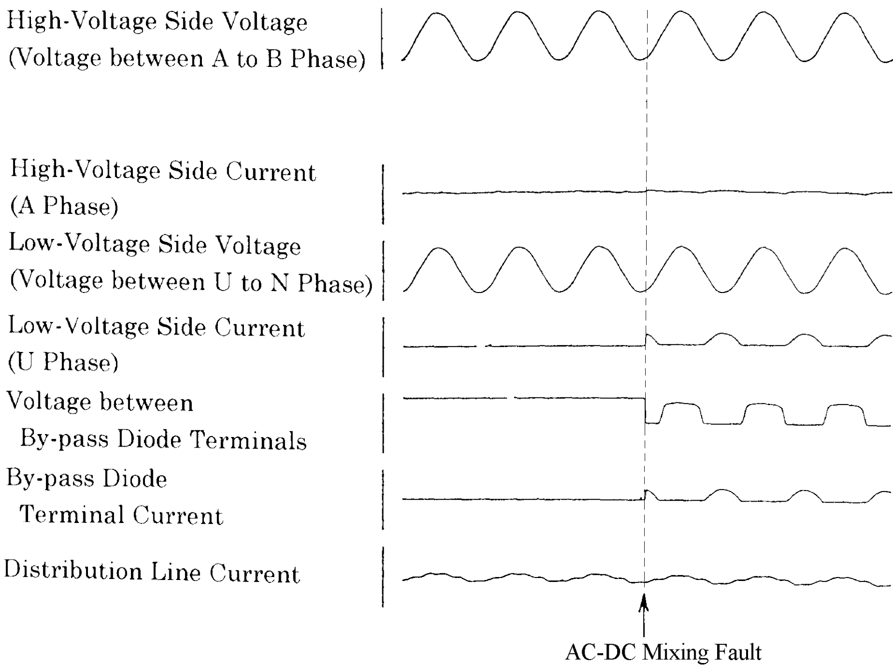

Fig. 6-7 Test result (before and after mixing fault)

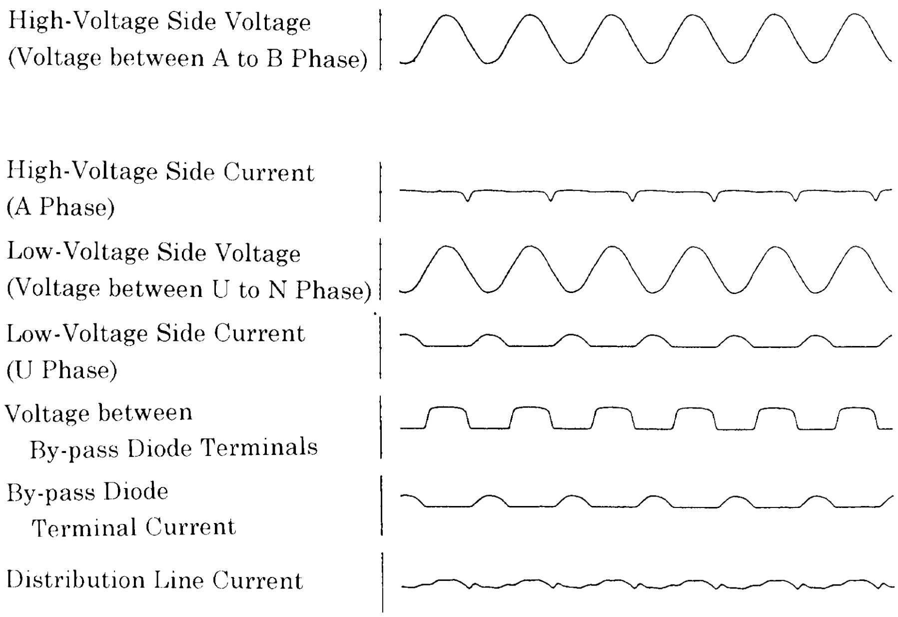

Fig. 6-8 Test result (9 seconds after fault)

6.4 Conclusions

The internal resistance of a photovoltaic module is very high in the absence of solar irradiation. Thus, if a mixing fault between the photovoltaic array DC circuit and AC circuit occurs, it is not a problem unless a by-pass diode is present. The DC current starts to increase immediately after fault contact and stabilises (saturated) within several seconds or tens of seconds. At this time, magnetic deflection of the magnetic circuit occurs and harmonics of even orders are generated on the high voltage side of the pole transformer. In the absence of solar radiation, if a photovoltaic array to which a by-pass diode is connected generates an AC-DC mixing fault, burnout of the by-pass diode may result in burnout of the blocking diode.

Distortion of the current waveform caused by an AC-DC mixing fault was seen in other photovoltaic power generation systems connected to the same low voltage distribution line. This phenomenon did not have any effect on these photovoltaic power generation systems, such as stopping power generation.

Distortion of the current waveform caused by an AC-DC mixing fault was seen in other pole transformers connected to the same high voltage distribution line. This was particularly noticeable in pole transformers located on the power supply side from the pole transformer generating the AC-DC mixing fault, but not in pole transformers located on the load side from the pole transformer generating the AC-DC mixing fault.

No effect was observed in photovoltaic power generation systems connected to the low voltage side of pole transformers located in the vicinity of the pole transformer generating the mixing fault. Thus, there is little detrimental effect such as overheating of pole transformer caused by mixing faults of photovoltaic power generation systems which continue for several minutes. Moreover, the existence of an AC-DC mixing fault in the system can be detected by monitoring the harmonics of even orders appearing in the AC system.

7. Output Fluctuation of PV Systems

7.1 Background

The output of photovoltaic power generation fluctuates with hourly changes in solar radiation. Solar radiation varies in second order owing to the movement of clouds except for on completely clear days and completely cloudy days. The hourly fluctuation in output of the photovoltaic power generation causes fluctuation in power flow, or fluctuation in voltage, in the connected distribution line. For photovoltaic power generation of a concentrated arrangement in a limited area, the output of each system fluctuates simultaneously compared with the load. Accordingly, the hourly fluctuation in voltage in the distribution line due to photovoltaic power generation becomes larger than the fluctuation induced from the load, and the speed of the hourly fluctuation is of second order. Such kind of fluctuation may become a technological issue affecting future introduction of photovoltaic power generation systems.

When the photovoltaic power generation system is installed on the roofs of individual houses, a large number of photovoltaic power generation systems are connected to the distribution line through which power is supplied to single-family houses. The power supply area per single distribution line in the Kansai Electric Power Co. area is normally within 1 km^2.

This report proposes a method of evaluating the output fluctuation in view of the magnitude and time of fluctuation when many photovoltaic power generation systems are connected to a distribution line that is densely located in an area such as a residential zone, and shows examples of the evaluation computation on the basis of measured data.

First, the output characteristics of a single array PV system are described, then the results of investigating the magnitude of the output fluctuation and characteristics of fluctuation speed in the case of many PV systems are described.

7.2 Theoretical Considerations

7.2.1 Output Characteristics of Single Array PV System

For describing the output of a single array PV system, various quantities for the sections shown in Fig. 7-1 are discussed. The inverter considered here is one that applies constant voltage control on the DC side.

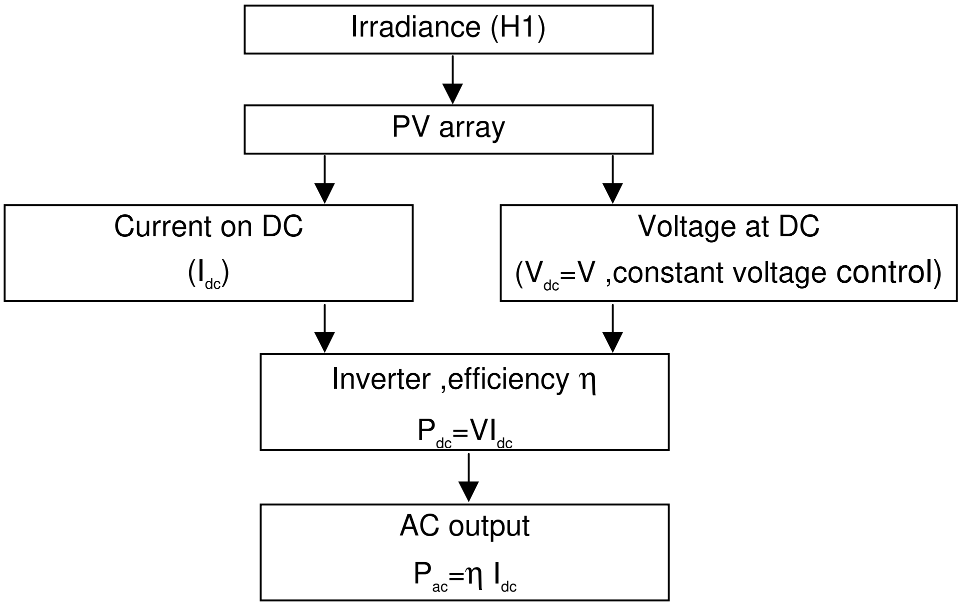

Fig. 7-1 Output of single array PV system

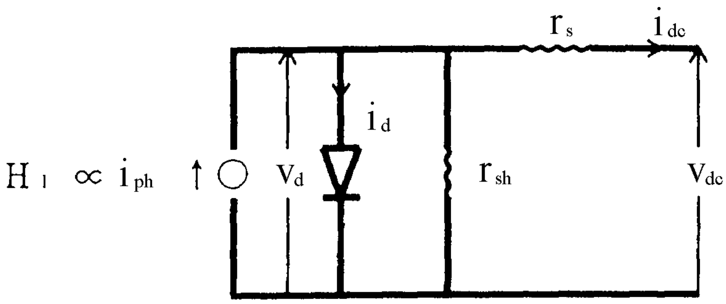

i_{ph}: constant current power source generating current responding to light intensity
r_s : series resistance collecting the generated current to terminals
r_{sh}: parallel resistance caused from leak current at pn junction
i_d : diode current
V_d: diode voltage
i_{dc} : terminal current at PV cell
V_{dc}: terminal voltage at PV cell

Fig. 7-2 PV equivalent circuit

The relation between irradiance H_1 and current I_{dc} on the DC side ideally follows the relation between i_{ph} ($\propto H_1$) and i_{dc} of the PV cell shown in Fig. 7-2. The relation between i_{ph} and i_{dc} is expressed by the equation given below based on the equivalent circuit of Fig. 7-2.

$$i_{dc} = i_{ph} - i_0 \cdot \left[\exp\left\{ \frac{q \cdot \left(v_{dc} + r_S \cdot i_{dc} \right)}{n \cdot k \cdot T} \right\} - 1 \right] - \frac{V_{dc} + r_S \cdot i_{dc}}{r_{sh}} \tag{1}$$

where, i_o: reverse saturation current at pn junction ,
n: diode performance index , k: Boltzmann constant ,
T: absolute temperature , q: element charge

From eq. (1), an actual silicon pn junction photovoltaic cell is assumed, and computation is given under the conditions of $n = 1$, $T = 300$ K, $r_{sh} = \infty$, $i_0 = 50$ pA/cm^2, $i_{ph} = 30$ mA/cm^2 (equivalent to 100 mW/cm^2 of incident light). The result is shown in Fig. 7-3. V_{oc} is the open circuit voltage of the PV cell, which is expressed by:

$$V_{0c} = \frac{n \cdot k \cdot T}{q} \cdot \ln\left(\frac{i_{ph}}{i_0} + 1\right) \qquad (2)$$

When $v_{dc} = 0$ V, then $i_{dc} = i_{sc}$ (i_{sc}: short circuit current of PV cell), and the (i_{sc} - i_{ph}) characteristic is independent of the value of r_s, giving the linear relation:

$$I_{sc} \fallingdotseq i_{ph} \qquad (3)$$

Therefore, i_{sc} is independent of the value of r_s, thus approximately expressing the irradiance (∞ i_{ph}).

For the recent crystalline silicon type, the value of r_s is 0.5 Ω or less, so the (i_{dc}-i_{ph}) characteristic changes very little even when the value of V_{oc} changes (generally to a negative temperature coefficient) owing to the temperature changes to vary the ratio of V_{dc}/V_{oc}, thus giving a nearly linear correlation as shown in Fig. 7-3(a). If the resistance of the external circuit of the PV cell becomes not negligible, and if r_s is equivalently larger than 0.5 Ω, then, when the temperature increases and V_{oc} decreases and so the ratio V_{dc}/V_{oc} increases, as shown in Fig. 7-3(b), then the (i_{dc}-i_{ph}) characteristic may become saturated in the upper convex zone. For a PV array, ideally the behaviour should be similar to that of a cell. The short circuit current of PV array I_{sc} and H_1 should be proportional to each other. Also, current I_{dc} on the DC side and H_1 should be proportional to each other in the case that the series resistance component of the PV array consists only of r_s (≤ 0.5 Ω) of the PV cell. Furthermore, when the inverter efficiency η is a constant value, all the PV system output (I_{dc}, P_{dc}, P_{ac}) should be proportional to H_1.

If, however, the series resistance becomes large due to connection resistance or other variables, the (I_{dc}-H_1(I_{sc})) characteristic may become non-linear with an upward convex profile owing to the temperature increase of the PV array, under a condition of constant V_{dc} value.

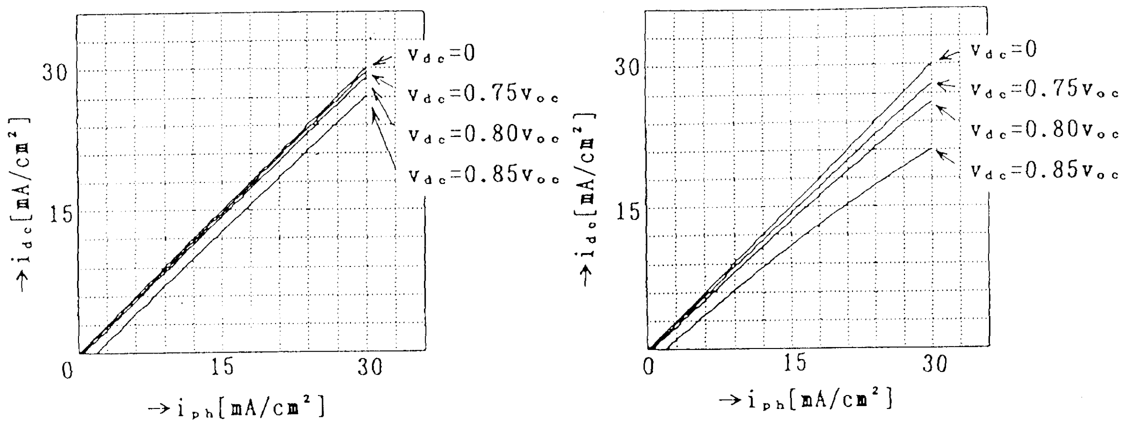

(a) $r_s = 0.5$ Ω (b) $r_s = 2$ Ω

Fig. 7-3 (i_{dc}-i_{ph}) characteristic

7.2.2 Total Output Fluctuation Characteristics of Many PV Systems

This section describes the relation between the fluctuation in total output ΣP_{ac} of individual PV systems in a system of distributed PV systems and the output fluctuation in individual PV systems. Figure 7-4 shows an example of distributed PV array systems, each containing a l [m] x w [m] PV array, in an area of L [m] in EW and W [m] in NS directions.

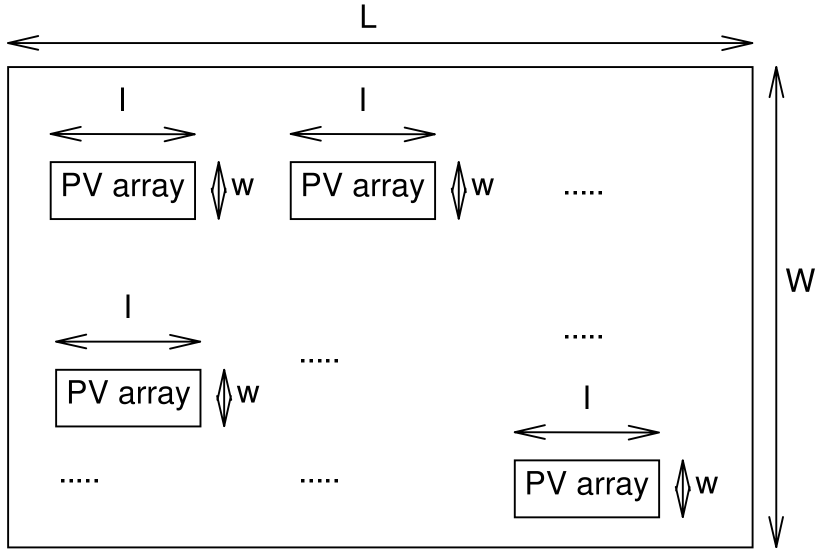

Fig.7-4 Example of PV systems distribution

When P_{ac0} [kW] is the rated output per single PV system and K_{cloud} is the output reducing coefficient due to cloud, then the output P_{ac} [kW] per single PV system is written as:

$$P_{ac} = k_{cloud} \cdot P_{ac0} \tag{4}$$

For the case that a cloud having a distinct boundary moves in the EW direction at a velocity of V_{cloud}, the P_{ac} fluctuation ΔP_{ac} [kW/s] per 1 second is expressed by:

$$\Delta P_{ac} = (1 - k_{cloud}) \cdot \frac{V_{cloud}}{l} \cdot P_{ac0} \tag{5}$$

The value of $\%\Delta P_{ac}$ [%/s] normalised by P_{ac0}, [k%/s] is written as:

$$\%\Delta P_{ac} = (1 - k_{cloud}) \cdot \frac{V_{cloud}}{l} \times 100\% \tag{6}$$

In a similar manner, the fluctuation $\%\Sigma P_{ac}$ [%/s] of ΣP_{ac} per 1 second normalised by the product of P_{ac0} and the number of array units is given by:

$$\%\Delta \Sigma P_{ac} = (1 - k_{cloud}) \cdot \frac{V_{cloud}}{L} \times 100\% \tag{7}$$

Consequently, the ratio of $\%\Delta P_{ac}$ and $\%\Sigma\Delta P_{ac}$, or the smoothing rate SM (smoothing effect: 1/SM) is defined by:

$$SM = \frac{\%\Sigma\Delta P_{ac}}{\%\Delta P_{ac}} = \frac{1}{L} \left(\leqq 1 \right) \tag{8}$$

Also for the case that a cloud having a distinct boundary moves in the NS direction, the SM is defined by:

$$SM = \frac{\%\Sigma\Delta P_{ac}}{\%\Delta P_{ac}} = \frac{w}{W} \left(\leqq 1 \right) \tag{9}$$

Equations (8) and (9) suggest that, when a cloud having a distinct boundary passes over the PV system, the fluctuation of total output of distributed PV systems decreases by the ratio of the length of each side between the PV array and the plane of the distribution arrangement. In other words, a larger area of distributed arrangement gives a larger smoothing effect.

If, however, the boundary of cloud is not distinct, and in the extreme case that the cloud thickness (k_{cloud}) varies over the whole area of the plane of the distributed PV array arrangement at a time, then the following equation applies:

$$\%\Sigma\Delta P_{ac} = \frac{d}{dt} \cdot k_{cloud} \times 100\% \tag{10}$$

Accordingly, from eqs. (8), (9), and (10) we derive:

$$\min\left[\frac{1}{L},\ \frac{w}{W}\right] \leqq SM \leqq 1 \tag{11}$$

7.3 Experimental Procedure

a. Experimental facility

The experiment was conducted at Rokko Test Centre for Advanced Energy Systems of Kansai Electric Power Co. using an experimental facility in which about one hundred 2 kW PV systems were connected to a simulated distribution line having a line constant (consisting of inductance and capacitance) equivalent to 10 km. For the experimental facility of the Test Centre as shown in Fig. 7-4, L is nearly equal to 110 meters and W nearly equal to 85 meters. The average size of the 100 PV arrays tested gives l nearly equal to 6.0 meters and w nearly equal to 2.4 meters (horizontal component). Therefore, the smoothing factor SM becomes maximum when the shade of a cloud having a distinct boundary passes over the Test Centre in the NS direction, giving SM = 0.028 (1/SM = 34.5).

b. Measurement circuit

Fig.7-5 shows the measurement circuit. The irradiance is normally determined by a pyrometer.

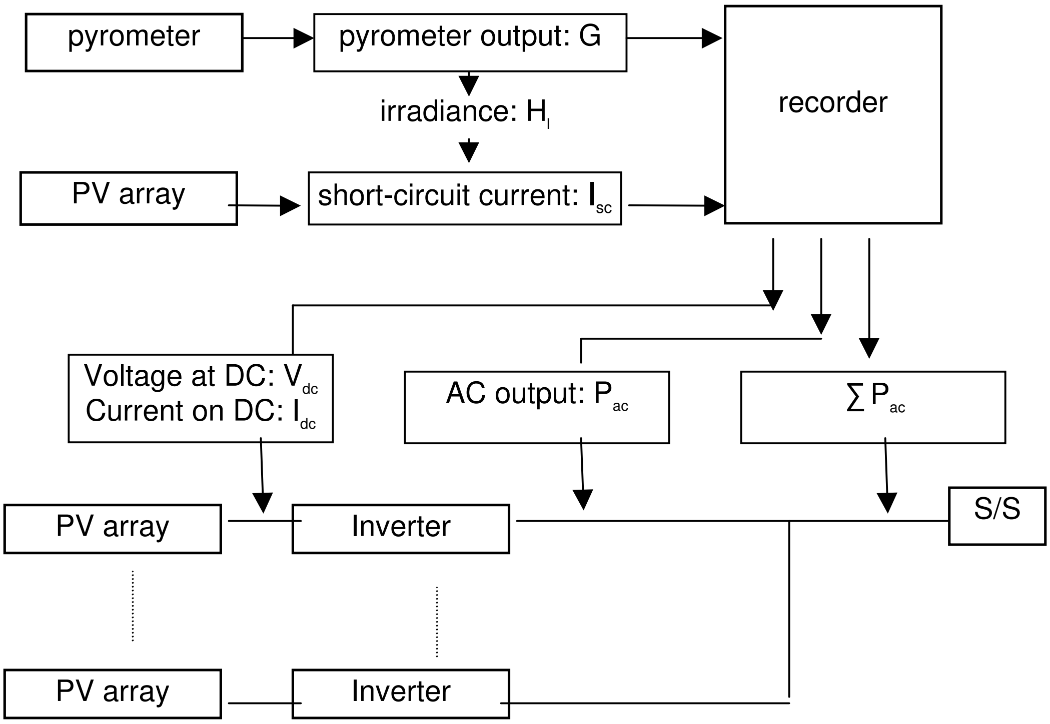

Fig. 7-5 Measurement test circuit

Table 7-1 Specifications of measurement test circuit

Device	Specifications
Pyrometer	Set with a 30% inclination Sensitivity 7.0 mV/kW/m^2 Internal resistance 500 Ω Response time 2.5 s Temperature characteristics 1% Incidence angle characteristics 2% Wavelength spectrum 300-2800 nm, Error under 1.5%
PV array	Max. output 2.33 kW (28℃) Voltage output 201 V (28℃) Optimum constant DC voltage 190 V Open-circuit voltage 252 V (28℃) Short-circuit current 13.0 A (28℃)
DC current transformer	Rated current 25 A Measuring range 0-37.5 A Max. error 0.1% of rated current Frequency characteristics 500 kHz Working temperature range -25 +70
Recorder	Sampling time 1.2 sec Measuring time 4 a.m. to 8 p.m.

As shown in Table 7-1, however, the response rate of the pyrometer used at the Rokko Test Centre is 2.5 seconds, which fails to accurately measure the fluctuation in irradiance of second order. Therefore, the measurement of fluctuation in irradiance is preferably done on the basis of fluctuation in short circuit current of the PV cell or module from the viewpoint of frequency characteristics, though the measurement is on an average irradiance on an incident surface. Since the minimum PV system unit which is evaluated by the experiment is a single PV array, the fluctuation in irradiance was evaluated by adding to the pyrometer output G the fluctuation in short circuit current I_{sc} of a PV array responding to the fluctuation in average irradiance on a single array face. In addition, to evaluate the fluctuation in output of the PV system of a single array, simultaneous measurement was performed on a single inverter for: the DC side current I_{dc}, DC side voltage V_{dc}, and AC output P_{ac}. Furthermore, to evaluate the fluctuation in total output in the case of many PV systems connected to a distribution line, the active power flow ΣP_{ac} at a substation of the simulated distribution line was measured. At this time, however, no fluctuating load was connected to the simulated distribution line to eliminate the effect of load fluctuation and to evaluate only the output of the PV system.

c. Method of computing fluctuation

During the experiment, the values of G, I_{sc}, V_{dc}, I_{dc}, P_{ac}, and ΣP_{ac}, which are described in section b, were measured with the maximum resolution of 12 bits, during a period of from 4 a.m. to 8 p.m. every day, with increments of Δt (=1.2s), for a total of 48,001 points. The method of computing the fluctuation of these measurement items is described below.

When the rated value of the measured items is expressed by Yo, and the measured value of the ith measurement (i = 0 - 48,000) is expressed by Y_i, then the fluctuation value of $\%\Delta Y_i$ [%/s] is written as:

$$\%DY_i = \frac{Y_i - Y_{i-1}}{Dt} \cdot \frac{1}{Y_0} \times 100\% \qquad (12)$$

The fluctuation of each measurement item was investigated for the fluctuation of 48,000 points per day computed by eq.(12).

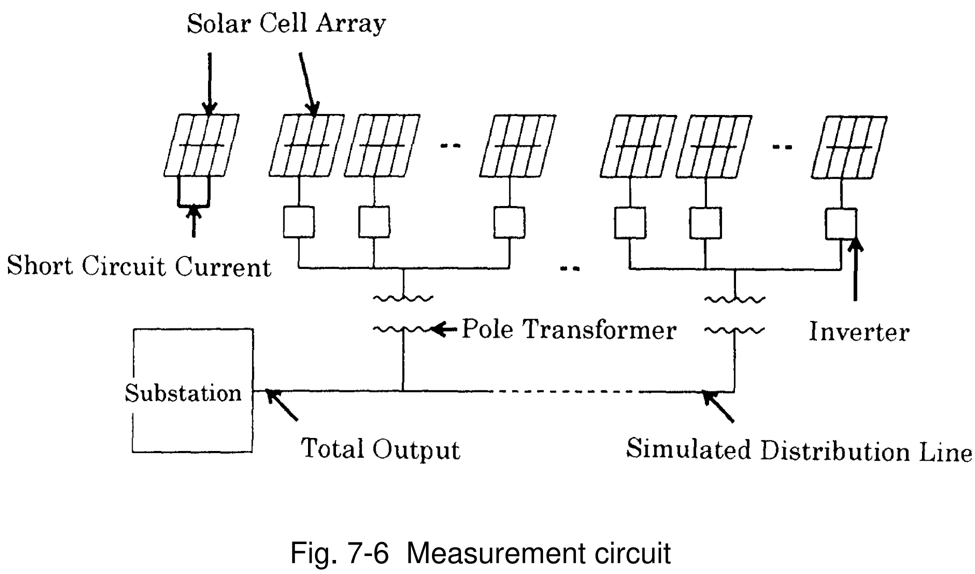

Fig. 7-6 Measurement circuit

To evaluate the hourly fluctuation of output of photovoltaic power generation, both the magnitude of fluctuation and the time of fluctuation (speed of fluctuation) must be considered. In this investigation, the definition is given as ΔY_i for the magnitude of fluctuation, Δt_i for the time of fluctuation, and $\Delta Y_i/\Delta t_i$ for the speed of fluctuation, as shown in Fig. 7-7.

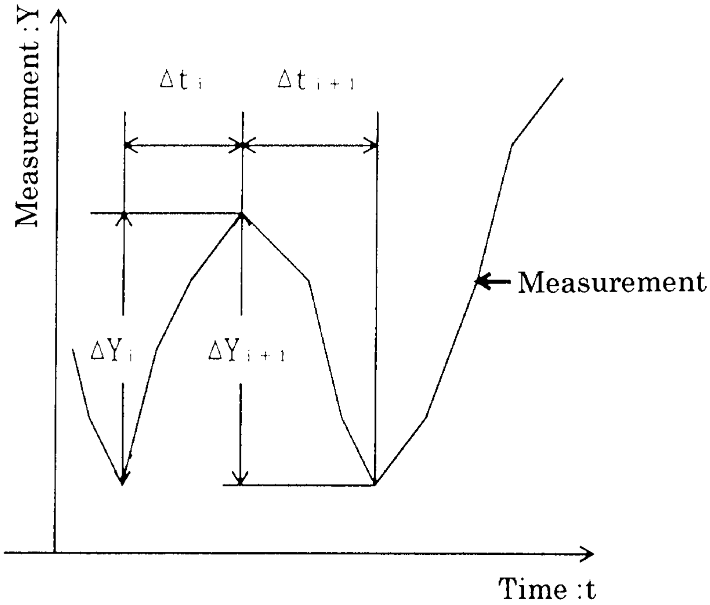

Fig. 7-7 Definition of magnitude and time of fluctuation

7.4 Experimental Results

7.4.1 Output Characteristics of Single Array PV System

(1) Relation between pyrometer output G and single PV array short circuit current I_{sc}
Figure 7-8 shows the relation between pyrometer output G and single PV array short circuit current I_{sc} (locus during the period from 4 a.m. to 8 p.m. on the same day) on each of the winter, spring, and summer days when the solar radiation is relatively stable. The figure shows that, as described in Section 7.2.1, there is a proportional relation between the short circuit current I_{sc} of the PV array and the irradiance H_1, independent of season.

Table 7-2 Measurement conditions

		Highest temperature	Average temperature
Winter days	February 23, 1995	10.8℃	5.6℃
Spring days	May 27, 1995	26.9℃	22.6℃
Summer days	August 5, 1995	38.7℃	34.6℃

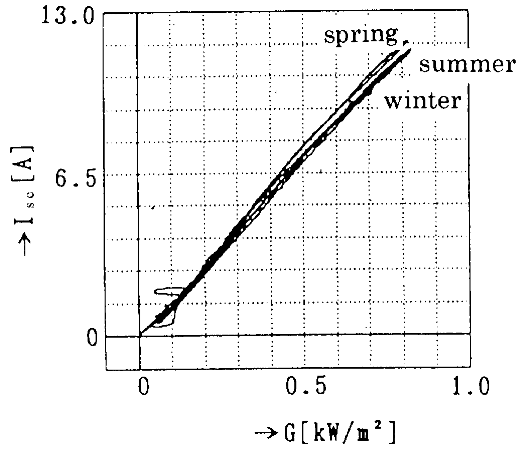

Fig. 7-8 G-I_{sc} characteristic

(2) Relation between DC side current I_{dc} and short circuit current I_{sc} for a single PV array
Figure 7-9 shows the relation between the DC side current I_{dc} and the short circuit current I_{sc} for a single PV array, which were measured on the same day with the acquired data of Fig. 7-8. The figure shows that the (I_{dc}-I_{sc}) characteristic is non-linear in upward convex profile, and the characteristic is stronger for seasons of higher temperature. As described in Section 7.2, the probably cause of this phenomenon is that the series resistance of the PV array is larger than the simple sum of each series resistance r_s (= 0.5 Ω) in the PV cell and that the temperature rise reduces the PV array open circuit voltage V_{oc}.

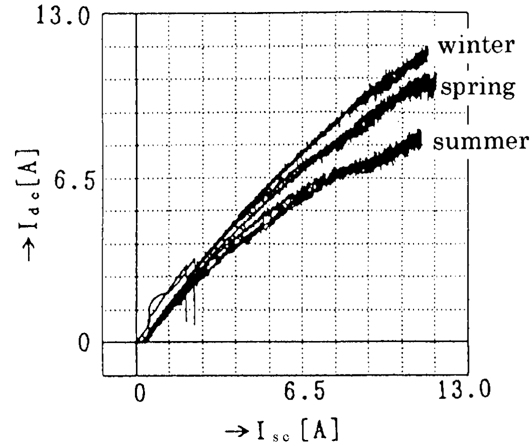

Fig. 7-9 (I_{dc}-I_{sc}) characteristic

(3) Fluctuation characteristics of PV system output
Figure 7-10 shows examples of the measured fluctuation characteristics of PV system output (as a percentage, normalised by rated values) during a winter day when the fluctuation in solar radiation was relatively intense. The fluctuation of $I_{sc,}$ which is the irradiance, and these fluctuations of a single inverter output P_{ac} appear in second order. Compared with the fluctuation, the fluctuation of output G of the pyrometer is less than the I_{sc} and P_{ac} fluctuations because the pyrometer has a response time of 2.5 seconds, as shown in Table 7-2. In addition, the fluctuation of total output ΣP_{ac} at a substation is also less than the I_{sc} and P_{ac} fluctuations.

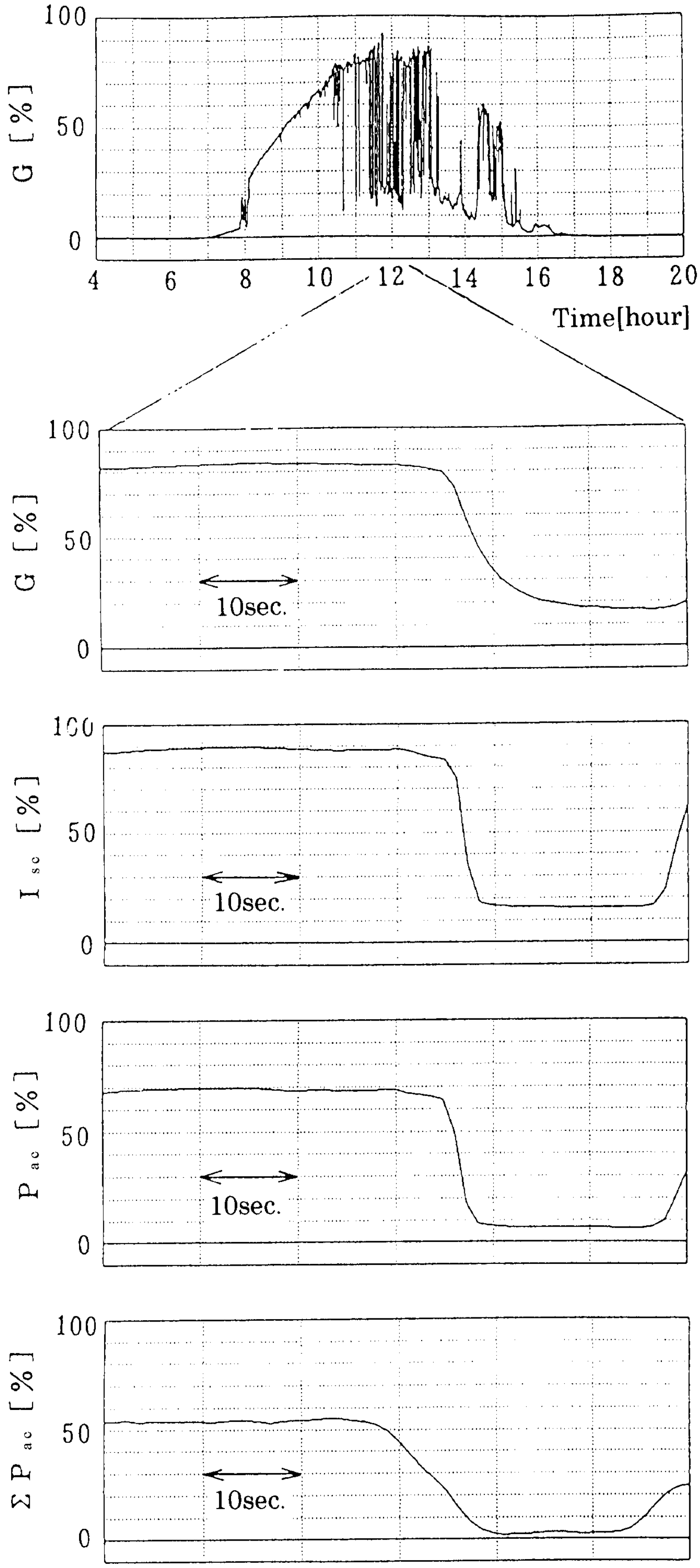

Fig. 7-10 PV system output fluctuation characteristics (January 1, 1995)

(4) One day cumulative characteristics of PV system fluctuation

Figure 7-11 compares the cumulative characteristics of each fluctuation [%/s] computed by the method described in Section 7.3c of a PV system over a single day (4 a.m. to 8 p.m.), (curves of cumulative 48,000 data in order from large to small). The values of %ΔG and %$\Delta\Sigma P_{ac}$ are suppressed by the values of %ΔI_{sc}, %ΔI_{dc}, and %ΔP_{ac}. The smoothing rate SM at near the maximum value is about 0.28. The value is ten times (or one tenth for the smoothing effect) the value (SM = 0.028) expected to maximise the smoothing effect in the experimental facility described in Section 7.3a.

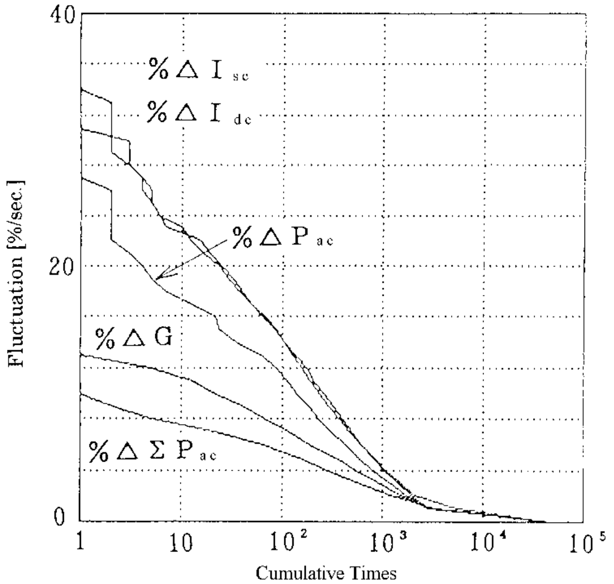

Fig. 7-11 Cumulative characteristics of fluctuation (January 1, 1995)

(5) Annual characteristics of each fluctuation of PV system

Figure 7-12 shows the values of %ΔI_{sc}, %ΔI_{dc}, %ΔP_{ac}, %$\Delta\Sigma P_{ac}$, and %ΔG at the point giving maximum %ΔG measured in each month. The period of measurement was one year beginning from July, 1994 and ending in June, 1995. During the measurement period, the value of %ΔI_{sc}, which presumably accurately simulates the fluctuation of solar radiation, gave about 50%/s in March and April in spring or October around autumn, and the value of %ΔP_{ac} reached about 35%/s in March. The tendency of the maximum values of %ΔI_{sc}, %ΔI_{dc}, and %ΔP_{ac} in each month was equal to the maximum wind velocity on the day of measurement. Thus, the day of intense fluctuation of PV system output was a day of strong wind.

The maximum value of %$\Delta\Sigma P_{ac}$ in each month, which shows the fluctuation on a flat plane on which about one hundred 2 kW PV systems were installed, was in a stable state not higher than 10%/s throughout the year. The smoothing factor SM in each month computed from Fig. 7-12 ranged from 0.11 (June) to 0.63 (September). These values are about 4 to 22.5 times larger than the case in which the smoothing effect is maximised in the experimental facility, (0.028) (giving a smoothing effect of about 1/22.5 to 1/4 fold) described in Section 7.3a.

The values of %ΔG giving poor response performance are not higher than 15%/s throughout the year.

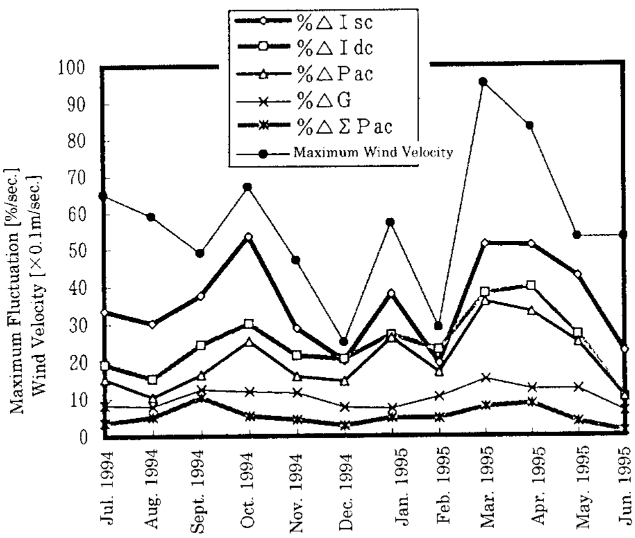

Fig. 7-12 Monthly maximum fluctuation characteristic in a year

7.4.2 Total Output Fluctuation Characteristics of Many PV Systems

Figure 7-13 shows the data measured on May 25, 1997, when the solar radiation varied relatively significantly. The maximum value of short circuit current of a photovoltaic array was about 16 A, and the maximum value of total output of the photovoltaic power generation system was about 100 kW.

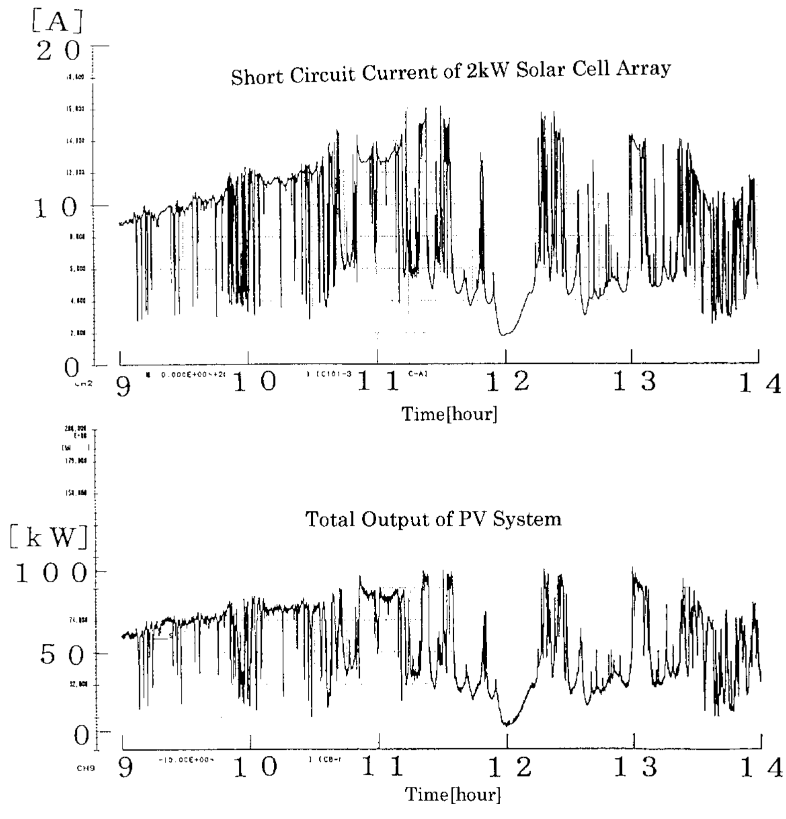

Fig. 7-13 Examples of measured data (May 25, 1997)

For the measured data, the computation described in Section 7.3 was applied to derive the values of (ΔY_i, Δt_i), (i = 1, 2,...), thus plotting the computed values on the (ΔY_i, Δt_i) plane and (ΔY_i, $\Delta Y_i/\Delta t_i$) plane, which were given in Fig. 7-14 and Fig. 7-15, respectively. For comparison of the short circuit current with total output, the scale of ΔY_i is set to a length that was normalised by the maximum value of the measured data in Fig. 7-13. The range of distribution of short circuit current and the range of distribution of magnitude of fluctuation in total output are almost equal to each other. The magnitude of fluctuation is proportional to the time of fluctuation. The short circuit current, however, does not give a proportional relation but, in some cases, shows a small fluctuation time even under large magnitude of fluctuation. As a result, the range of speed of fluctuation in total output becomes much narrower than the case of short circuit current.

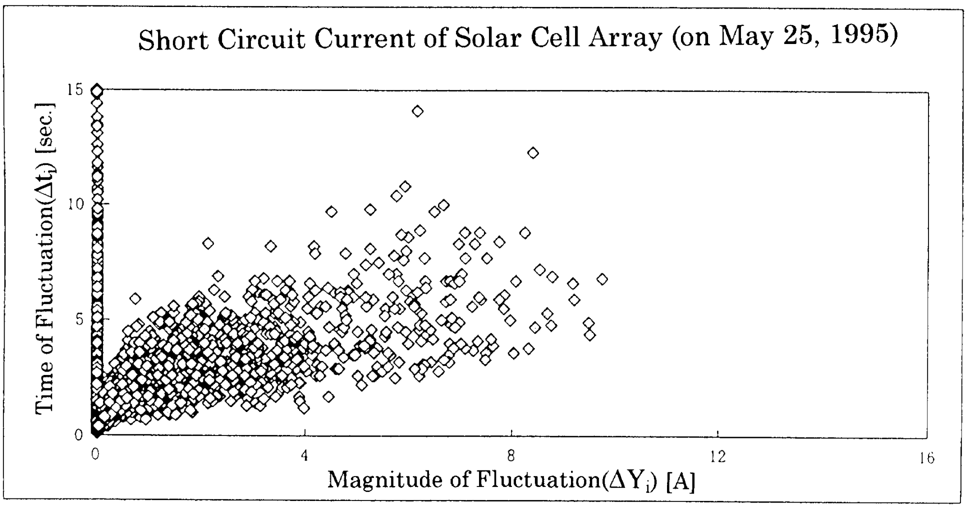

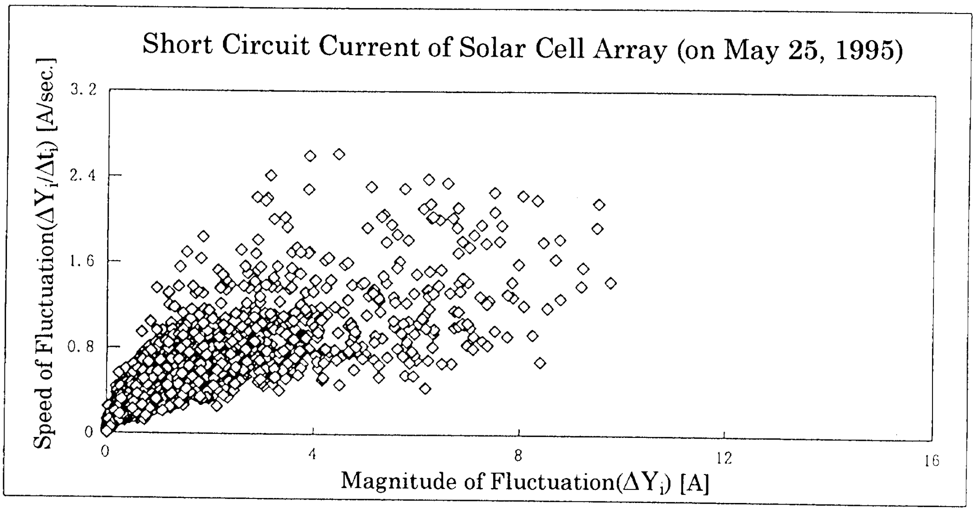

Fig. 7-14 Short circuit current of 2 kW photovoltaic array (May 25, 1997)

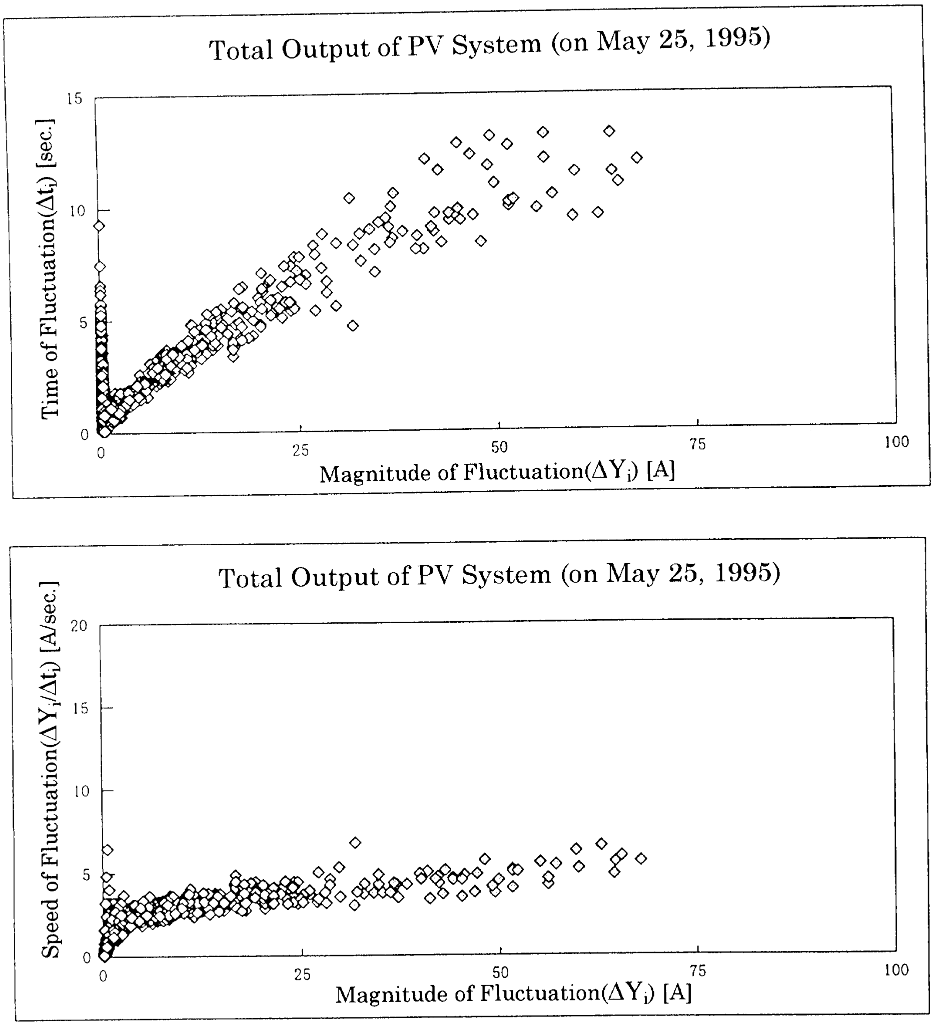

Fig. 7-15 Total output of photovoltaic power generation system (May 25, 1997)

7.5 Conclusions

It is difficult to measure the actual speed and magnitude of output fluctuations of multiple interconnected photovoltaic power generation systems. It was found that the value measured by a pyrometer having a slow response is similar to the actual values of the speed and magnitude of output fluctuation of multiple interconnected photovoltaic power generation systems. Therefore, the speed and magnitude of total output fluctuation can be measured with a pyrometer having a slow response.

In the case when many PV systems are connected uniformly along the distribution line, even if the output fluctuation of each PV system is large, both the magnitude and speed decrease and level off for the whole system. Accordingly, the distribution voltage fluctuation due to output fluctuation also decreases. For the remaining work in future, local voltage fluctuation for the case of distributed and concentrated installation of PV system should be examined.

8. Measurement of PV Array Temperature

8.1 Background

The surface temperature of an array is an important factor in evaluating the characteristics of photovoltaic power generation systems. However, since it is not clear whether the temperature is for the output period or for no output period, the difference in surface temperature of the array "for the case in which the inverter is connected to the photovoltaic array and output at full capacity" and "for the case in which the output terminal of the array is opened, i.e., no output" is clarified and the effect is described.

8.2 Experimental Procedure

Of the one hundred 2 kW arrays installed in Rokko Test Centre, three adjacent arrays, which are located around the centre, were selected for measurement. An output terminal of one of these arrays is opened. Another unit is connected to a system interconnection inverter and allowed to output by maximum power tracking control. The array between these two units repeatedly switches back and forth between output and no output at appropriate intervals. This "on-off array" is used to detect the change in surface temperature of the array caused by switching off and on.

The surface temperature of the photovoltaic array is strongly influenced by the intensity of solar radiation and velocity and direction of wind. Furthermore, the response speed to temperature of the array itself has an effect. To minimise these effects, three adjacent arrays were used. The intervals between switching on and off were 15 minutes, 30 minutes and 60 minutes. Thermocouples were used for measuring temperature.

8.3 Experimental Results

1) The result of changing the output at intervals of 15 minutes is shown in Fig. 8-1. Because the temperature response time of photovoltaic arrays used is significantly long, the interval is not long enough to cause a temperature change and the difference is not shown clearly. A temperature difference was seen between "array with output" and "array without output". The surface temperature of "array with output" is slightly lower than that of "array without output".

2) The result of changing the output at intervals of 30 minutes is shown in Fig. 8-2. Under this condition, a temperature change was clearly shown. The surface temperature of the array switched from no output to output, approaches that of "array with output" 30 minutes after switching. The surface temperature of the array switched from output to no output, approaches that of "array without output" 30 minutes after switching. The surface temperature of "array with output" is slightly lower than that of "array without output".

3) The result of changing the output at intervals of 60 minutes is shown in Fig. 8-3. Under this condition, a temperature change was also clearly shown. The surface temperature of the array switched from no output to output, approaches that of "array with output" 30 minutes after switching. The surface temperature of the array switched from output to no output, approaches that of "array without output" 30 minutes after switching. The surface temperature of "array with output" is slightly lower than that of "array without output".

4) The result of 24-hour operation of "array with output" and "array without output" is shown in Fig. 8-4. The surface temperature of "array with output" is slightly lower than that of "array without output". Although the temperature difference between the two arrays was 5℃ at the most, it is expected that the temperature difference varies depending on weather conditions and the time of day and further tests are needed.

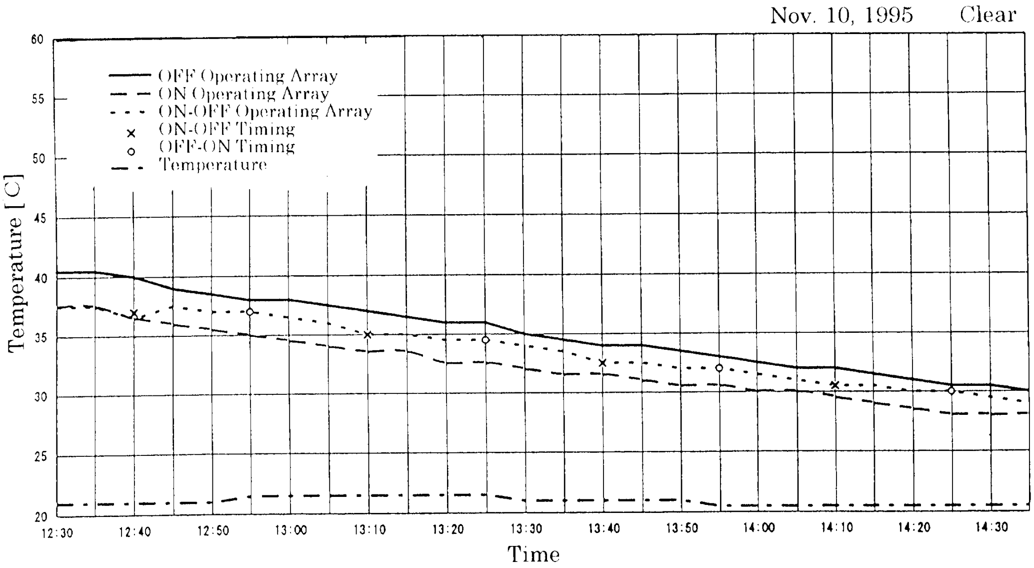

Fig. 8-1 Temperature measurement of photovoltaic power generation array (changing output at intervals of 15 minutes)

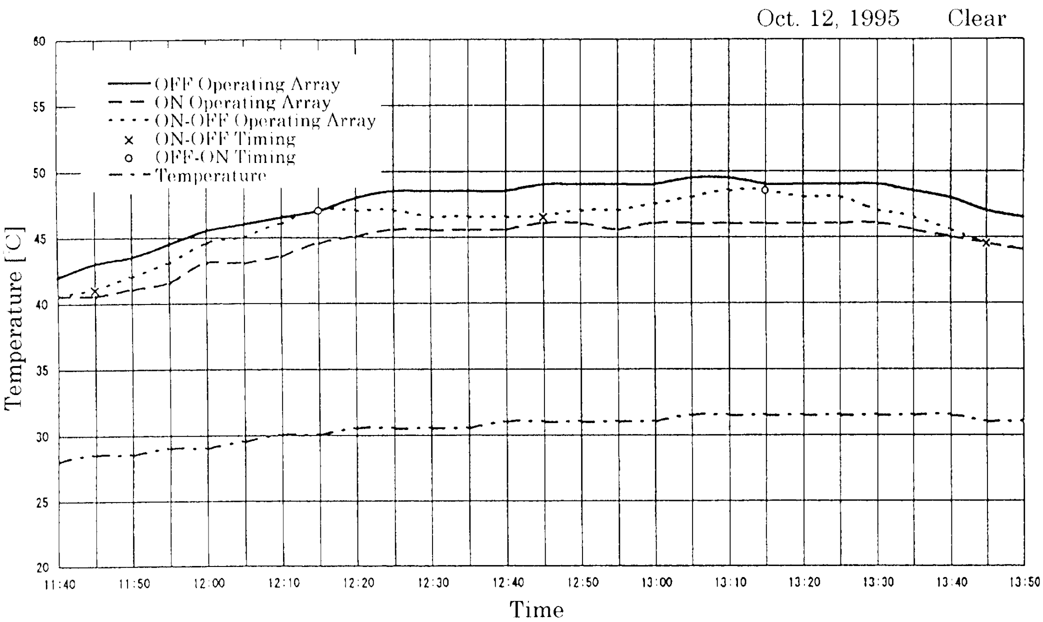

Fig. 8-2 Temperature measurement of photovoltaic power generation array (changing output at intervals of 30 minutes)

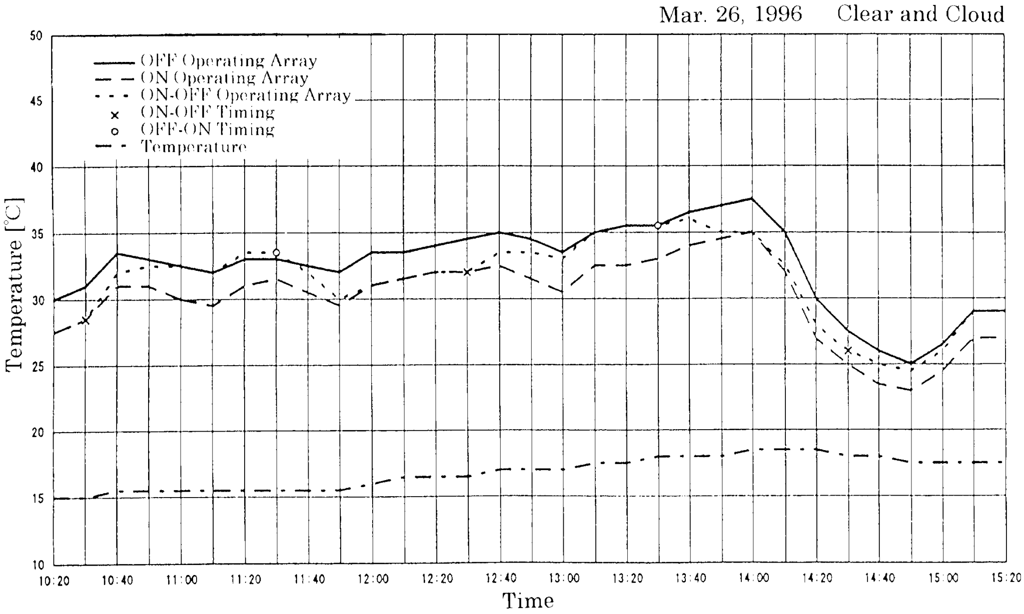

Fig. 8-3 Temperature measurement of photovoltaic power generation array
(changing output at intervals of 60 minutes)

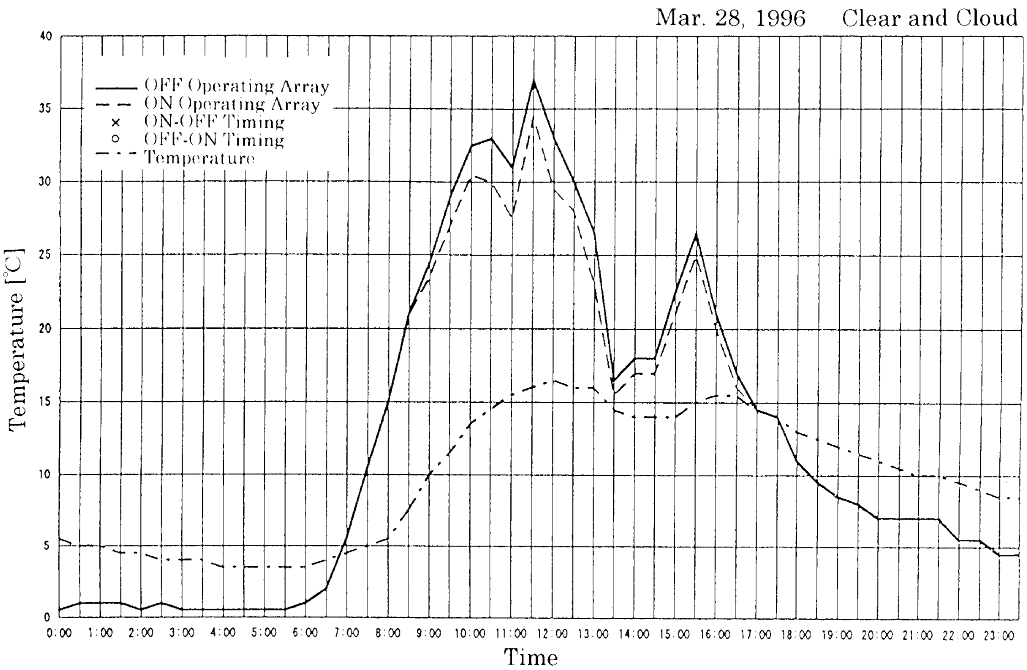

Fig. 8-4 Temperature measurement of photovoltaic power generation array
(24 hours, unchanged output)

8.4 Conclusions

The surface temperature of the array of a photovoltaic power generating system is lower when the array delivers power than when the array output is open circuited. This was confirmed from the measurements with three photovoltaic power generating arrays. Although the measured temperature difference was as low as 5℃ at the most in this measurement, the difference is considered to be bigger under actual conditions.

Future studies should investigate whether it is appropriate to measure the surface temperature of an array with or without the output connected The appropriate interval for evaluating the conversion efficiency of photovoltaic power generating systems should also be determined.

9. Conclusions

In subtask 30, experimental studies using the test facilities at the Rokko Test Centre for Advanced Energy Systems were conducted. Experiments were conducted for various aspects such as harmonics, islanding, distribution line short circuit, AC-DC mixing fault, PV system output variation, and PV array temperature evaluation. These experiments were conducted to provide reference data for grid interconnection of PV systems. Subjects like harmonics, islanding, AC-DC mixing fault and PV system output variation are closely related to the activities of subtask 20, while some of the subjects such as distribution line short circuit and PV array temperature measurement were not directly related to subtask 20 activities.

Test results showed that grid interconnection of multiple photovoltaic power generation systems has little effect on distribution line short circuit, AC-DC mixing fault, and output variation, but does affect harmonics and islanding. Further consideration of these effects, especially the islanding conditions, is required.

ANNEX LIST OF PARTICIPANTS

Sub-task 30 : Experimental tests using the Rokko Island and/or other test facilities
Leader: Akio Kitamura, The Kansai Electric Power Company, Japan

Names and addresses of Task V experts

The members of Tasks V are listed below (in alphabetic order and per 1999):

Country: Australia
Name Phil Gates
Company energyAustralia
Address L18 227 Elizabeth St.
GPOBox 4009
City Sydney
Zip code NSW 2001
Tel +61 2 9269 7366
Fax +61 2 9269 7372
E-mail pgates@energy.com.au

Country: Australia
Name Grayden L. Johnson
Company energex
Address 150 Charlotte Street
BPO Box1461
City Brisbane
Zip code Qld 4001
Tel +61 7 3407 4130
Fax +61 7 3407 4612
E-mail gj008@energex.com.au

Country: Austria
Name Gerd Schauer
Company Verbundgesellschaft
Address Am Hof 6a
City Wien
Zip code A-1011
Tel +43 1 53113 52439
Fax +43 1 53113 52469
E-mail schauerg@verbund.co.at

Country: Austria
Name Christoph Panhuber
Company Fronius KG
Address Gunter-Fronius-Strasse 1
City Wels-Thalheim
Zip code A-4600
Tel +43 7242 241-0
Fax +43 7242 241-226
E-mail panhuber.christoph@fronius.com

Country: Denmark
Name Arne Faaborg Povlsen
Company Elsamprojects A/S
Address Kraftvaerksvej 53
City Frederica
Zip code DK-7000
Tel +45 7923 3236
fax +45 7556 4477
E-mail afp@elsamprojekt.dk

Country: Germany
Name Hermann Laukamp
Company Fraunhofer ISE
Address Oltmannsstrasse 5
City Freiburg
Zip code D-79100
Tel +49 761 4588 275
Fax +49 761 4588 217
E-mail helau@ise.fhg.de

Country: Italy
Name Francesco Groppi
Company ENEL S.p.A.
Address Via A. Volta 1, Cologno Monzese
City Milan
Zip code 20093
Tel +39 2 7224 5770
Fax +39 2 7224 5235
E-mail groppi@pel.enel.it

Country Japan
Name Takuo Yoshioka (OA)
Company NEDO
Address Sunshine 60, 29F, 1-1, 3-Chome, Higashi-Ikebukuro, Toshima-ku
City Tokyo
Zip code 1706028
Tel +81 3 3987 9406
Fax +81 3 3590 5803
E-mail yoshiokatko@nedo.go.jp

Country: Japan
Name Tadao Ishikawa
Company CRIEPI
Addres 2-11-1 Iwato-kita Komea-shi
City Tokyo
Zip code 2018511
Tel +81 3 3480 2111
Fax +81 3 3430 4014
E-mail ishikawa@criepi.denken.or.jp

Country: Japan
Name Akio Kitamura
Company The Kansai Electric Power
Address 11-20, Nakoji 3-chome,
City Amagasaki, Hyogo
Zip code 661
Tel +81 6 6484 9786
Fax +81 6 6494 9827
E-mail -

Country: The Netherlands
Name Bas Verhoeven
Company KEMA T&D power
Address Utrechtseweg 310
City Arnhem
Zip code NL-6812
Tel +31 26 356 3581
Fax +31 26 351 3683
E-mail s.a.m.verhoeven@kema.nl

Country: Portugal
Name António Venâncio
Company EDP-GID
Address Av. Infante Santo, 17-6
City Lisbon
Zip code 1350
Tel +351 3955900
Fax +351 3902531
E-mail avenancio@edinfor.pt

Country: Switzerland
Name Peter Toggweiler
Company Enecolo AG
Address Lindhof 235
City Monchaltorf
Zip code 8617
Tel +41 1 994 9001
Fax +41 1 994 9005
E-mail enecolo@active.ch

Country: UK
Name Alan Collinson
Company EA Technology Ltd.
Address Capenhurst
City Chester
Zip code CH1 6ES
Tel +44 151 347 2396
Fax +44 151 347 2139
E-mail abc@ealt.co.uk

Country: UK
Name James Thornycroft
Company Halcrow Gilbert Associates
Ltd.
Address Burderop park
City Swindon, Wiltshire
Zip code SN4 OQD
Tel +44 1 793 814756
Fax +44 1 793 815020
E-mail thornycroftjm@halcow.com

Country: USA
Name Ward Bower
Company Sandia National labs.
Address MS 0753
City Albuquerque, New Mexico
Zip code 87185-0753
Tel +1 505 844 5206
Fax +1 505 844 6541
E-mail wibower@sandia.gov